ADAPTATION OF AUSTROADS MECHANISTIC-EMPIRICAL PAVEMENT DESIGN FOR TROPICAL CLIMATES

Rajapakshe Pathirannehelage Piyumee Kaushalya Premarathne

(178064C)

A thesis submitted in partial fulfilment of the requirements for the

degree Master of Philosophy

Degree of Master of Philosophy

Department of Civil Engineering

University of Moratuwa
Sri Lanka

March 2022

DECLARATION

This is my Master of Philosophy (MPhil.) dissertation. This dissertation does not integrate any previously published work submitted for a degree or diploma at another university or school of higher education without acknowledgement. Unless acknowledged in the literature, this research thesis contains no already published material created by another individual.

Furthermore, I authorise the University of Moratuwa the non-exclusive right to reproduce and disseminate my dissertation, in whole or in part, in print, electronic, or other media. I reserve the right to utilise this content in future publications, including scientific papers and journals.

Signature: ……. Date: 23/04/2023

R.P.P.K. Premarathne

The above candidate has researched for a Master of Philosophy (MPhil.) under my supervision.

Signature of the supervisor: …… Date: 30/04/2023

Professor. W.K. Mampearachchi

Signature of the supervisor: …… Date: 30/04/2023

Professor. M. Gunaratne

ABSTRACT

Many road agencies have employed conventional empirical pavement design methods, such as the American Association of State Highway and Transportation Officials (AASHTO) and Transport Research Laboratory (TRL) Overseas Road note 31 guidelines, to design and analyse flexible pavements. Empirical pavement design methods utilise empirical formulae based on past experiments conducted in extreme weather conditions. They have significant drawbacks permitting limited freedom for pavement designers, leading to material constraints in road projects. Such restrictions may result in high costs for hauling materials from far sites, leading to increased costs for road construction projects. Road agencies have identified the advantages of mechanistic-empirical (M-E) pavement design methods that accommodate available materials resulting in economical designs. However, performance models given in M-E methods are derived under laboratory conditions and require calibrations to the field. Austroads is one of the most recognised M-E guidelines widely used in Australia and New Zealand. It accompanies a user-friendly and time-efficient software package-CIRCLY. This research was focused on adapting the Austroads M-E pavement design guidelines for tropical climates. Austroads suggests two performance models, each for fatigue cracking and subgrade rutting. This research focused on calibrating the default performance models proposed by Austroads by finding the most suitable damage exponent (b) and shift factor (SF) for tropical climates. Calibrating the default fatigue performance model was only considered. Data from two A-class roads were obtained for model development and model validation. Cumulative damage factor (CDF) representing the accumulated fatigue damage was estimated at varying damage exponents (b) and shift factors (SF) using the mechanistic design software-CIRCLY. The alligator cracking index (ACI) suggested by the Federal Highway Administration (FHWA), quantifying the fatigue damage level, was calculated using visual surveys to detect and classify pavement distresses. It could be observed that the CDF have a strong relationship with the ACI. The most robust relationship between the ACI and the CDF could be observed at the damage exponent (b)= 5.1 and the shift factor (SF)= 2.5. CDF values were computed for the model validation by inputting the calibrated damage exponent (b=5.1) and shift factor (SF=2.5) to the mechanistic design software-

CIRCLY. ACI values were predicted by substituting these calculated CDF values for the derived regression model. When the observed ACI values were plotted against the predicted ACI values, it could be noticed that the best-fit curve for the observed ACI and predicted ACI has $R^2 = 0.99$ and slope = 1.007. This observation emphasizes the accuracy of the derived model, thereby justifying its use for the design and analysis of flexible pavements for tropical climatic conditions. Therefore, it can be justified that adapting the Austroads mechanistic pavement design guideline for tropical climates is highly favourable by modifying the default performance relationships. The use of mechanistic tools to design and analyse pavements was strongly emphasised during the analysis steps, ensuring the reliability of such tools in pavement design and analysis. As the M-E design procedure allows the designer to use available materials, adapting the M-E design procedure will address the material constraint in road construction projects and deliver more cost-effective designs. This will finally help reduce unwanted expenditures and improve the economic aspect of road construction projects.

Keywords: Mechanistic-Empirical (M-E) Pavement Design, Austroads, Modified failure functions, Alligator Cracking Index (ACI), CIRCLY, Cumulative Damage Factor (CDF), Tropical climates

DEDICATION

To

My Loving Motherland, Sri Lanka

ACKNOWLEDGEMENTS

I want to offer my immense gratitude to my research supervisor Professor. Wasantha Kumara Mampearachchi, at the Department of Civil Engineering, University of Moratuwa, Sri Lanka, offered me this excellent opportunity to pursue my passion for research and academia. I am thankful for the great exposure you gave me to build my confidence and the invaluable support throughout these years to achieve this most extraordinary milestone.

I want to thank my second supervisor, Professor Manjriker Gunaratne, University of South Florida, Tampa, for his outstanding support throughout the research and positive input to make this research a success. I am grateful to Professor. J.M.S.J. Bandara, Dr. H. R. Pasindu at the Department of Civil Engineering, University of Moratuwa, Sri Lanka and Dr S. P. Jayakody at the Southeastern University, Sri Lanka, for your timely instructions and valuable advice in making this research a success.

My genuine appreciation goes to all the Road Development Authority (RDA) staff, who supported the collecting and analysing of data. I want to thank all the Planning Division directors and the RDA's Research and Development (R and D) for providing me with the necessary data. I want to thank the RDA's audit director (retired), Mr Keerthi Damboragama, for your immense support for the data collection. I thank Senior Engineer Mr Sugeeth Samarasinghe for his invaluable support throughout the research. I am obliged to Mr Kasun Muthunayake and Mr Imesh Pushpakantha at the Planning Division of RDA for serving me in obtaining the required data on time.

Further, I would like to thank Ms Melani Jayakody, Mr Uditha Padmaperuma, and Mr Pathum Fernado for supporting me throughout this project. I want to thank all the academic and non-academic staff members at the Civil Engineering Department, University of Moratuwa, Sri Lanka, who helped me.

Last but not least, throughout this study, I appreciate the encouragement and support from my loving family and friends. I would not be who I am without my family and friends.

R.P.P.K. Premarathne

TABLE OF CONTENT

LIST OF FIGURES

LIST OF TABLES

LIST OF ABBREVIATIONS

AASHTO	American Association of State Highway and Transportation Officials
AADT	Average Annual Daily Traffic
ABC	Aggregate Base Course
AC	Asphalt Concrete
ACI	Alligator Cracking Index
CBR	California Bearing Ratio
CDF	Cumulative Damage Factor
CESAL	Cumulative Equivalent Standard Axle Load
DBST	Double Bitumen Surface Treatment
DESA	Design Equivalent Standard Axles
ESAL	Equivalent Standard Axle Load
FHWA	Federal Highway Administration
FHWA RIP	Federal Highway Administration's Road Inventory Program
FWD	Falling Weight Deflectometer
M-E	Mechanistic-Empirical
M_R	Resilient Modulus
MCC	Manual Classified Count
MEPDG	Mechanistic-Empirical Pavement Design Guide
MSE	Mean Squared Error
NCHRP	National Cooperative Highway Research Program
NDT	Non-Destructive Testing
NPS	National Park Service
PCI	Pavement Condition Index
PMS	Pavement Management Systems
PSI	Present Serviceability Index
RDA	Road Development Authority
RF	Reliability Factor
RI	Roughness Index
SAR	Standard Axle Repetitions
SF	Shift Factor
TLD	Traffic Load Distribution
TRL	Transport Research Laboratory
WMAAT	Weighted Mean Annual Air Temperature
WMAPT	Weighted Mean Annual Pavement Temperature
SAST	Single Axle Single Tyre
SADT	Single Axle Dual Tyre
TAST	Tandem Axle Single Tyre
TADT	Tandem Axle Dual Tyre
TRDT	Tridem Axle Dual Tyre

LIST OF APPENDICES

1 INTRODUCTION

With the country's industrial advancement and economic development, there is an extraordinary demand for improved road infrastructure. The improvement of road infrastructure has been very significant over the past century, and road infrastructure needs are rapidly increasing in conjunction with Sri Lanka's economic growth. Road development authority (RDA) in Sri Lanka encounters critical limitations due to conventional pavement design methods currently used in Sri Lanka, such as Transport Research Laboratory (TRL) Road Note 31 (Transport Research Laboratory, 1993) and American Association of State Highway and Transportation Officials (AASHTO) (AASHTO, 1993), permitting limited freedom in pavement design procedures.

These conventional pavement design procedures utilize empirical formulae based on past experiences and results. Most empirical methods have no provision for using alternate materials, and this is a critical factor to consider when addressing the constraint of good quality material in pavement construction. As conventional pavement design procedures suggested, the unavailability of recommended materials results in the high cost of hauling materials from far sites, leading to a higher total cost of road construction projects. In developing countries, including Sri Lanka, material, economic, and environmental constraints are unfavorable for the road construction industry as well as for the economy of the country. Consequently, these conventional pavement design procedures are more conservative and do not often provide cost-effective designs. These design procedures recommend designing pavements by considering design traffic volume in Equivalent Standard Axle Load (ESAL) and subgrade strength.

TRL Road Note 31 (Transport Research Laboratory, 1993) is an empirical guideline that specifies layer thicknesses for a selected set of materials. However, it does not establish a mechanism for integrating materials having characteristics other than those defined in the standard. They are developed by acknowledging the worst possible condition, and it is hard to expect cost-effective pavement designs from empirical pavement design procedures like TRL Road Note 31 (Transport Research Laboratory, 1993) and AASHTO (AASHTO, 1993). TRL Road Note 31 (Transport Research

Laboratory, 1993) can only accommodate traffic loading up to 30 million Cumulative Equivalent Standard Axle Load (CESAL) in one direction. Hence, this guideline does not apply to traffic loadings exceeding 30 million CESALs. Compared to TRL Road Note 31 (Transport Research Laboratory, 1993), the AASHTO (1993) design method can be adopted to design heavy-volume roads, and it is flexible in the hands of road designers. AASHTO (1993) guideline also does not provide a precise method to alter the design according to the available conditions and materials.

Considering the drawbacks of conventional pavement design procedures, road development agencies have recognized the necessity of new pavement design procedures to overcome limitations in traditional pavement design procedures to resolve these constraints. Mechanistic-Empirical (M-E) pavement design procedures have drawn the attention of pavement designers and road development agencies. It has also become a global trend due to its significant advantages. Many road agencies have shifted from conventional pavement design procedures to M-E pavement design procedures considering the design, construction, and maintenance improvements provided by M-E pavement design methods over purely empirical pavement design methods.

Applying M-E design methods for designing and analyzing pavements has several benefits. Reducing material and economic constraints in the road construction industry is a significant enhancement. As the mechanistic pavement design method accommodates available materials, there can be a substantial reduction in the hauling cost of materials from far sites and time wastage. Hence, a particular project's economic aspect and progress will be improved. M-E methods are flexible to adapt in practice without acquiring a vast database.

Road development agencies look forward to developing and adopting M-E design procedures, which permit the use of available materials during road construction. Utilizing mechanistic tools by incorporating expertise and experience obtained from empirical approaches with real-time performance, traffic loading, material properties, and environmental conditions is essential in that perspective. As a consequence of those investigations, in February 2004, the Mechanistic-Empirical Pavement Design

Guide (MEPDG) was delivered to the National Cooperative Highway Research Program (NCHRP) under project 1-37 A. This initiative constitutes a substantial breakthrough in pavement design since it redirected the emphasis away from the conventional empirical-based techniques and more towards M-E-based processes, which benefitted from analytical modelling features and the real-time performance of in-service roadways (Mehta & Roque, 2003).

Several mechanistic design procedures incorporate various software packages related to mechanistic pavement design. Mechanistic design software is adopted to make the pavement design process cost-effective and time efficient. Austroads pavement design guideline, broadly practiced in Australia and New Zealand, also has an inbuilt mechanistic design software named CIRCLY. This mechanistic design software is based on the performance models proposed by the Austroads pavement design guide. The Austroads pavement design method defines two performance models for asphalt fatigue cracking and subgrade rutting. Adapting the Austroads mechanistic pavement guideline to any country is highly favorable since it has this inbuilt pavement design software - CIRCLY- making the design process user-friendly and time-efficient. Using mechanistic design tools to incorporate Austroads' pavement design approach has several advantages, including choosing a wide range of vehicle categories, wheel layouts, layer thicknesses, and material properties and improving the analysis's descriptiveness.

These M-E pavement design procedures are timely for developing counties like Sri Lanka. M-E methods have shown successful applications in assessing early failure of roads, diminishing the maintenance cost due to subsequent failures, examining road failures, and recommending the most suitable rehabilitation methods. Developing a pavement design and performance evaluation tool in the Sri Lankan development sector for pavement design and analysis based on M-E procedures will benefit future road implementation projects. Ensuring the reliability of using a mechanistic tool for local roads improved under TRL Road Note 31 (Transport Research Laboratory, 1993) and AASHTO guidelines (AASHTO, 1993) is a real challenge to achieve.

A recent study by Jayarathna (2017) favorably applied Austroads mechanistic pavement design methods by accommodating mechanistic design software-CIRCLY to investigate the applicability of Austroads mechanistic pavement design guidelines for tropical climates. Jayarathna (2017) concluded that the Austroads mechanistic design guideline could effectively design flexible pavements in tropical climates. However, initially, mechanistic pavement design software-CIRCLY was used effectively to evaluate pavement conditions based on Cumulative Damage Factor (CDF) for Double Bitumen Surface Treated (DBST) roads in Northern Province (Jayarathna, 2017). It was identified that the mechanistic design software-CIRCLY based on Austroads could be further improved as a reliable tool for pavement designing and performance evaluation process locally.

Performance models based on Austroads should be calibrated by incorporating design parameters such as materials properties, traffic, and environmental factors under local conditions for all structural pavement designs to adapt the Austroads M-E procedures. Austroads pavement design guide accommodates material properties such as resilient modulus and Poisson's ratio as inputs to the design process. This pavement design process also accommodates the number of standard axle repetitions (SAR) induced by the design traffic. Consequently, traffic data such as axle load survey data, manual classified count (MCC) data, and average annual daily traffic (AADT) data are also required for calculating the design equivalent standard axles (DESA). The resilient modulus of the pavement layers is usually obtained from the back-calculation of falling weight deflectometer (FWD) data. The back-calculation process should be conducted by correcting the asphalt modulus at the weighted mean annual pavement temperature (WMAPT) recommended by the Austroads guideline.

Consequently, adapting the Austroads mechanistic design procedure will be highly beneficial for the long-term and short-term aspects of the highway construction industry in local tropical climatic conditions. Available conventional empirical pavement design methods such as TRL Road Note 31 and AASHTO do not allow the use of available materials, which costs much money to haul materials from far sites and time to complete design steps. Therefore, checking the possibility of adapting Austroads mechanistic procedures for local tropical climatic conditions is highly

required. Since it was already validated by Jayarathna (2017) that the Austroads mechanistic design can be successfully utilized for the design and analysis of flexible pavements in tropical climatic conditions, further research on how to adapt Austroads mechanistic pavement design was necessary. Adapting Austroads mechanistic pavement design guidelines will allow the use of available and novel materials, thereby reducing constraints in construction materials, design, cost, and time. The availability of such flexible mechanistic pavement design methods will allow the designers and engineers to design and construct cost-effective and time-efficient road construction projects, thereby reducing the high hauling cost of materials, overestimation and underestimation of pavement layer thicknesses and reducing the total cost of highway construction projects. Adapting Austroads mechanistic pavement design can be achieved by calibrating the default failure functions to suit local tropical climatic conditions. Considering the availability of the data and limitations in analytical resources, only the calibration of the default fatigue performance model suggested by the Austroads mechanistic pavement design guide was only considered in this study.

2 OBJECTIVES

This research was focused on adapting the Austroads mechanistic pavement design guidelines for local tropical climatic conditions by determining a calibrated failure function for asphalt fatigue.

The objectives of this research were,

1. Identifying the requirements of calibrating default failure function for Asphalt fatigue suggested by Austroads mechanistic pavement design guidelines.
2. Calibrating the default failure function for asphalt fatigue suggested by Austroads mechanistic pavement design guidelines to suit tropical climatic conditions.

2.1 Scope of Work

The research was focused on adapting the Mechanistic-Empirical (M – E) pavement design procedure developed by the Austroads pavement design guide for tropical climatic conditions. Since these performance models were laboratory-derived under controlled conditions, validating and calibrating (if required) before adapting for pavement design and analysis procedures is vital. Failure functions suggested by the Austroads pavement design guide may not directly apply to tropical climatic conditions since it was designed to suit Australian conditions by default. Therefore, these models may require specific modifications/calibrations to suit the local tropical conditions. The Austroads mechanistic pavement design guideline integrates its mechanistic design software named CIRCLY, a user-friendly and time-efficient mechanistic pavement design software package. Using mechanistic design software – CIRCLY is straightforward, making the design and analysis process quick and efficient. The mechanistic design software-CIRCLY based on the Austroads guide, was used in this study to check the requirement to calibrate the default failure functions suggested in the Austroads pavement design guide. The analysis was only focused on calibrating the failure function for fatigue cracking in asphalt layers considering the available data and other limitations imposed during the analysis procedure. All material properties were obtained from in-situ data of the selected roads for analysis. The alligator cracking index (ACI), representing the fatigue damage in the asphalt

layers, was analyzed against the Cumulative Damage Factor (CDF), representing the accumulated damage in the asphalt layers, to identify calibration requirements and to conclude the most suitable calibrated failure function for asphalt fatigue for tropical climatic conditions.

3 LITERATURE REVIEW

3.1 Flexible pavements

Flexible pavement is a multi-layered elastic system supported by a subgrade that facilitates vehicle mobility (Singh & Sahoo, 2021). Flexible pavements generally consist of asphalt concrete (AC), aggregate base course (ABC), subbase, and subgrade layers. These layers have distinct material properties. The asphalt concrete layer is composed of crushed aggregates, fines, and bitumen blended to meet the defined material properties to withstand the traffic loads without causing failure throughout the life of the pavement. The asphalt concrete performs like a waterproof layer, limiting water infiltration to the lower layers. ABC consists of crushed aggregates and fines which meet the specified limits. The subbase layer is constructed with natural granular materials, and the subgrade layer is the existing earth soil. Accommodation of materials and properties may vary with subgrade support, environmental factors, traffic loads, and drainage provisions (Leonards, 1982).

The layers of the pavement are organized in ascending order of load-bearing capacity. The material having the highest load-bearing potential (and thus the costliest) is placed at the top. The material with the lowest load-bearing potential (and, therefore, the least expensive) is placed at the bottom. (Singh & Sahoo, 2021). The stresses imposed by automobile movement are distributed through the granular structure of aggregates via grain-to-grain contact (Singh & Sahoo, 2021). Stress intensity is higher on the top layers. Accordingly, the topmost layer (Asphalt) should have the highest strength to withstand high-intensity stress conditions. Stress intensity gradually diminishes with the depth of the pavement as the weak layers experience a minor stress intensity (Leonards, 1982).

Stress distribution on a flexible pavement due to traffic loads is depicted in Figure 3.1.

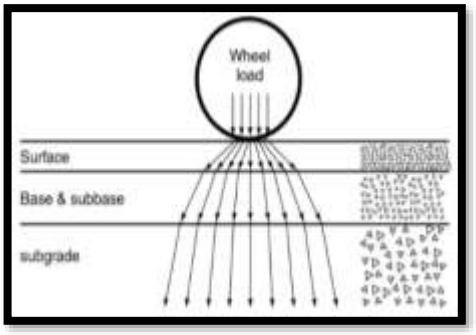

Figure 3.1: Traffic Loading and stress distribution in a flexible pavement (Austroads, 2010)

While the asphalt layer's modulus is temperature-dependent and viscous-elastic, the base course and subbase moduli are stress-dependent and nonlinear (Claessen et al., 1977; Dorman & Metcalf, 1965; Shook, 1982). The road structure relies on the strength and stability of the subgrade, which eventually relaxes the loads exerted on the road surface. The California bearing ratio (CBR) and resilient modulus (M_R) of subgrade are well-known empirical strength indicators used to determine road thickness. Although the CBR value specifies the stiffness and strength of pavement layers, it is inadequate for designing pavements (Brown, 1996).

3.2 Flexible Pavement Design Methods

The two major pavement design procedures for the design and analysis of flexible pavements are.

1. Empirical Pavement Design
2. Mechanistic-Empirical (M – E) Pavement Design

While the objective for M-E-based design is primarily to have a sound scientific and engineering background, empirical approaches remain attractive in many other fields of technology, owing to their extensive history of experience and familiarity with the methodologies. Thus, M-E approaches retain the tremendous potential for increased use and validation, which presents a significant challenge for pavement engineers (Haas et al., 2007a).

3.3 Empirical Pavement Design Procedure

Techniques for empirical pavement design are supported by empirical formulae or experimental studies undertaken in adverse weather conditions (Jayarathna, 2017). American Association of State Highway and Transportation Officials (AASHTO) method (AASHTO, 1993) and Transport Research Laboratory (TRL) Road Note 31 (Transport Research Laboratory, 1993) are the most widely used empirical guidelines for pavement design in Sri Lanka. TRL Road Note 31 (Transport Research Laboratory, 1993) is particularized for tropical countries like Sri Lanka.

The CBR value is a standard input in pavement design procedures like AASHTO (1993) and TRRL procedures (Powell et al., 1984), and even analytical road design procedures like the Shell method (Shell International Petroleum Company, 1978) rely on the CBR test to obtain, through empirical correlations, the fundamental stress-strain parameters required as input to the calculation of stresses and strains in pavements (Gillett, 2001).

3.3.1 Limitations in TRL Road Note 31

The Road Note 31 is an empirical approach-based catalogue pavement design guide, falling within the first generation of pavement design methodologies. The current designs for road pavement are based on empirical techniques, first presented in Road Note 31 by the Transport Research Laboratory and published 30 years ago. Roads in Sri Lanka are structurally designed and constructed following Road Note 31, limiting the indirect material property to a specified California Bearing Ratio value limit. As a result, the country's abundant in-situ soil and aggregate resources have not been utilized in the best possible way to construct roads. Most of the soil and aggregates available in the country cannot be used for highway construction in an ideal way since empirical techniques confine the material qualities to predetermined limits.

Consequently, a scarcity or excess of materials has resulted from this circumstance. Without considering a pavement system's structural capability, this may also lead to over- or under-estimated catalogues of the present pavement design recommendations. The limitations of adopting the empirical catalogue design technique include the inability to integrate novel pavement systems that use in-situ materials considering the

optimal quantity and the absence of a mechanistic-empirical material property database.

Due to the lack of supplies like aggregates, the road development agencies plan to employ the mechanistic-empirical approach to design the thickness of the road pavement as a solution. To address this issue, the Sri Lankan government anticipates using the mechanistic-empirical design approach to determine the thickness of new or overlay pavements, particularly for low-traffic roads. Because the pavement thickness design can be determined by mechanical responses, such as strain or stress in a crucial location of a layered pavement system, rather than by indirect material properties like the California Bearing Ratio value, mechanistic-empirical design can offer flexibility in using a wide range of material properties.

In order to establish the mechanistic-empirical design concept and methodology for new road construction and the rehabilitation of existing roads, as well as to guide the Road Development Authority in developing a comprehensive database system for pavement management and analysis soon, a technical assistance initiative between the Asian Development Bank and the Road Development Authority of Sri Lanka was launched in January 2017 (Yoo & Park, 2018).

3.3.2 Limitations in AASHTO 1993 pavement design guideline

The AASHTO 1993 design process is based on empirical formulae obtained from the AASHO Road Test, carried out on a test track in Ottawa, Illinois, in the late 1950s. For now, the test gave highly beneficial information for pavement design. Unfortunately, the current material improvements and the sharp rise in traffic quantities made this empirical design process extremely problematic.

The AASHTO pavement design method has several limitations, including empirical equations created based on a particular subgrade type, one environmental condition, and a restricted range of traffic loads and material characterization. These factors are directly relevant to the location where the AASHO road test was conducted. The accuracy and consistency of layer thickness calculations made using inputs much more significant than those utilized for the AASHO Road test are seriously in doubt.

Furthermore, roads designed and built-in accordance with the AASHTO 1993 did not perform as well after their design periods, according to recent research comparing the Flexible Pavement Design AASHTO 1993 and Mechanistic-Empirical Pavement Design (MEPDG). This study also found that AASHTO 1993 overestimates pavement layer thicknesses. Terminal Present Serviceability Index (PSI) values are different for different traffic levels and locations. A similar tendency to the final PSI values might be seen in predicted fatigue cracking and rutting. According to the study's parameters, predicted fatigue cracking shows considerable sensitivity to design inputs. Additionally, it was discovered that the main determining input elements for the chosen pavement performance indices were environmental factors and traffic loads (Aguib, 2021).

3.4 Mechanistic-Empirical Pavement Design Methods

Until the end of World War II (the mid-1940s), pavement design was nearly entirely empirical or experience-based, at which point fundamental or theoretically based concepts began to develop. The inaugural International Conference on the Structural Design of Asphalt Pavements held at Ann Arber, Michigan, in 1962 is widely regarded as the starting point for applying these principles to pavement design (Monismith, 2004). Numerous advancements toward what we now refer to as the mechanistic-empirical (M-E) pavement design methodology occurred over the next several decades in a wide range of countries worldwide. Thus, M-E approaches retain the considerable potential for further application and verification, posing a severe challenge to pavement engineers (Haas et al., 2007b).

Identify the most critical remarks when converting the process to a mechanistic-empirical framework:

i. Consideration of fatigue cracking by Miner’s law,
ii. Prediction of low-temperature cracking
iii. Development of a mechanistic subsystem for predicting permanent deformation (Uzan, 2004)

The design of new and rehabilitated pavements has relied on empirical methods that have been advanced incrementally over time. Nevertheless, these procedures have several limitations due to their empirical nature. Consequently, studies have been conducted to overcome those limitations. As a result, in February 2004, the Mechanistic-Empirical Pavement Design Guide (MEPDG) was delivered to the National Cooperative Highway Research Program (NCHRP) under project 1-37 A. This project was a notable improvement in pavement design because it shifted from traditional empirical-based design techniques toward M-E-based approaches that benefit analytical modelling capabilities and in-service pavement performance (Mehta et al., 2008).

Pavement design and lifetime estimation are often accomplished using M-E pavement design methods (Walther & Wistuba, 2012). The advantage of an M-E technique is that it enables explicit determination of in-situ material properties. In-situ material properties can be established by estimating field deflection measurements on a pavement structure. Such evaluations ascertain the pavement's current structural support and anticipated lifetime, leading to a more appropriate design for the specific condition. M-E design can also identify critical locations in a road structure, allowing the designer to foresee the ultimate distress mode by analyzing the pavement responses in a specific layer and designing correspondingly.

Additionally, the M-E pavement approach has the following benefits over a solely empirical approach:

i. Increased reliance on readily available materials
ii. Provision for advanced materials
iii. Improved specification of layer characteristics
iv. Supports a variety of load types.
v. Predictions of performance that are more accurate.
vi. Accommodating materials' environmental and ageing impacts (Austroads, 2017)
vii. Capability to examine additional variables and perform sensitivity tests.

viii. Rationally evaluate innovative materials' projected performance and loading conditions (Wardle, 2010).

However, implementing the ME procedures has several challenges, including the enormous amount of traffic and climatic data needed, the advanced characterization of the pavement materials, and the calibration and validation of the local conditions. Accordingly, an increased required time to develop and evaluate the design is warranted. Furthermore, lacking experience with the ME pavement design approaches is an additional challenge. (Saudy et al., 2023). As a result, a study was conducted by Jayarathna (2017) on the validation of the mechanistic-empirical design approach for pavement design - a case study for Sri Lanka to assess the applicability of mechanistic-empirical (M-E) models developed by AUSTROADS guide for tropical climatic conditions prevailing in Sri Lankan roads. The research accommodated the mechanistic pavement design software - CIRCLY, based on the default failure functions suggested by the AUSTROADS pavement design guideline to make the analysis procedure straightforward and time efficient. The researcher facilitated the Cumulative Damage Factor (CDF) of the asphalt layer, representing the accumulated damage and the in-service pavement condition for the analysis. The pavement Condition Index (PCI) representing the pavement condition was calculated only for structural-based distresses as assessed by type, severity, and density according to the ASTM method. Then these obtained CDF values were verified with the PCI values, and it was found that the CDF values obtained from the mechanistic design software – CIRCLY have a significant relationship with PCI values. Consequently, it was concluded that mechanistic design software - CIRCLY, based on Austroads pavement design guidelines, could be introduced as an effective pavement design and analysis tool for designing road pavements in tropical climatic conditions. The same research also evaluated the possibility of using the mechanistic pavement design software – CIRCLY to investigate pavement failure. Results showed that the subbase layer's inadequate strength was the reason for the failure. The mechanistic design software investigated failure and proposed a reliable reclamation method. The above research findings successfully concluded that the AUSTROADS mechanistic pavement design

method could be accommodated in designing and analyzing flexible pavements in tropical climates.

The variation of pavement condition index (PCI) with Cumulative damage factor (CDF), as found by Jayarathna (2017), is presented in Figure 3.2.

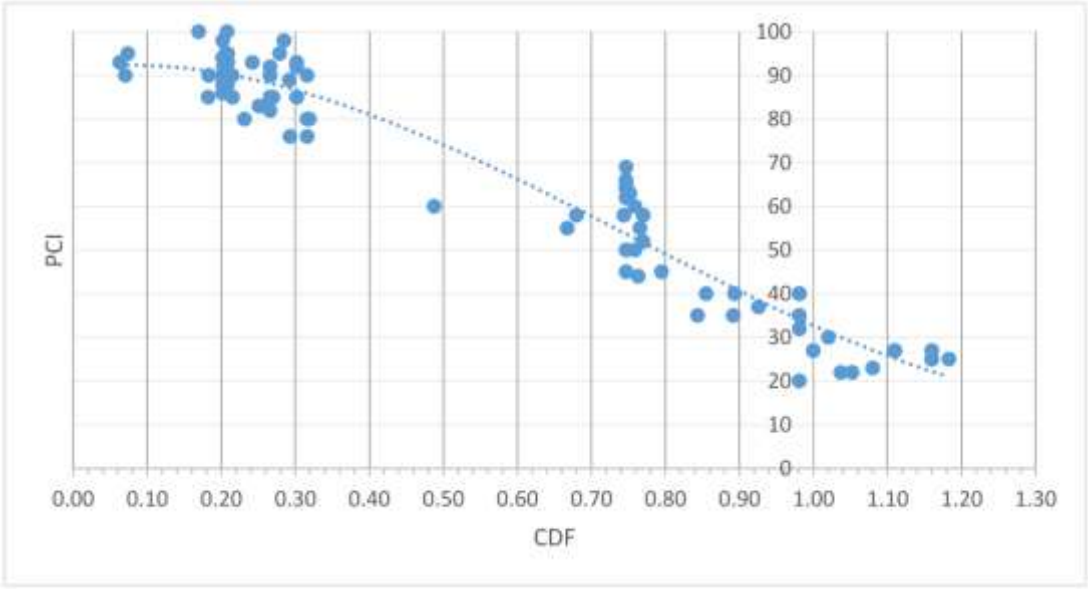

Figure 3.2: Variation of PCI with CDF (Jayarathna & Mampearachchi, 2017)

According to (Jayarathna & Mampearachchi, 2017), the best form of model that represents the expected behavior of PCI versus CDF takes the following form as in the Equation 3.1:

$$y = 63.404x^3 - 143.08x^2 + 20.834x + 91.589$$ ----------*Equation 3.1*

(Jayarathna & Mampearachchi, 2017) used another data set to validate the above-derived model. Figure 3.3 shows the variation of observed PCI with the measured PCI.

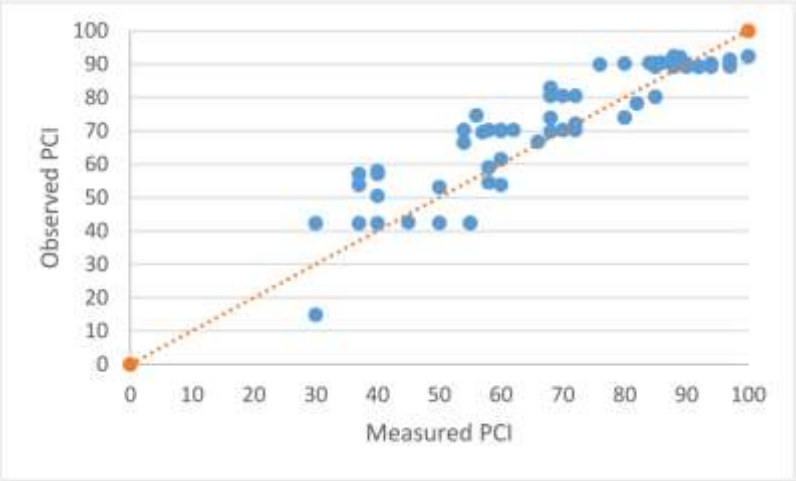

Figure 3.3: Model Validation (Jayarathna & Mampearachchi, 2017)

The R^2= 0.71 for the above graph shows that the PCI values predicted from the model are more reliable (Jayarathna & Mampearachchi, 2017).

Furthermore, a study on the calibration of the mechanistic–empirical pavement design guide for flexible pavement design in Arkansas by Hall et al. (2011) identified that The Mechanistic-Empirical Pavement Design Guide (MEPDG) should be adjusted to a local scale due to possible discrepancies amongst national and local conditions. The study focused on the initial local calibration of flexible pavement models in the MEPDG for Arkansas, and data from the local pavement management system (PMS) and the Long-Term Pavement Performance (LTPP) database were utilized for this requirement.

The analysis also required traffic, climate, structure, and performance data. The LTPP database contained necessary traffic data, such as volume count, vehicle classification, and axle load distribution, to be utilized directly in the MEPDG. For this research, climate data were obtained from nearby climate stations by interpolation, considering each location's GPS coordinates. The MEPDG provides five flexible pavement performance predictions: alligator cracking, longitudinal cracking, transverse cracking, rutting, and international roughness index (IRI). For LTPP sections, the corresponding measured performance data are recorded in Monitoring. As with national calibration (Guide, 2004), low-, medium-, and high-severity alligator cracking were summed as “alligator cracking” without adjustment; low-, medium-, and high-

severity in-wheel path longitudinal cracking was added without adjustment as "longitudinal cracking"; and low-, medium-, and high-severity transverse cracking was summed as "transverse cracking" by use of the same weighting function as in the national calibration. Only new flexible pavement was included in this study. All manual distress surveys followed the LTPP 'Distress Identification Manual' (Miller & Bellinger, 2003).

The solver function in Microsoft Excel was utilized to optimize the coefficients for alligator cracking. Iterative runs of the MEPDG employing discrete calibration coefficients were done to optimize rutting models. Consequently, the alligator cracking and rutting models suggested by MPEDG were improved by calibration.

MEPDG was run with the national default calibration coefficients at the verification stage. The comparisons of predicted and measured alligator cracking, longitudinal cracking, transverse cracking, and IRI and total rutting were then presented, and they are illustrated in Figure 3.4 to Figure 3.8.

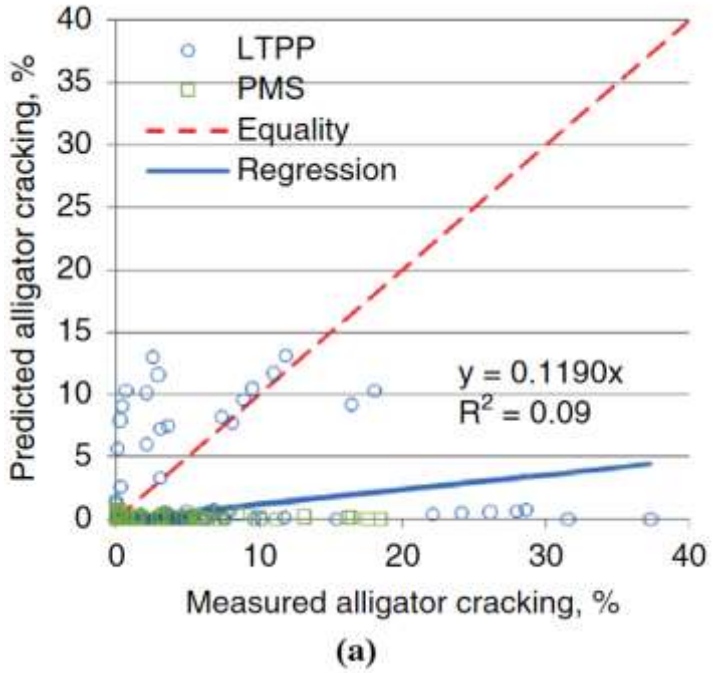

Figure 3.4: Alligator cracking model: (a) verification (Hall et al., 2011)

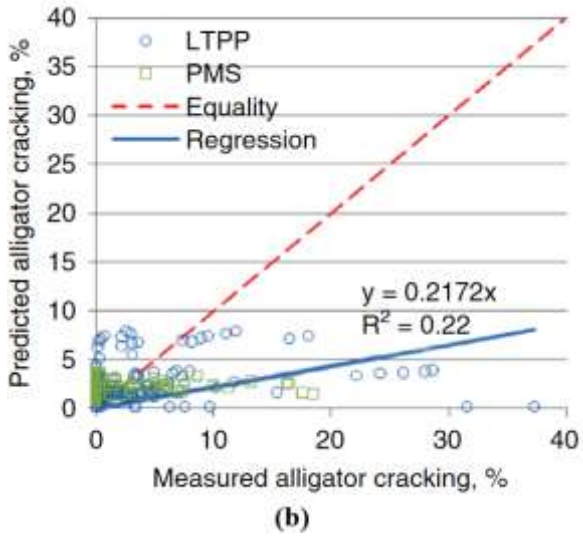

Figure 3.5: Alligator cracking model: (b) calibration (Hall et al., 2011)

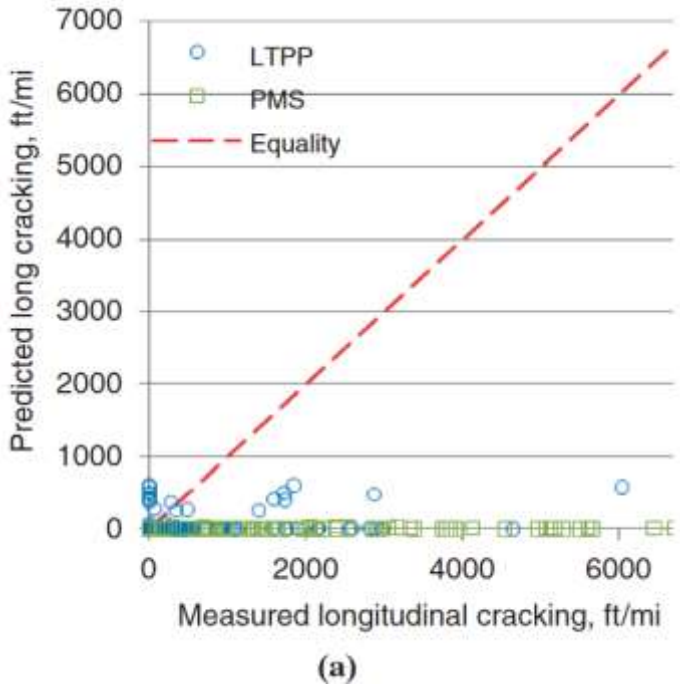

Figure 3.6: Verification of national calibrated model: (a) longitudinal cracking (Hall et al., 2011)

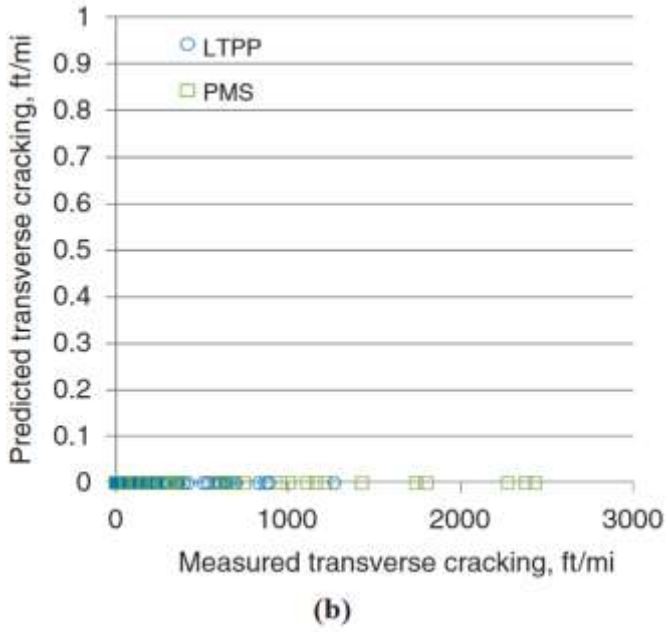

Figure 3.7: Verification of national calibrated model: (b) transverse cracking (Hall et al., 2011)

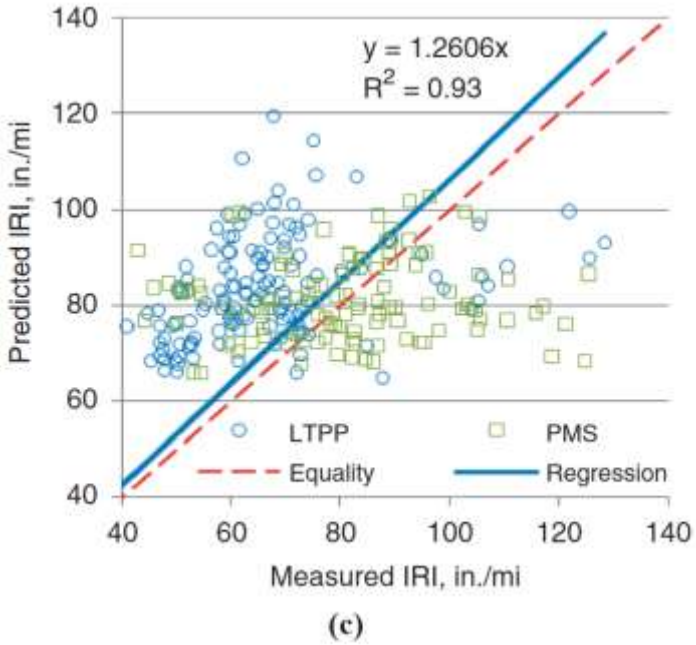

Figure 3.8: Verification of national calibrated model (c) IRI (Hall et al., 2011)

Predictive distresses did not match well with measured distresses, particularly for longitudinal and transverse cracking. Furthermore, alligator cracking and longitudinal cracking predicted by MEPDG are forms of fatigue cracking. Transfer functions predict visual cracking from mechanistic damage at the bottom and top of HMA layers.

Thus, HMA layer thickness has a highly significant effect on performance predictions. In this research, because of the nature of the data, longitudinal cracking and transverse cracking models were not calibrated. In addition, the smoothness model (IRI) was not calibrated because the predicted IRI is a function of other predicted distresses. The solver function in Microsoft Excel was used to optimize the coefficients in the alligator cracking model (Hall et al., 2011).

Hall et al. (2011) summarized the initial local calibration of flexible pavement models in the MEPDG for Arkansas. The following conclusions were drawn from this study:

The procedure for local calibration of the MEPDG by using LTPP and PMS data in Arkansas was established. Overall, alligator cracking and rutting models were improved by local calibration. However, more sites and data collection are recommended before implementing the MEPDG in Arkansas. The availability and quality of design, materials, construction, and performance data are critical for local calibration. States like Arkansas will likely need additional calibration sites to supplement available LTPP and PMS data (Hall et al., 2011).

3.5 Fundamental Outputs of Mechanistic-Empirical Pavement Design

The mechanistic component of the M-E design evaluates one or more responses in the pavement structure as a function of material characteristics, layer thickness, and loading conditions. The empirical component of the M-E design is connecting pavement response(s) to observed performance, namely smoothness deterioration, fatigue crack development, and rutting development (Haas et al., 2007b). The mechanistic approach establishes the structural responses of a pavement system, such as stresses, strains, and deflections, resulting from road traffic (Stubbs, 2011). Vertical compressive strain (z) at the subgrade layer's top and horizontal tensile strain (t) at the asphalt layer's bottom are the primary factors that contribute to fatigue and rutting failures, respectively (Brown, 1996). Empirical transfer functions derived from the structural responses are correlated to the performance of the pavement. Unlike conventional empirical pavement design approaches, it considers the effects of traffic, material characteristics, and environmental variables on the structural responses of the pavement. Furthermore, it provides a more rational way to characterize pavement

structures and associated factors. (Stubbs, 2011). Figure 2.9 illustrates fundamental pavement responses as a function of load, material properties, and layer thicknesses.

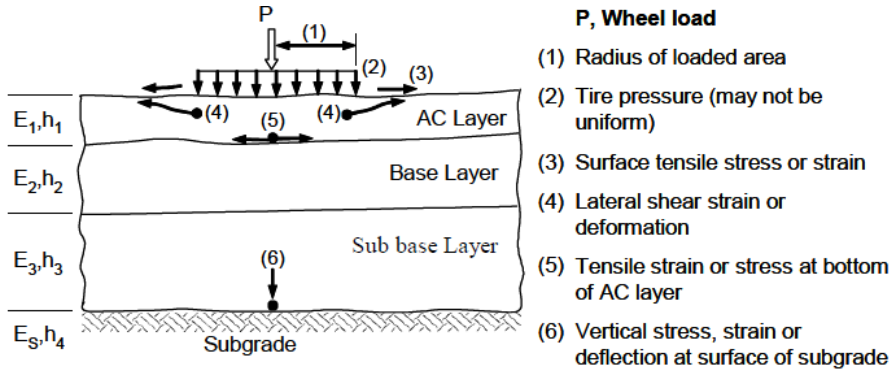

Figure 3.9: Fundamental Pavement Responses as a Function of Load, Material Properties, and Layer Thicknesses (Mechanistic part) (Haas et al., 2007b).

Figure 2.10 illustrates the pavement performance to which mechanistic response(s) must be related / correlated (empirical part).

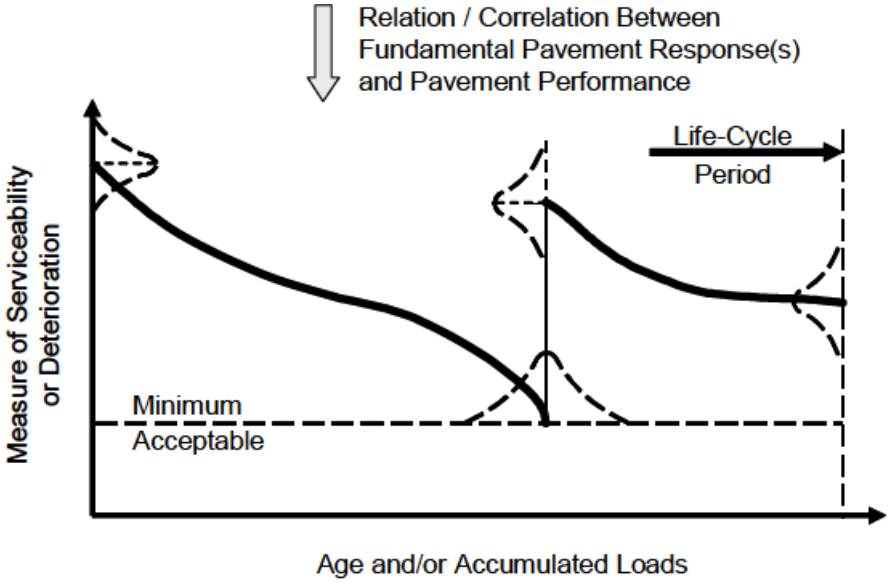

Figure 3.10: Pavement Performance to Which Mechanistic Response(s) Must be Related / Correlated (Empirical Part) (Haas et al., 2007b).

M-E procedures typically comprise several steps. Firstly, critical responses causing distress are identified. Next, the pavement layers' critical responses (stresses, strains, and deflections) are determined. Subsequently, these critical responses are empirically

related to distress. Moreover, it can be identified that various models are available for each distinct distress and each pavement type. These models are referred to as 'performance models.' Ultimately, the pavement section, which is at an acceptable level of distress at the end of the design life, is chosen (Chou & Lytton, 1991). In establishing the thickness of pavement layers, the intention was to render a minimum thickness of overlaying material that would lessen the unit stress on the succeeding lower layer, commensurate with the material's load-carrying capacity.

The thicknesses of the pavement layers should be verified by fulfilling the following specifications.

i. Select pavement thickness to restrain the vertical compressive strains on the top of the subgrade layer.
ii. Select pavement thickness to restrain the horizontal tensile strains on the bottom of the Asphalt layer.

3.6 Distress Modes for Flexible pavements

Finn et al. (1977) defined the terms damage and distress as follows:

i. "Damage is the effect of a single, repetitive load application contributing to cracking or rutting."
ii. "Distress is the cumulative effect of damage, resulting in a detectable and quantifiable level of cracking or rutting."

"Pavement distress, referred to as pavement failure, is defined as any indication of a crack or fracture in the pavement layer and an indicator of substandard or unacceptable pavement performance" (Erlingsson, 2013). Distress in flexible pavements has been challenging in many countries as road traffic and vehicle loads have increased (Elnashar et al., 2019). The serviceability of a pavement system reduces with increasing pavement distresses due to the expansion of various distresses. Besides, several agencies have devised several definitions for failures in pavements. AASHTO (1993) defines failure as "when 20% of the pavement surface is cracked". Austroads (2012) describes failure as "when the flexural stiffness approaches 50% of the initial value measured at 50 cycles or reached one million cycles".

Austroads (2010) has identified the following distress modes in flexible pavements depicted in Table 3.1. Table 3.1 is also inclusive of reasons for such distress types.

Table 3.1: Major distress types and reasons for distresses (Austroads, 2010)

Distress	Traffic Associated / Non–Traffic Associated	Reasons
Rutting	Traffic Associated	Densification
Cracking	Traffic Associated	Single or low repetitions of high load
		Many repetitions of normal loads
	Non-Traffic Associated	Swelling of subgrade materials
		Reflection of shrinkage cracks from underlying materials
		Thermal cycling
Roughness		Variability of density
		Material properties

Fatigue cracking is one of the most significant distress mechanisms to consider when designing pavements. While considerable progress has been made in past years in assessing fatigue performance and the design process for flexible pavements, future research should attempt to overcome the difficulty of forecasting fatigue cracking in terms of damage distribution when pavement life and traffic repetitions are unknown (Elnashar et al., 2019).

3.7 Asphalt Fatigue Cracking and Asphalt Fatigue Models

3.7.1 Distresses in Asphalt Pavements

Asphalt is a mixture of bituminous binder and numerous, often uniform-sized aggregate fractions spread and compacted while hot to form a pavement layer (Khattak & Baladi, 2013). Asphalt concrete is a commonly used form of pavement due to its high stability, durability, and resistance to water damage (Moghaddam et al., 2011). Asphalt mixtures are typically viscoelastic; their stress and strain response are time-rate-temperature dependent. Asphalt pavements usually have multiple layers, including asphalt concrete, base, subbase and subgrade.

The strength/modulus of asphalt is derived from the following:

i. The friction between the aggregate particles
ii. The viscosity of the bituminous binder under operating conditions

iii. The cohesion within the mass resulting from the binder itself.
iv. The adhesion between the binder and the aggregate (Austroads, 2017)

The most likely causes of asphalt layer distress on moderate-to-heavy-trafficked pavements are as follows:

i. Rutting and shoving due to insufficient resistance to permanent deformation
ii. Cracking due to fatigue
iii. Durability (oxidation) leads to top-down cracking (Austroads, 2017)

Fatigue and rutting are the most common types of pavement distress, resulting in shorter pavement life, maintenance, and road user costs. They are primarily caused by more vehicles, particularly those with high axle loads, adverse environmental conditions, and construction and design faults. As a result, the service life of asphalt pavement is reduced (Moghaddam et al., 2011). Figure 2.11 shows fatigue cracking in flexible pavements.

Figure 3.11: Fatigue cracking in flexible pavements

Typically, fatigue cracks begin towards the bottom of the HMA layer, where the tensile stress and strain are maximum. Cracks propagate to the surface due to the increasing amount of load applications. They occur as one or more longitudinal fractures joined by transverse cracking to create an alligator hide-like pattern (Khattak & Baladi, 2013). Identifying strategies to delay the deterioration of asphalt pavements and extend their service life is critical. Numerous studies have been undertaken to improve the properties of road pavements to give a more comfortable ride and ensure greater

durability and service life in light of climatic change and traffic loading (Moghaddam et al., 2011).

3.7.2 The Fatigue Life of Asphalt

Defining fatigue life (the number of loading cycles required to cause failure) is challenging, particularly in the controlled-strain mode. Among numerous options, (Hicks et al., 1993), (Williams, 1998), and (Smith & Hesp, 2000) considered a 50% drop in stiffness or modulus relative to the initial value (Xiao, 2006). It is critical to predict the fatigue life of hot mix asphalt mixes (HMA) while designing pavements (TB Moghaddam et al., 2011). Numerous factors contribute to the fatigue life of HMA pavements, including the asphalt binder's tensile strength, traffic volume, construction practices, aggregate angularity and gradation, the AC's relative stiffness, the base material, and environmental conditions such as temperature and moisture (Khattak & Baladi, 2013). Specific adverse effects are possible due to the high volume of vehicles imposing repetitively high axle loads on roads, environmental conditions, and structural defects. These typically result in permanent deformation (rutting), fatigue, and low-temperature cracking, reducing the road pavement's service life (Sengoz & Topal, 2005).

In basic terms, the factors affecting the fatigue life of asphalt are as follows:

i. The supporting (modulus) is given by the underlying road structure to the asphalt.
ii. The asphalt layer's contribution to the overall stiffness of the roadway
iii. The modulus of the asphalt and its variation with temperature
iv. The type of binder used in the mixture.
v. The traffic loading spectrum
vi. The ambient temperature in which the asphalt is functioning.

Only the latter three are unaffected by other variables (Austroads, 2017)

3.8 Fatigue life prediction for flexible pavements

Asphalt mixes' fatigue resistance is commonly described as their capacity to withstand repeated traffic loading under the existing environmental conditions without

substantial cracking or premature failure. Asphalt pavements' fatigue cracking resistance depends on the thickness of the pavement layers, the mix volumetrics, the mixture type, and the pavement structure. Thus, the capacity to evaluate and model an asphalt binder's inherent fatigue performance is a vital first step toward developing mixtures and pavements resistant to premature fatigue failure. The fatigue cracking resistance of asphalt pavement is determined by the structure (layer thickness), the type and volumetrics of the mixture, and the asphalt binder's intrinsic fatigue cracking resistance (Safaei et al., 2016). It is critical to assess the fatigue characteristics of certain mixtures under a diverse array of traffic and climatic circumstances when designing asphalt concrete pavements such that fatigue considerations may be integrated into the design process.

A model for fatigue life prediction can be established based on an accurate characterization of fatigue failure. There are two distinct approaches: phenomenological and mechanistic. The phenomenological fatigue model is simple to apply but does not consider damage progression during the fatigue mechanism. Mechanistic models are based on fracture or damage mechanics. Although this approach is intrinsically more sophisticated than the phenomenological approach, it is more frequently accepted since it is based on the stress-strain relationship (Kim et al., 2003).

Numerous recent studies have been conducted to model and forecast fatigue cracking. Performance models can be characterized as deterministic or probabilistic based on their predicted results. There are three types of deterministic models: mechanistic, empirical, and mechanistic-empirical (M–E). (Ferreira et al., 2011; Lytton, 1987). Mechanistic models are based on mechanics theories. The stresses and strains in a pavement layer could be computed using basic assumptions and simplifications such as isotropic, linear-elastic, homogenous material, minor strain, and static loading. Due to the simplicity of such models and their ability to correctly define the general responsive behavior of the pavement, they are counterproductive at determining pavement deterioration given the high nonlinearity of the behavior of pavement materials that are not only anisotropic but also dependent on time, temperature, and other parameters (Schwartz & Carvalho, 2007).

Experimental data and statistical approaches are used to develop empirical models. They are incorporated to overcome the constraints of the mechanistic approach's simplified theoretical models. The empirical models relate pavement distress to traffic loadings and deflection and calculate the load repetitions required to cause pavement failure. One main drawback of empirical models is that they are empirical and were established for certain pavement areas. As a result, they cannot be applied directly to different pavement sections. In other words, they are restricted to a specific area of the section (Ferreira et al., 2011; Li, 2005; Lytton, 1987).

3.9 Mechanistic approach for fatigue life prediction of Asphalt

Asphalt fatigue properties are a critical structural design parameter. The mechanistic design approach assumes tensile strain at the base of the asphalt layer to reduce fatigue cracking. One of the primary goals of the mechanistic approach to pavement design is to minimize horizontal tensile strain and fatigue cracking in the asphalt layers. Mechanistic pavement design techniques require extensive laboratory material characterization under actual loading conditions (traffic speeds, rest durations amid traffic stresses, and multi-axle loading) (temperature, healing, ageing). The laboratory characterization of asphalt suited to local conditions and the performance relationships established from laboratory data are critical for developing field performance prediction models. The number of cycles of a standard axle loading necessary to induce substantial fatigue cracking in-service is commonly acknowledged to be much greater than the number of cycles to failure (as defined by the number of cycles required to reduce the flexural stiffness of an asphalt mix to half its initial value) in a laboratory fatigue test (Finn et al., 1977). This variance between laboratory and in-service fatigue lives is due to changes in loading conditions, such as vehicle types and axle configurations, rest periods between vehicle loads (effects of residual stresses and healing), traffic distribution (mixed traffic effect), vehicle wander, and mix compaction levels achieved, as well as environmental factors such as seasonal temperature variations and temperature gradients in the pavement.

The variations in the pavement fatigue lifetimes of laboratory-measured and in-service conditions (cracking in the wheel path) have been linked to changes in the following:

i. Loading conditions including vehicle type and axle configurations, rest periods between vehicle loads, and vehicle wandering in the wheel paths.
ii. Environmental factors.
iii. Ageing and micro-damage healing in the asphalt pavement.
iv. Crack propagation mechanism; and
v. Asphalt compaction and properties.

These differences between laboratory and field conditions require using a “shift factor" to predict field fatigue life from the laboratory-measured or predicted life. Consequently, several asphalt fatigue performance relationships have been developed. However, the relationships were developed for local conditions, considering the environment, climate, traffic, pavement materials, and pavement configurations. Further, these relationships were derived from assessing asphalt mixes using laboratory fatigue tests specific to the specific test methods, conditions, and equipment; additional variability can be introduced if these relationships are applied to other conditions (Baburamani, 1999). The existing fatigue life prediction models established by the Asphalt Institute, Shell, and SHRP scientists are based on laboratory fatigue relationships obtained in controlled stress or strain loading of asphalt beams in flexure. These models are acceptable only in the spectrum of mix types (mainly asphalt mixes with conventional binders), volumetric compositions and loading conditions investigated, and the extent to which field validation was conducted. Any divergence from these values may lead to a different prediction of life. Tensile strain and the stiffness of the asphalt mix are the two primary variables affecting fatigue life. The exponents employed in the prediction formulas for these variables vary according to the laboratory test method, loading conditions employed, and the asphalt mixtures assessed.

3.9.1 Mechanistic-Empirical models for fatigue damage in Asphalt

M–E models integrate mechanistic and empirical techniques into a single general model to capitalize on each model's strengths and overcome some of the models' flaws when used separately (Li, 2005). M- E models determine the strains induced at critical locations by the vehicle's single-wheel load. Consequently, the pavement life can be

estimated using the empirical fatigue model. (Ferreira et al., 2011; Li, 2005; Lytton, 1987).

Mechanistic pavement design aims to maintain distress and damage to the pavement within specified tolerances. As a result, M-E pavement design methodologies rely heavily on response and performance prediction models (Ahmed & Erlingsson, 2015). The following aspects are included in the establishment of pavement damage prediction models.

1. Laboratory assessment of material properties
2. Investigation of the structural response of pavement layers
3. Establishment of performance criteria and models for predicting distress (Finn et al., 1977)

The fatigue properties of asphalt mixes are commonly described as a relationship between the initial stress or strain and the number of load repetitions required to fail. These relationships are ascertained through repeated flexure, direct tension, or diametral tests conducted at various stress or strain levels. The fatigue behavior of a particular mixture can be characterized by the slope and relative stress level or strain level vs the number of load repetitions required to fail (Monismith et al., 1985). Equation 3.2 presents the equation for number of load applications to failure.

$$N_f = A\left(\frac{1}{\epsilon_t}\right)^b \left(\frac{1}{S_{mix}}\right)^c$$ ----------*Equation 3.2*

N_f = number of load applications to failure

ϵ_t = tensile strain

S_{mix} = mixture stiffness

A, b, c = experimentally determined coefficients

Numerous models were proposed to predict the fatigue life of pavements based on laboratory test results provided in equation 3.2 (Claessen et al., 1977; Finn et al., 1977; Shook, 1982). In the modern era, mechanistic-Empirical (M-E) pavement design requires complete, digitalized packages. This condition, nevertheless, introduces significant calibration and validation issues, selecting appropriate input values and resource needs for implementation and striking a balance between complexity and

comprehensiveness and comprehensibility and practicality (Haas et al., 2007a). Table 3.2 summarizes numerous researchers' and agencies' computer-based analytical solutions for asphalt concrete pavements.

Table 3.2: Summary of Some Computer-Based Analytical Solutions for Asphalt Concrete Pavements (Haas et al., 2007a)

Program and Ref.	Theoretical Basis	No. Layers (max)	No. of Loads (max)	Program Source	Remarks
BISAR (De Jong, 1979)	MLE	5	10	Shell International	The program BISTRO was a forerunner of this program.
CIRCLY (Wardle, 1977)	MLE	5+	100	MINCAD, Australia	Includes provisions for horizontal loads and frictionless as well as full-friction interfaces
ELSYM (Ahlborn, 1972)	MLE	5	10	FHWA (UCB)	Widely used MLE analysis Program
FENLAP (Brunton & De Almeida, 1992)	FE		1	University of Nottingham	It was specifically developed to accommodate non-linear resilient materials properties.
ILLIPAVE (Thompson & Elliott, 1985)	FE		1	University of Illinois	
PDMAP (PSAD) (Finn et al., 1977)	MLE	5	2	NCHRP Project 1-10	Includes provisions for iteration to reflect non-linear response in untreated aggregate layers
SAPSI-M (Chatti & Yun, 1996)	Layered, damped elastic medium	N layers resting on elastic half-space or rigid base	Multiple	Michigan State Univ./Univ. of California Berkeley	Complex response method of transient analysis-continuum solution in the horizontal direction and finite element solution in the vertical direction
VEROAD (Nilsson et al., 1996)	MLVE	15 (resulting in half-space)		Delft Technical University	Viscoelastic response in shear; elastic response for volume changes

MLE – multilayer elastic
MLVE – multilayer viscoelastic
FE – finite element

However, implementing the ME procedures has many challenges, including the enormous amount of traffic and climatic data needed, the advanced characterization of the pavement materials, and the calibration and validation of the local conditions. Accordingly, an increased required time to develop and evaluate the design is warranted. Furthermore, lacking experience with the ME pavement design approaches is considered an additional challenge.

Recent research by (Jayarathna & Mampearachchi, 2017) concluded that the mechanistic design software- CIRCLY, based on the AUSTROADS mechanistic pavement design guideline, can be used as an effective mechanistic tool for the design and analysis of flexible pavements in tropical climates like Sri Lanka. So, it can be justified that the use of mechanistic design software – CIRCLY for the design and analysis of flexible pavements is highly effective compared to other mechanistic design software available, given that mechanistic design software – CIRCLY is already validated to be used for the design and analysis of roads in tropical climates as in Sri Lanka. Using mechanistic design software – CIRCLY is a straightforward methodology to accommodate AUSTROADS pavement design guidelines as integrated with Austroads mechanistic pavement design guidelines. Furthermore, the Austroads flexible pavement design method utilizes CIRCLY to compute load-induced elastic stresses, strains and deflections in model pavements (Wardle, 2010).

This situation proves that the Austroads mechanistic design method can be adopted to design and analyze flexible pavements in tropical climates like Sri Lanka.

3.10 Asphalt Fatigue Criteria in Austroads Pavement Design Guide

For conventional bituminous binders used in asphalt placed on moderate-to-heavily trafficked pavements, the general relationship between the maximum tensile strain in asphalt produced by a specific load and the allowable number of repetitions of that load is given by Equation 3.3.

$$N = \frac{SF}{RF}\left[\frac{6918(0.856V_b + 1.08)}{E^{0.36}\mu\varepsilon}\right]^5 \quad \text{----------Equation 1.3}$$

N = allowable number of repetitions of the load-induced tensile strain

με = load-induced tensile strain at the base of the asphalt (micro-strain)

V_b = percentage by volume of bitumen in the asphalt (%)

E = asphalt modulus (MPa)

SF = shift factor between laboratory and in-service fatigue lives (presumptive value = 6)

RF = reliability factor for asphalt fatigue

Reliability factors are transfer functions that link the mean fatigue life in the laboratory to the fatigue life in service. The Austroads guide's guidelines should determine the desired level of project reliability. Table 3.3 summarizes the reliability factors recommended for various reliability levels as the Austroads design guide specified.

Table 3.3: Reliability factors for different project reliability (Austroads, 2010)

Desired project reliability				
80%	85%	90%	95%	97.5%
2.5	2.0	1.5	1.0	0.67

3.10.1 Fatigue Criteria for Cement treated Materials in Austroads Pavement Design Guide

The in-service fatigue relationship for cement treated materials is of the following general form as in the Equation 3.4.

$$N = RF\left(\frac{K}{\mu\varepsilon}\right)^{12} \text{----------Equation 3.4}$$

N = Allowable number of repetitions of the induced load-induced tensile strain

με = Load-induced tensile strain at the base of the cemented material (micro strain)

K = a constant, calculated by multiplying the laboratory fatigue constant k by the laboratory-to-field tolerable strain shift factor (SF), 1.55 is the presumptive SF value

ϵ = Horizontal tensile strain on the underside of the cement-treated layer

3.11 Subgrade Rutting

Rutting is the principal mode of distress in flexible pavements, caused by repeated traffic loading movement. Pavement deformation comprises recoverable (elastic) and irrecoverable (plastic) components. All pavement components contribute to the overall deformation of the flexible pavement system due to continuous vehicular movement. Permanent deformation of granular material – rutting and shoving, particularly along the outer wheel path along the pavement shoulder – occurs due to inadequate stability to withstand the existing loading and environmental conditions (Austroads, 2017). Figure 3.12 illustrates the definition of recoverable strain and soil resilient modulus.

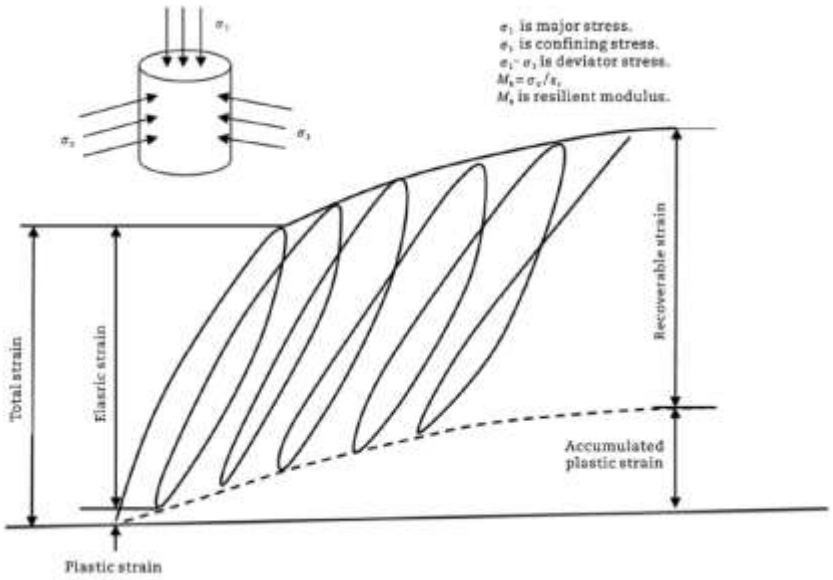

Figure 3.12: Definition of recoverable strain and soil resilient modulus (Huang, 1993)

Rutting can be reduced by.

i. Limiting the vertical compressive strain on top of the subgrade
ii. Limiting the total accumulated permanent deformation on the pavement surface

Rutting or permanent deformation is regarded as a prominent distress mechanism in flexible pavements, depending on the permanent deformation characteristics of each layer. Thus, a thorough understanding of the phenomenon is required to avoid severe rutting during the pavement's life. Excessive loads, repeated traffic loadings, soil volume changes, compressive material beneath the pavement system, and frost-

sensitive pavement geomaterials are only a few causes of pavement rutting. Over the last few decades, work has contributed to developing empirical models for calculating the rut depth formed in pavement systems with different structure compositions and environmental conditions.

3.12 Subgrade Permanent Deformation (Rutting) Models

Numerous investigators have developed empirical models for assessing and forecasting rutting accumulation in various pavement elements. The accumulated permanent strain has been presented as a function of the number of load and deviator stress applications in the majority of proposed models; nevertheless, factors including stress state, moisture content, material type, and environmental conditions all have a significant impact on the permanent deformation characteristics of pavement materials under cyclic loading (Singh & Sahoo, 2021). Current empirical design methods for flexible pavements prevent rutting by limiting vertical strain at the top of the subgrade (Claessen et al., 1977; Shook, 1982). The Asphalt Institute, Shell Design (Shell International Petroleum Company, 1978), and several other organizations have developed an equation to determine the maximum number of load repetitions (N_d) to limit rutting using vertical compressive strain (ϵ_c) on the top of the subgrade. Equation 3.5 represents the fundamental rutting model (Jayarathna & Mampearachchi, 2017)

$$\boldsymbol{N_d = f_4(\in_c)^{f_5}} \quad \text{----------}\textit{Equation 3.5}$$

Constant values for f_4 and f_5, which several agencies introduced, can be shown in Table 3.4.

Table 3.4: f_4 and f_5, introduced by different agencies (Jayarathna & Mampearachchi, 2017)

Agency	f_4	f_5	Rut depth (inches)
Asphalt Institute	1.365 × 10-9	4.477	0.5
Shell (revised 1985) 50% reliability 85% reliability 95% reliability	 6.15×10^{-7} 1.94×10^{-7} 1.05×10^{-7}	 4.0 4.0 4.0	
U.K. Transport & Road Research Laboratory (85% reliability)	6.18 × 10-8	3.95	0.4
Belgian Road Research Centre	3.05×10^{-9}	4.35	Belgian Road Research Centre

3.13 Limiting Subgrade Criteria in Austroads Pavement Design Guide

Interestingly, the vertical compressive strain at the subgrade's top is crucial in evaluating the severity of surface rutting in the pavement structure's unbound components. Monismith et al. (1988) express the rationale for using subgrade strain to measure surface rutting. The intensity of the plastic strain is proportional to the magnitude of the (vertical) elastic strain in paving materials. The elastic strain increases from the subgrade to the surface in a road structure. Accordingly, by setting the elastic strain at the subgrade surface at a specific value, the elastic strain in the components above this plane is controlled, as are the values for the associated plastic strains. Incorporating the plastic strains across the pavement section yields information about the pavement's permanent deformation (rut depth).

The limiting strain criterion for the subgrade is given in Equation 3.6.

$$\boldsymbol{N = \left(\frac{9150}{\mu\varepsilon}\right)^{7}} \quad \text{----------}\textit{Equation 3.6}$$

N = the allowable number of repetitions of a Standard Axle at this strain before an unacceptable level of pavement surface deformation develops (units of ESAs)

$\mu\boldsymbol{\varepsilon}$ = the vertical compressive strain (in terms of micro strain), developed under a Standard Axle at the top of the subgrade

By incorporating this relationship into the mechanistic-empirical approach, designs that are typically compatible with the observed performance of roadways across Australia in terms of pavement surface deformation development will be generated. Nevertheless, it should be used with extreme caution when building pavements that carry significantly different loads to roadways (Austroads, 2017).

3.14 Pavement Design and Analysis Using Austroads Mechanistic Pavement Design Guide

3.14.1 Mechanistic-Empirical Procedure by Austroads pavement design guide

The mechanistic-empirical technique enables the designer to produce various pavement types to support a variety of loading conditions and configurations. The design procedure's fundamental premise was to choose pavement thickness limiting vertical (compressive) strains in the subgrade and horizontal (tensile) strains at the bottom of the bituminous concrete caused by design vehicular traffic loads at selected levels. The techniques outlined in this chapter apply to moderately to heavily traffic pavements.

The summary of the design procedure can be shown as follows.

i. Evaluating the input parameters (material properties, traffic parameters, and environmental conditions)
ii. Selecting a trial pavement
iii. Analyzing the trial pavement to determine the allowable traffic.
iv. Comparing the allowable traffic with the design traffic
v. Accepting or rejecting the trial pavement

The appropriate design inputs are.

i. Desired Project Reliability
ii. Construction and Maintenance Policy Influences
iii. Environment
iv. Subgrade
v. Materials and Performance Criteria
vi. Design Traffic Loading

The design procedure is based on the structural analysis of a multi-layered pavement subjected to normal road traffic loading.

3.15 Pavement model for mechanistic-empirical procedure

The critical locations of the strains within a pavement model – and the idealized loading situations are shown in Figure 2.13.

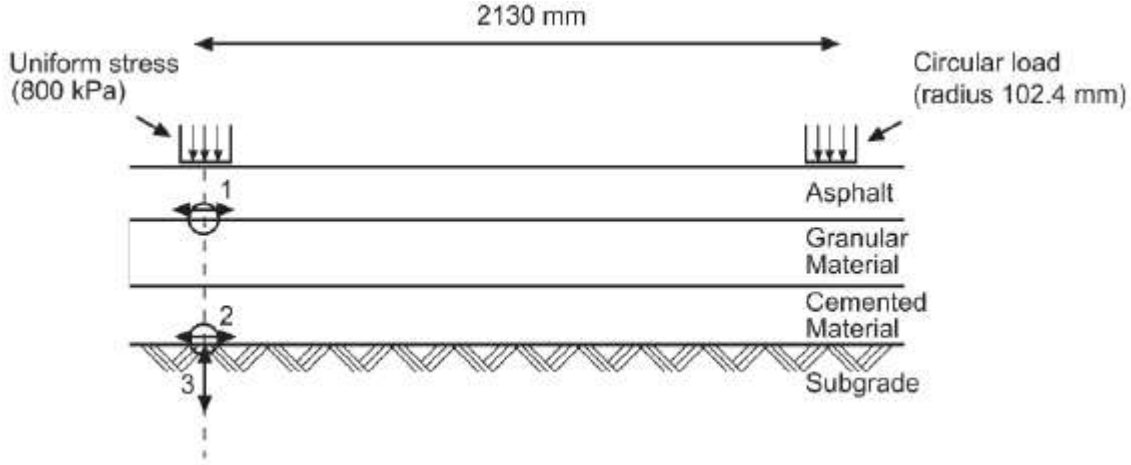

Figure 3.13: Axle with single tires (Austroads, 2017)

Calculations of critical strains are made using the multilayer elastic theory. These critical strains are then utilized to calculate the maximum number of axle repetitions applied to the pavement before the critical layer fails. This is accomplished using experimentally derived performance models (Jayarathna & Mampearachchi, 2017).

3.16 Estimation of Design Traffic in Austroads pavement design guide

The pavement design is based on the proposition that it will provide good service for the cumulative traffic anticipated over a specific time frame - the design period. Serviceability implies the road will not require considerable restoration over the design lifetime (Austroads, 2012).

The damage caused by a heavy vehicle depends on the gross weight and how the weight is distributed.

It depends on the following:

i. The number of axles on the vehicle
ii. How these axles are grouped – into axle groups

iii. The loading is applied to the pavement through each axle group – the axle group load.

The design traffic for flexible pavement design is defined in the Austroads pavement design approach as "the total number of Standard Axle Repetitions (SAR) during the design period, which causes damage similar to that caused by cumulative traffic". The Austroads guide notes that light cars make a negligible contribution to road defects. As a result, design traffic only accounts for heavy vehicles. When adjacent axles are shorter than 2.1 meters apart, the Axle group is considered. Considering this circumstance, all potential axle configurations are classified into six types.

i. Single Axle with Single Tires (SAST)
ii. Single Axle with Dual Tires (SADT)
iii. Tandem Axle with Single Tires (TAST)
iv. Tandem Axle with Dual Tires (TADT)
v. Triaxle with Dual Tires (TRDT)
vi. Quad Axle with Dual Tires (QADT)

All tires specified are standard tires.

Cumulative pavement loading over time is essentially a record of each axle group traversing the pavement over this period, together with its type and load. This cumulative loading is defined as follows:

i. The cumulative number of axle groups traversing the pavement during the period.
ii. The proportions of each axle group type in this total
iii. The frequency distribution of the axle group loads for each axle group type.

The procedure of determining the design traffic in Austroads is sequenced as follows.

i. Select a design period.
ii. Identify the most heavily trafficked lane in the carriageway.
iii. Estimate the average daily number of heavy vehicles in the design lane during the first year of the project's life (Average Annual Daily Traffic - AADT)

iv. Calculate the percentage of heavy vehicles (%HV) in the traffic stream.
v. Determine the Lane Distribution Factor (LDF)
vi. Estimate heavy traffic growth throughout the design period (Cumulative Growth Factor - CGF)
vii. Estimate the average number of axle groups per heavy vehicle (NHVAGs)
viii. Calculate the cumulative heavy vehicle axle groups over the design period.
ix. Estimate the proportion of axle group types and the distribution of axle group loads.
x. Calculate ESA per axle group and SAR per ESA
xi. Calculate design ESA and design SARs for each distress type (Austroads, 2017)

3.17 Determining Cumulative Heavy Vehicle Axle Groups (HVAG)

The primary consideration of a pavement design is that it should be sufficient for the cumulative traffic loads predicted in the design lane over the design period. This loading involves determining the cumulative number of heavy vehicle axle groups (HVAG) and Design Traffic (NDT) over the design period. It is critical to remember that the N_{DT} applies to flexible and rigid pavements and that further calculations are required to determine standard axles of loading for flexible pavements.

3.17.1 Selection of Design Period

The design period adopted by the pavement designer is the amount of time deemed adequate for the road to operate without requiring substantial rehabilitation or reconstruction. It is a critical parameter in the overall process of pavement management. Along with its direct involvement in estimating design traffic for the pavement design process, it also serves as the foundation for expectations regarding the performance of the built pavement. Additionally, it serves as a basis for long-term network-wide programming of future substantial rehabilitation or reconstruction projects. Generally, the design period for a particular pavement type falls in the range specified in Table 3.5. It must be emphasized that while a road is supposed to offer excellent services during a defined design period, this performance can be anticipated if actual cumulative traffic does not exceed the estimated cumulative traffic throughout

the period. Thus, the reasonable duration of satisfactory service is determined by the design traffic value, not the design period value.

Table 3.5: Typical pavement design periods (Austroads, 2010)

Pavement Type	Typical Design Period
Flexible pavements	20–40 years
Rigid pavements	30–40 years

3.17.2 Identification of Design Lane

The design lane is readily identifiable as the more heavily trafficked lane for a two-way roadway (one lane in each direction).

The design lane is always left (or outermost) on multi-lane single-direction highways. Calculations of traffic loading for this type of roadway are generally offered for this whole road, with no lane-specific data. Weigh-in-motion (WIM) technologies provide lane-specific data on the loading of heavy vehicles on a highway. Without project-specific data, Table 3.6 guides the proportion of heavy vehicle traffic loading given to the design lane. The percentage of vehicles allotted to a specific lane is the lane distribution factor (LDF).

Table 3.6: Lane Distribution Factors (LDF) *(Austroads, 2010)*

Location	Lanes each direction	Lane distribution factor (LDF)		
		Left lane	Centre lane	Right lane
Rural	Two-lane	1.00[(1)]	N/A	0.50
	Three lanes	0.95	0.65	0.30
Urban	Two-lane	1.00[(1)]	N/A	0.50
	Three lanes	0.65	0.65	0.50

[1] This value is the suggested limit for a lane, and it may be reduced if sufficient traffic survey data indicates that a lower LDF is appropriate.

3.17.3 Initial Daily Heavy Vehicles in the Design Lane

an assessment of the average daily number of heavy vehicles in the design lane during the first year of operation (of the project) is required to calculate the cumulative HVAG

in the design lane. This year-long averaging ensures that the forecast is unaffected by daily (or, more typically, seasonally) fluctuations in daily traffic loadings.

The equation (Equation 3.7) to derive the initial daily heavy vehicles (N_i) traversing the design lane is as follows.

$$\boldsymbol{N_i = AADT \times DF \times \frac{\%\,HV}{100} \times LDF} \text{ ----------Equation 3.7}$$

N_i = initial daily heavy vehicles in the design lane

AADT = Average Annual Daily Traffic 2 in vehicles per day in the first year

DF = direction factor is the proportion of the two-way AADT travelling in the direction of the design lane

%HV = average percentage of heavy vehicles

LDF = lane distribution factor, the proportion of heavy vehicles in the design lane

The designer is reminded of the crucial significance of ensuring that the data used in this assessment work appropriately represents traffic loads for the year the project is open. Improvements may be challenging to facilitate seasonal traffic variations, such as those associated with transporting harvested vegetables. Extra caution is advised when heavy traffic loads are concentrated over a brief period, as the typical pavement performance models employed in this section may not be appropriate.

3.17.4 Cumulative Number of Heavy Vehicles when Below Capacity

Estimating cumulative traffic in the design lane over the design period requires an assessment of the probable daily traffic loading variations throughout this time. Once the impacts of these variations are determined, they are integrated into the calculation of cumulative loading. This section covers the growth in traffic volumes. Assume that the project involves realignment, reconstruction, or overlay in this scenario; it is fair to estimate traffic volume growth using historical data for the existing pavement. Based on historical information, it is appropriate to anticipate an increase in daily traffic volume (including light and heavy vehicles) for the design period or until the road's traffic capacity is reached. Additionally, this finding illustrates that the growth

is geometric because it can be represented using conventional compound growth formulae.

The compound growth of traffic volumes is usually and conveniently specified as a percentage increase in annual traffic volumes – a typical statement being 'the annual growth rate is R%.' Adopting this specification of growth and with compound growth occurring throughout the design period, the cumulative growth factor (CGF), when constant, over the design period, is readily calculated as in Equation 3.8.

$$\boldsymbol{CGF = \frac{(1+0.01R)^{P}-1}{0.01R}\ for\ R > 0} \text{ ----------Equation 3.8}$$

$$P\ for\ R = 0$$

CGF = cumulative growth factor

R = annual growth rate (%)

P = design period (years)

In the case of below-capacity traffic volumes throughout the design period, the equation (Equation 3.9) to derive the Design Traffic (N_{HV}) – in cumulative heavy vehicles – traversing the design lane during the specified period is.

$$\boldsymbol{N_{HV} = 365 \times CGF \times N_i} \text{ ----------Equation 3.9}$$

N_{HV} = design traffic in cumulative heavy vehicles

CGF = cumulative growth factor

N_i = average daily number of heavy vehicles in the first year of opening to traffic

The cumulative number of heavy vehicles estimated using the abovementioned techniques is premised on the idea that the design lane operates at or below capacity for the entire design period. For projects where the cumulative number of heavy vehicles predicted using the methodologies mentioned above surpasses 10^7, it is recommended that an evaluation be carried out in compliance with section 7.4.6 of the Austroads guide (Austroads, 2017) concerning the issue of whether the number of heavy vehicles has surpassed capacity before the completion of the design life. If capacity is attained, Section 7.4.6 specifies how to estimate the cumulative number of heavy vehicles by limiting annual heavy vehicle loading.

3.17.5 Determining Cumulative Heavy Vehicle Axle Groups

The average number of axle groups per heavy vehicle (N_{HVAG}) is required to calculate the cumulative heavy vehicle axle groups in the design lane over the design period (N_{DT}) can be calculated as given in Equation 3.10.

$$\boldsymbol{N_{DT} = N_{HV} \times N_{HVAG}} \text{ ----------} \textit{Equation 3.10}$$

N_{DT} = the cumulative heavy vehicle axle groups in the design lane over the design period

N_{HV} = cumulative number of heavy vehicles

N_{HVAG} = average number of axle groups per heavy vehicle

3.18 Estimation of Traffic Load Distribution (TLD)

Along with the total HVAG, the project's traffic load distribution (TLD) is necessary to compute the design traffic loading.

The TLD contains data important for determining the extent of pavement damage produced by the HVAG, particularly:

1. The proportions of all axle groups that are a particular axle group type.
2. The proportion of axles applied at each load magnitude for each axle group type.

3.19 Damage to Flexible Pavements

"Design traffic loading" refers to the number of Equivalent Standard Axles (ESA). For the mechanistic-empirical design of pavements comprising bound materials, the cumulative HVAG and the traffic load distribution (TLD) are needed to define the Design Traffic when considering fatigue damage to asphalt, cement materials and lean-mix concrete.

3.20 Pavement Damage in Terms of Equivalent Standard Axle Repetitions

The Standard Axle is a single axle with dual tires (SADT) applying a load of 80 kN to the pavement. The loads on axle configurations that are considered to cause the same damage (i.e., overall pavement damage when using the empirical procedure and rutting and loss of surface shape in the mechanistic-empirical design procedure) are given in

Table 3.7 and Table 3.8 to determine Design Traffic in ESAs. It denotes this axle group load (which causes the same damage as a Standard Axle) as the axle group's Standard Load (SL_i), ESAs of damage are evaluated as in the Equation 3.11.

$$\boldsymbol{ESA_{ij}} = \left(\frac{\boldsymbol{L_{ij}}}{\boldsymbol{SL_i}}\right)^{\boldsymbol{4}} \text{----------} \textit{Equation 3.11}$$

ESA_{ij} = number of repetitions of a Standard Axle which causes the same amount of damage as a single passage of axle group type i with load L_{ij}

SL_i = Standard Load for axle group type i

L_{ij} = j^{th} load magnitude on the axle group type i

Table 3.7: Loads on axle groups with dual tires cause the same damage as a Standard Axle *(Austroads, 2010)*

Axle group type	**Load (kN)**
Single axle with dual tires (SADT)	80
Tandem axle with dual tires (TADT)	135
Triaxle with dual tires (TRDT)	182
Quad-axle with dual tires (QADT)	226

Table 3.8: Loads on axle groups with single tires cause the same damage as a Standard Axle *(Austroads, 2010)*

Axle group type	Nominal tire section width	Load (kN)
Single axle with single tires (SAST)	Less than 375 mm	53
	At least 375 mm but less than 450 mm	58
	450 mm or more	71
Tandem axle with single tires (TAST)	Less than 375 mm	89
	At least 375 mm but less than 450 mm	98
	450 mm or more	119
Triaxle with single tires (TRST)	Less than 375 mm	121
	At least 375 mm but less than 450 mm	132
	450 mm or more	162
Quad-axle with single tires (QAST)	Less than 375 mm	150
	At least 375 mm but less than 450 mm	164
	450 mm or more	201

Calculating the ESAs of damage due to the design traffic requires estimating the average number of ESAs per heavy vehicle axle group (ESA/HVAG) from a project's Traffic Load Distribution (TLD). The TLD may be based on the following:

i. Project-specific WIM data
ii. Data selected from the WIM data.

The design number of Equivalent Standard Axles of traffic loading (DESA) is calculated using the following Equation 3.12.

$$\boldsymbol{DESA = \frac{ESA}{HVAG} \times N_{DT}} \text{ ----------} \textit{Equation 3.12}$$

ESA/HVAG = average number of Equivalent Standard Axles per Heavy Vehicle Axle Group

NDT = cumulative number of Heavy Vehicle Axle Groups over the design period

3.21 Effect of the weighted mean annual pavement temperature (WMAPT) on design traffic

There is a growing realization that asphalt mixtures exhibit accelerated crack healing with rising temperature to a significant level than the asphalt fatigue relationship. As a temporary solution, awaiting more research quantifying the increase in crack healing with increasing temperature, an upper limit may be used in the design traffic loading used in the asphalt fatigue damage calculations. Table 3.9 provides suggested limiting design traffic loadings in ESA. The limit decreases as the temperature rises due to increased crack healing. Using the ESA limits and the number of ESAs per heavy vehicle axle group, the upper limit in cumulative HVAG used in the asphalt fatigue damage calculations is determined using Equation 3.13.

Table 3.9: Suggested upper limits on design traffic for asphalt fatigue (Austroads, 2010)

WMAPT	**≤ 25 °C**	**26–34 °C**	**≥ 35 °C**
Design traffic loading limit (DESA)	4×10^8	2×10^8	10^8

WMAPT = Weighted Mean Annual Pavement Temperature

$$N_{DT\ limit} = \frac{DESA_{limit}}{ESA/_{HVAG}} \quad \text{----------Equation 3.13}$$

$N_{DT\ limit}$ = upper limit of the cumulative number of Heavy Vehicle Axle Groups over the design period for use in the asphalt fatigue damage calculations

$DESA_{limit}$ = upper limit of the design traffic expressed as Equivalent Standard Axles (ESA) for use in the asphalt fatigue damage calculations.

ESA/HVAG = average number of ESA per HVAG from the project traffic load distribution

It is important to note that these design traffic loading limits apply exclusively to asphalt fatigue computations; they do not apply to cemented materials, lean-mix concrete fatigue, or permanent deformation damage estimates.

3.22 Introduction to Mechanistic Design Software – CIRCLY

CIRCLY is a significant element of the Austroads Pavement Design Guide, extensively used in Australia and New Zealand. Compared to other accessible mechanistic tools, Mechanistic Design Software - CIRCLY has several distinguishing characteristics. It permits us to employ vehicle types and load configurations, wheel layout, braking or vertical loads, damage model, layer thickness combination, and elastic modulus combination. It is exceptional amongst commercial software since it supports the Austroads method's requirement for cross-anisotropic capabilities. Additionally, it automates several of the Austroads method's prerequisites, such as the sub-layering of unbound granular layers.

Furthermore, the parametric analysis tool allows for fine-tuning layer thicknesses, saving pavement costs. It can calculate load-induced stresses, strains, and deflections at any point in the multilayer system. CIRCLY Mechanistic Design Software could also consider various load types, including vertical, horizontal, and torsional. Non-uniform surface contact stresses can be expressed using a polynomial distribution. Additionally, with the advancement of Mechanistic Design Software – CIRCLY has been closely aligned with Austroads' mechanistic flexible pavement design method (Wardle, 2010). Figure 2.14 shows the pavement model for mechanistic design procedure by mechanistic design software – CIRCLY.

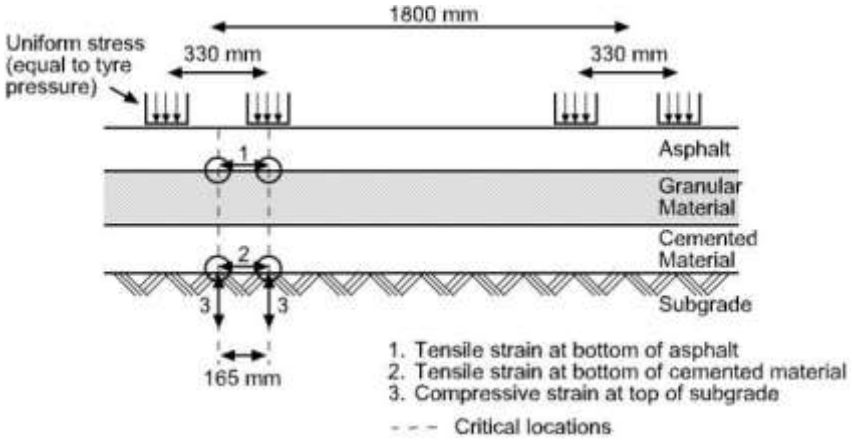

Figure 3.14: Pavement Model for Mechanistic Design Procedure by Mechanistic Design Software – CIRCLY (Wardle, 2010)

The Austroads mechanistic design method involves calculating pavement damage from these critical strains using empirical equations called 'failure criteria' or 'performance relationships' of the form in the Equation 3.14.

$$\boldsymbol{N = [\frac{K}{\varepsilon}]^{b}} \text{ ----------} \textit{Equation 3.14}$$

N = predicted life (repetitions of ε)

k = material constant.

b = damage exponent of the material.

ε = load-induced strain

The empirical parameters 'K' and 'b' are determined by calibrating the design method against the observed performance of test pavements or pavements in service (Wardle, 2010).

3.23 Cumulative Damage Factor (CDF) and Miner's Hypothesis

Even though the Austroads flexible pavement design approach does not specify the Cumulative Damage Factor (CDF) theory, it has been used as the primary way for presenting findings numerically and graphically in Mechanistic Design Software - CIRCLY. After that, the CDF concept is required to forecast the overall damage to a road structure. This method uses the magnitude of the pavement strain response to vehicle loading as a direct indicator of pavement damage over the pavement's life. The cumulative damage from all vehicles contributes to pavement failure according to the strain imposed by the individual vehicles.

The damage factor for the i^{th} loading is defined as the number of repetitions (n_i) of a given strain divided by the 'allowable' repetitions (N_i) of the strain that would cause failure.

The damage factor for the i^{th} loading is given by Equation 3.15.

$$\boldsymbol{DF = \frac{n_i}{N_i}} \text{ ----------} \textit{Equation 3.15}$$

n_i = Number of repetitions of the load group i

N_i = Allowable repetitions of the response parameter that would cause failure

Using Miner's hypothesis, CDF is obtained by summing the damage factors over all the loadings in the traffic spectrum.

The Total Damage Factor is defined by the Equation 3.16:

$$\boldsymbol{CDF_{Total} = \sum_{i=1}^{Load\ Cases} CDF_i} \qquad \text{----------} \textit{Equation 3.16}$$

'i' is summed over the mix of loads, for example, different container vehicles.

Once the CDF approaches 1.0, the pavement has reached its design life. If the CDF value is less than 1.0, the road has extra capacity; the CDF value illustrates the proportion of pavement life consumed by design traffic. If the CDF exceeds 1.0, the pavement is declared undesirable and must be adjusted during the subsequent trial to rectify the deficit. For instance, this may result in a rise in pavement thickness or a change in pavement stiffness. The procedure is repeated until a satisfactory output is obtained (Wardle, 2010).

3.24 Input Parameters for Mechanistic Pavement Design Using Mechanistic Design Software – CIRCLY

In Austroads, the modulus and Poisson's ratio of a layer are used to characterize its properties. These properties enable the application of layered elastic theory to compute pavement responses (stresses, strains, and deflections) across the pavement structure (Jayarathna & Mampearachchi, 2017). It is a one-of-a-kind method of pavement design. It assumes that the unbound granular materials have anisotropic moduli; most other design approaches assume they have isotropic moduli (Gribble & Patrick, 2008).

Seyhan et al. (2005) support the assumption of anisotropic moduli as the study has observed vertical resilient moduli commonly found to be larger than horizontal moduli. This observation is consistent with the fact that unidirectional compaction results in a preferred void orientation and an anisotropic structure.

3.24.1 Anisotropic Material Characterization

Compared to anisotropic materials, isotropic materials have the same characteristics in all directions. The cross-anisotropic case has an axis of symmetry of rotation. The attributes are supposed to be identical in all directions perpendicular to this axis but different from those in the direction of the axis.

Isotropic properties of materials assumed in Mechanistic Design Software – CIRCLY can be summarized as follows.

i. Asphalt - Isotropic
ii. Cement Treated - Isotropic
iii. Unbound Granular - Anisotropic
iv. Subgrade – Anisotropic (Wardle, 2010)

3.24.2 Unbound Granular Materials

Unbound granular pavement materials such as graded crushed rock, base course, and natural gravels involve specific consideration since their elastic stiffness depends on the stress state at each point in the material. The layered elastic approach is incapable of thoroughly addressing stress dependence. This condition is due to the method's critical constraint that elastic moduli must remain constant within each horizontal layer. Stress diminishes with distance from the wheels, so the modulus will also change horizontally and vertically with distance from the wheels.

However, the layered elastic method can consider stress dependence to some degree by dividing granular layers into sub-layers and assigning moduli to each sub-layer. This characteristic enables the modulus to vary with depth. CIRCLY automatically subdivides granular layers and assigns moduli by the Austroads guide, and this procedure was formerly done manually by the designer. The modulus of asphalt is highly temperature-sensitive, while the modulus of unbound granular materials is moisture-content dependent (Wardle, 2010).

3.25 Determination of Modulus of Pavement Materials

3.25.1 Selection of Resilient Modulus Testing Method

In the usual approach, many highway engineers have prioritized assessing the performance of existing roads. Designers must focus on an effective way to identify the structural condition to make proper rehabilitation and management decisions. The structural condition of a pavement provides sufficient information to estimate the remaining life of the pavement and determine a viable rehabilitation and reconstruction plan. Determining the material characteristics, specifically the stiffness of each pavement layer, is essential when designing mechanistic pavement (Goktepe et al., 2006). In-situ layer moduli values are crucial in determining allowable loads for existing pavement structures, overlay thickness, and assessing rehabilitation needs (Mehta & Roque, 2003).

Structural analyses and rehabilitation choices are frequently provided on project-level investigations through design charts and mechanistic methods utilizing multi-layered linear elastic theory and back-calculation techniques. Pavement deflection measurements are utilized to conduct structural assessments for pavement rehabilitation design and network monitoring. Older apparatus, such as the Benkelman beam and La Croix deflectograph, was widely used. Institutions such as Shell, the Asphalt Institute, and TRRL established several empirical relationships for analysis and overlay design (Horak & Emery, 2006).

Nondestructive testing (NDT) methods are increasingly being employed as they evaluate the structural performance of the road in a non-destructive approach and can be applied rapidly. The NDT approach is based on the principle that the structural performance of a pavement system is inversely proportional to the number of surface deflections caused by an applied load. Nondestructive testing techniques are classified as Deflection Basin Methods and Surface Wave Methods (Goktepe et al., 2006). Back-calculation of pavement layer moduli from non-destructively determined deflection basins has evolved into the industry-standard approach for evaluating the structural integrity of pavements (Chou & Lytton, 1991). In NDT methods, the mechanical properties of flexible pavement layers are measured at low strain levels (Goktepe et al., 2006). Generally, inconsistencies between deflection-based NDT methods are due

to differences in loading parameters (type, duration, and magnitude) and deflection measurement locations. We may classify load applications into static, steady-state vibratory, and time-domain impulses by emphasizing the loading condition.

Static loading is the most scenario, but it cannot accurately represent existing traffic loads; hence, displacements along the road surface are measured when subjected to a steady-state harmonic or a transient dynamic load (Lytton, 1989; Ullidtz, 2000; Uzan, 1994). The Benkelman beam and La Croix deflectometer are nondestructive testing (NDT) equipment operating under static loading. Dynamic loading is a highly accurate and effective method of simulating the effect of existing traffic loads.

Dynamic testing is generally conducted longitudinally throughout the roadway, and recorded deflection basins are used to describe the structural integrity of the pavement system when subjected to actual dynamic traffic loads (Goktepe et al., 2006). The steady-state dynamic condition is equivalent to a vehicle travelling over a section of pavement, and the loading period is related to the vehicle's speed. Dynaflect and Road Rater are two well-known examples of dynamic loading devices that operate in a steady state.

An impulse load is applied to the road surface in time domain impulse loading, and deflection measurements are acquired in the time domain. Numerous sensors are often employed to determine the deflection values at multiple locations on the road surface. A falling weight deflectometer (FWD) is a transient impulse loading device (Mamlouk, 1985; Sebaaly et al., 1985; Tawfiq et al., 2000). Falling weight deflectometer (FWD) testing has been used widely to evaluate pavement layers' structural integrity and calculate their moduli. Even if the estimated and measured deflection basins agree within acceptable limits, the modulus values for pavement layers acquired through the back-calculation procedure may not be valid (Mehta & Roque, 2003).

3.25.2 Falling Weight Deflectometer

The falling weight deflectometer (FWD) is a well-established and effective non-destructive road-testing equipment for analyzing global roads' structural integrity. The FWD is generally used for rehabilitation design investigations and network-wide

Pavement Management System (PMS) monitoring (Horak & Emery, 2006). FWD testing has been used frequently to analyze road pavements' structural integrity and calculate their moduli (Mehta & Roque, 2003). During the procedure, a varying load, typically 9,000 lb. (40 kN), is confined to fall vertically under gravity onto a spring-loaded plate with a diameter of 30 cm (11.82 in.) lying on the road surface (Husain & George, 1982; Sharma & Stubstad, 1980; Shen, 1993; Van Cauwelaert et al., 1989). Geophones, in particular, assess transient surface deflections at various locations (usually at six or seven locations). As a result, the deflection basin curve is plotted using the peak values for each geophone. Figure 2.15 depicts a typical FWD test result. As illustrated in Figure 2.15, the geophone just below the load application spot measures the maximum deflection. In contrast, more distanced geophones record minor deflections. Deflection curves display haversine behavior, meaning they rise nonlinearly to the peak and decrease after the peak with time elapsed.

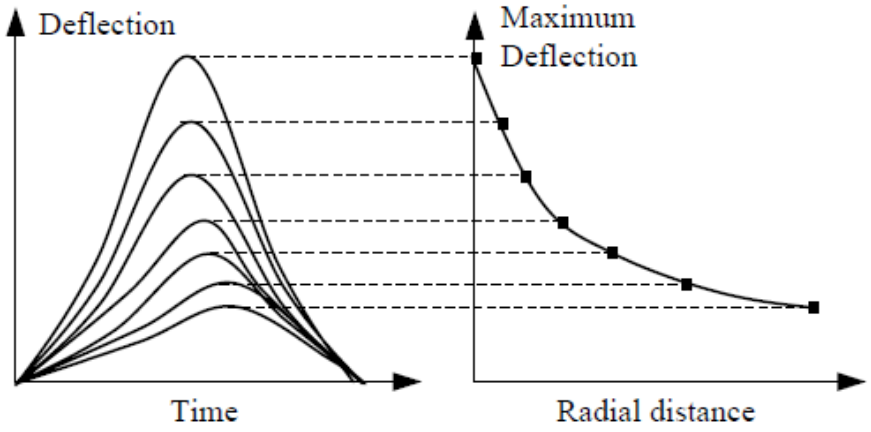

Figure 3.15: Illustration of typical FWD deflection graph

Several FWDs are commercially available, such as the Dynatest FWD, the KUAB FWD, and the Phoenix FWD (Bentsen et al., 1989; Hoffman & Thompson, 1982; Meier & Rix, 1995; Newcomb, 1987; Sebaaly et al., 1985; Stolle, 1991; Tawfiq et al., 2000; Tholen et al., 1985; Zhou, 2000). The fundamental downside of FWD is that it must wait for a few minutes at every test point throughout the measurement process, reducing efficiency (Goktepe et al., 2006).

3.25.3 Back-Calculation of Resilient Modulus of Pavement Layers

Back-calculation problems are frequently encountered in various scientific areas, alternatively, parameter identification problems. It is an optimization used to generate an inverse mapping of a known relationship defined by discrete or continuous data points (Goktepe et al., 2006). The primary objective of back-calculation is to determine the in-situ elastic moduli (E) of the numerous pavement layers. The deflection values are computed for assumed elastic moduli and compared to the observed deflection values in this procedure. As a result, the assumed moduli values are altered for the following iteration. The iteration process is repeated until the computed and observed deflection values are almost identical.

Additionally, the thickness of the existing pavement may be undetermined, which can be approximated iteratively using the back-calculation procedure (Das, 2010). The core issue addressed by the back-calculation approach is establishing a series of layer moduli theoretically consistent with input data comprised of specified pavement layer thicknesses and Poisson's ratios, a defined applied load, and a measured pavement deflection basin caused by the applied load. This issue does not have closed-form resolution, and multiple solutions may exist for every input data set. Consequently, the analyst's judgment is required when analyzing the back-calculation technique (Richter, 2006). Even if the calculated and measured deflection basins agree within accepted ranges, the modulus values for pavement layers acquired through the back-calculation procedure may be inaccurate (Mehta & Roque, 2003). Numerical inconsistencies are created throughout iterations, and – due to the inverse nature of the issue – no unique solution can be obtained through the back-calculation procedure owing to the idealizations required for pavement structure analysis (Ceylan et al., 2005; Chou & Lytton, 1991; Hall & Mohseni, 1991; Ullidtz & Stubstad, 1985). Efforts are being made to evolve a complete back-calculation scheme to reach the solution accurately, reliably, and quickly (May & Von Quintus, 1994).

3.25.4 KUAB PVD back-calculation software

Load impact systems are classified into two types: single-mass (e.g., Dynatest, Carl Bro, PaveTesting) and double-mass (e.g., Dynatest, Carl Bro, PaveTesting) (KUAB). The double mechanism results in a high loading time representing a wheel. The

double-mass technique is more reproducible and produces more precise results on roads constructed on soft soils. The single-mass approach may overestimate the capacity of pavements built on soft soils. The KUAB program estimates the moduli of the layers in a pavement provided the thickness and Poisson's ratio of each layer. It accomplishes this through an iterative approach in which theoretical deflection values in a mathematical model are compared to measured deflection values. The software alters the layer modules until there is no further enhancement possible. The software then analyses the strains in the layers and determines which layer will underperform initially based on the strain criterion permitted and how many years this would require. Ultimately, the program determines the overlays needed to guarantee that the road can support a specified load for a specified lifespan. The KUAB software employs the equivalent thicknesses method. All other layers are transformed to have the same modulus as the layer under consideration to discern the compression of a particular layer. The deflection at the top and bottom of the corresponding pavement layer is estimated using Boussinesq. The distinction between the two is the layer's compression. The cumulative deflection on the top is the summation of all layer deflections. The Poisson's ratio, modulus, and thickness of each layer are seed parameters for the mathematical model's initial computation of theoretical deflections. The modulus value that perfectly meets the calculated and measured deflection is chosen (Aher & Loya, 2019).

3.26 Pavement Management Systems (PMS)

Electronics, wireless networks and web-based software enhancements have fueled the emergence and evolution of a new generation of project management systems combining quantitative and qualitative goals. This novel architecture must handle a road system more effectively and function better. Numerous transportation agencies globally have implemented pavement management systems (PMS). These systems are essential technology to provide organizations with the desired benefits. Pavement management systems are highly effective at managing massive pavement systems (McGovern et al., 2016; Pan et al., 2015). The efficacy of these methods is contingent upon how pavement distress is measured, and data is obtained. PMS requires establishing a pavement inventory database that contains information about the status

of the pavement, as well as construction, maintenance, and rehabilitation records. Additionally, it enables decision-makers to assess the impact of different funding levels on road conditions (Yoder & Witczak, 1991).

3.27 Importance of Alligator Cracking information in Pavement Management Systems

Cracking data is a crucial component of distress data that every pavement management system must have (Lee & Kim, 2005). Cracking is among the most prevalent distresses that impair the pavement's functionality (Zhaoyun et al., 2009). Early pavement degradation is characterized by four distinct types of cracking: transverse, longitudinal, block, and alligator/fatigue cracking (Al-Suleiman et al., 2017). Fatigue damage reduces asphalt concrete (AC) stiffness caused by repeated loading. Tensile strain develops at the bottom of the AC of asphalt paving upon each cycle of traffic loading. Due to this tensile strain, specific localized damage is caused on a minute level in the material. This damage reduces material stiffness (E) as traffic loads increase. While the damage produced by a single vehicle is minimal, the cumulative damage is significant when considering the life span of road pavements. Once a certain amount of damage has been accumulated, bottom-up fatigue cracking occurs, resulting in alligator cracking at the surface (Islam & Tarefder, 2016). Exposure to environmental circumstances and traffic loads amplifies field distresses' emergence, development, and coalescence. Once distress develops, it will continue to perpetuate, resulting in severe road damage (Zhang et al., 2017). Over time, road systems degrade mainly owing to fatigue. This degradation occurs over time and is strongly affected by repetitive axle loadings caused by automobile movement. To correctly manage roads, it is necessary to monitor such cracks’ growth and ensure the security of workers accountable for road monitoring (Al-Suleiman et al., 2017).

3.28 Alligator Cracking Index (ACI)

Highway infrastructure's most important commodity is its roads. Maintaining and rehabilitating these roads to the necessary serviceability is among the most challenging tasks that pavement experts and highway administrators encounter. Road performance assessment using pavement condition indicators is integral to any Pavement Management System. Numerous indices, such as the Pavement Condition Index (PCI),

the Present Serviceability Rating (PSR), and the Roughness Index (RI), have already been widely utilized to determine the appropriate maintenance plan for existing roadways (Shah et al., 2013). The traditional techniques for identifying road cracks in the present specifications are labor-intensive, time-consuming, hazardous, and subjective (Zhaoyun et al., 2009).

Assessing road conditions, including distress, roughness, friction, and structure, is crucial for pavement design, rehabilitation, and management. The majority of cost-effective maintenance and rehabilitation (M and R) solutions produced with the use of a Pavement Management System (PMS) are the result of precise pavement assessment (Huang, 1993). Pavement management systems necessitate systematic monitoring of road surfaces to decide when preventative and remedial repairs should be performed. The procedure entails collecting large amounts of visual data during site visits. The road surface condition would then be compared to a pavement distress index calculated using a rating methodology developed beforehand by state or federal authorities. The rating system identifies whether a road segment needs maintenance, overlaying, or reconstruction.

The alligator crack index is one of the surfaces distresses forming part of the overall pavement distress index. The alligator crack distress index is used to visually assess the severity of cracks in an area of the roadway. This analysis could then determine the alligator crack index through an equation (Vallejo, 2012). The distress identification manual developed for the long-term pavement performance project (Miller & Bellinger, 2003) has been frequently used to describe the many varieties of cracks found in asphalt pavements (Cook et al., 2004; Federal Highway Administration, 2006; McQueen, 2004; Minnesota Department of Transportation, 2011).

3.29 Pavement Distress Identification Manual for the National Park Service (NPS) Road Inventory Program

The Federal Highway Administration's Road Inventory Program (FHWA RIP) is founded on the notion that applying automated crack identification technologies to photographs may thoroughly predict the pavement's surface condition. Numerous

criteria for measuring the condition of pavements have progressed with varying precision and recognition levels. Throughout the last decade, digital imaging to capture photographs of pavements and subsequent crack identification and classification has improved significantly. Digital cameras with excellent resolution have got more accessible, and crack detection software's unique programming code and algorithms have been enhanced (Federal Highway Administration, 2006).

The Federal Highway Administration (FHWA) has used the "Distress Identification Manual for the Long-Term Pavement Performance Program," Publication No. FHWA-RD 03-031, June 2003, as a guideline for determining the type of distress on National Park Service (NPS) pavement (Miller & Bellinger, 2003). The FHWA RIP distress classifications are identical to those outlined in the LTPP manual, with minor adjustments. The "Distress Identification Manual for the National Park Service Road Inventory Program, Cycle 4, 2006–2008" was prepared to utilize the "Distress Identification Manual for the Long-Term Pavement Performance Program" as a reference. The severity levels defined in this publication are consistent with the LTPP Distress ID Manual. The description of Alligator Cracking and the method for determining the severity have been modified. Additionally, this manual covers Rutting and Roughness and their applicability to RIP. This "Distress Identification Manual for the National Park Service Road Inventory Program" will guide crack detection and classification, determine the severity and extent of distress, and calculate distress index values for the FHWA RIP Cycle 4 (Federal Highway Administration, 2006).

3.30 Calculation of Alligator Cracking Index

3.30.1 Description

Alligator cracking can be conceived as a combination involving fatigue and block cracking. It is a network of interconnected cracks at distinct developmental stages. Alligator cracking forms a complex pattern like chicken wire or alligator skin. It may occur at any point along the lane Alligator cracking must have a quantifiable area.

3.30.2 Severity Levels

i. LOW

"An area of cracks with no or very few interconnecting cracks, and the cracks are not spalled. Cracks are ≤ 6mm in mean width. Cracks in the pattern are no further apart than 0.328 m. May be sealed cracks with sealant in good condition and a crack width that cannot be determined".

ii. MEDIUM

"An area of interconnected cracks that form a complete pattern. Cracks may be slightly spalled. Cracks are > 6 mm and ≤ 19 mm or any crack with a mean width ≤19 mm and adjacent low severity cracking. Cracks in the pattern are no further apart than 150 mm".

iii. HIGH

"An area of interconnected cracks forming a complete pattern. Cracks are moderately or severely spalled. Cracks are >19mm or any crack with a mean width ≤ 19mm and adjacent medium to high severity random cracking".

The total severity of alligator cracking is determined using a combination of observed crack width and pattern. Figure 2.16 to Figure 2.21 shows the alligator crack identification. According to the preceding explanation of each severity level, the highest crack width and pattern level determine the overall severity. Table 3.10 illustrates this.

Table 3.10: Alligator Crack Severity Levels (Federal Highway Administration, 2006)

Alligator Cracking Severity Levels		**Crack Pattern**		
		LOW	**MEDIUM**	**HIGH**
Crack Width	LOW	L	M	H
	MEDIUM	M	M	H
	HIGH	H	H	H

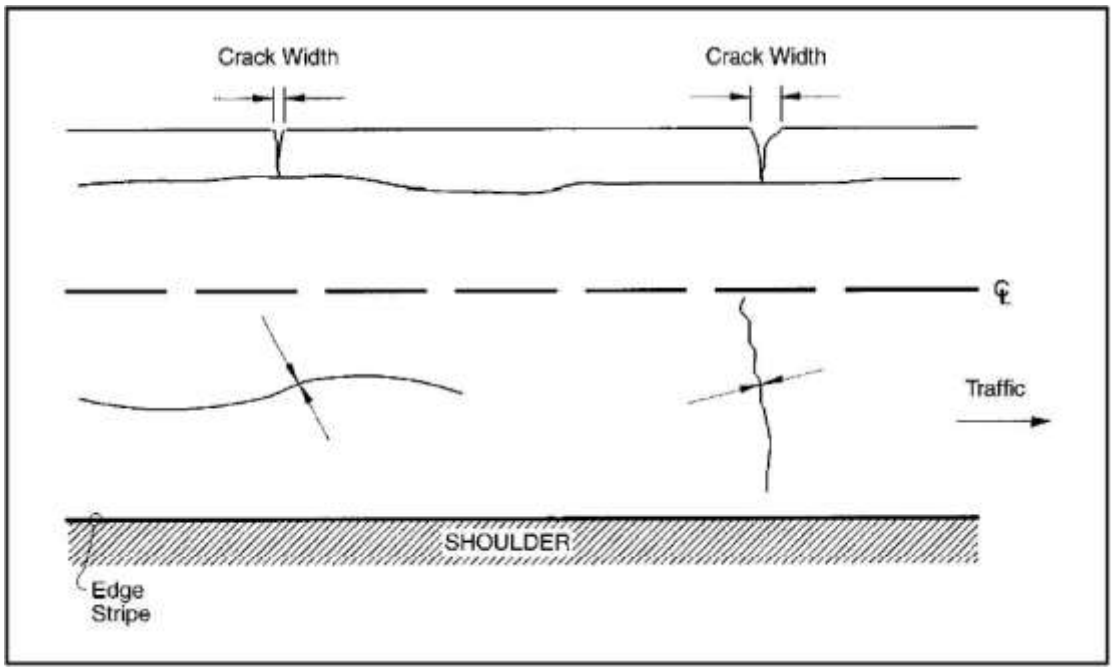

Figure 3.16: Measuring Crack Width on Asphalt Pavement (Federal Highway Administration, 2006)

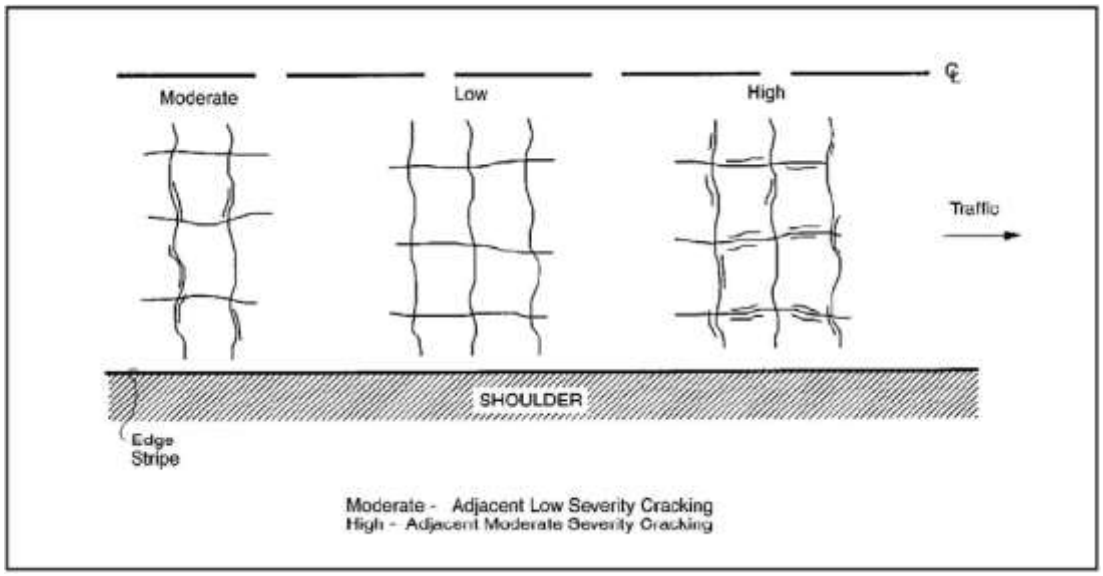

Figure 3.17: Effect on Severity Level of Alligator Cracking due to Associated Random Cracking (Federal Highway Administration, 2006)

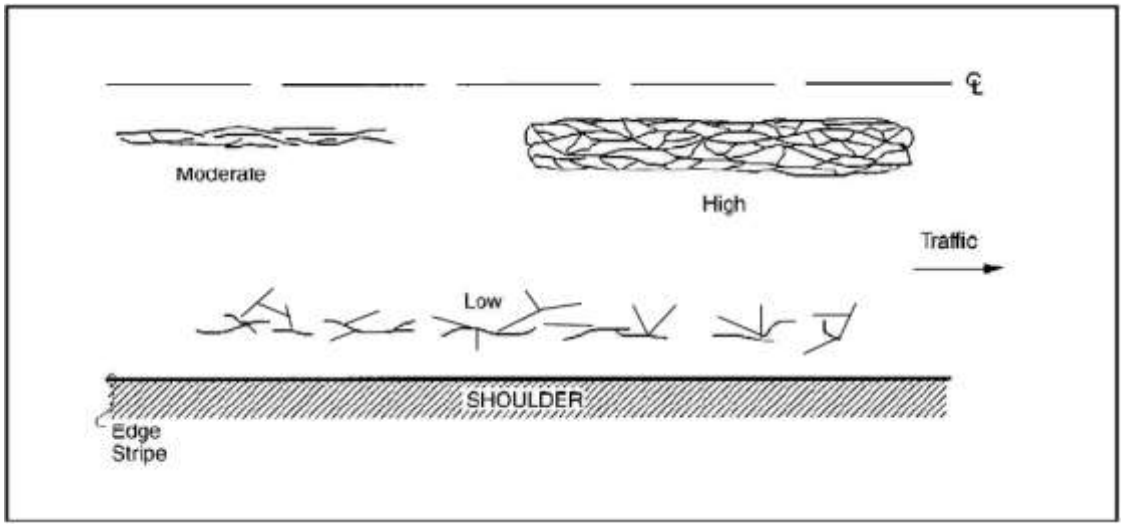

Figure 3.18: Alligator Crack Patterns of Differing Severity (Federal Highway Administration, 2006)

Figure 3.19: High Severity Alligator Cracking (Federal Highway Administration, 2006)

Figure 3.20: Medium Severity Alligator Cracking (Federal Highway Administration, 2006)

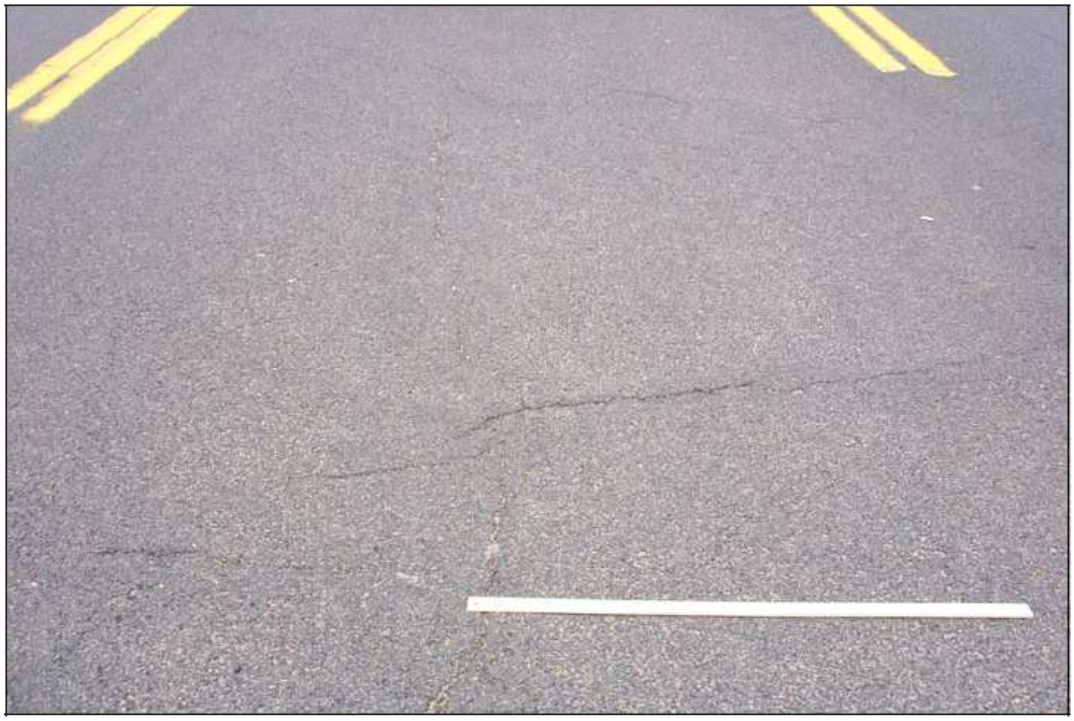

Figure 3.21: Low Severity Alligator Cracking with Few or No Interconnecting Cracks (Federal Highway Administration, 2006)

3.31 Alligator Crack Index Formula

Note: All index formulas below contain Maximum Allowable Extents (MAE) applicable to 32 m intervals. ACI can be calculated using Equation 3.17.

$$\boldsymbol{AC\ Index = 100 - 40 \times \left[\left(\frac{\%LOW}{70}\right) + \left(\frac{\%MED}{30}\right) + \left(\frac{\%HI}{10}\right)\right]} \text{ ------Equation 3.27}$$

The values of %LOW, %MED, and %HI report the percentage of the observed pavement (32 m, primary lane) that contains alligator cracking within the respective severities. These values range from ≥ 0 to ≤ 100.

%LOW = Percent of total area (primary lane, 32 m in length), low severity
%MED = Percent of total area (primary lane, 32 m in length), medium severity
%HI = Percent of total area (primary lane, 32 m in length), high severity

Percent of the total area is computed as in the Equation 3.18:

$$\boldsymbol{Percent\ of\ the\ total\ area = \frac{square\ meter\ area\ of\ alligator\ crack\ severity}{32\ m * lane\ width(m)}} \text{ ------}$$

Equation 3.38

"In AC_INDEX, the denominators 70, 30, and 10 are the MAE for each severity. In other words, we will allow up to 70% of low-severity alligator cracking for a 32 m interval before failure and 30% for medium severity. If any severity reaches MAE, the resulting index value is 60 or failure" (Miller & Bellinger, 2003).

3.32 OriginPro Statistical Analysis Software

OriginPro is the preferred statistical software and graphical program for over 500,000 researchers and technologists globally working in commercial enterprises, academics, and authorities. OriginPro provides an intuitive interface for amateurs while allowing for extensive customizing as the consumer gains experience with the software (OriginLab Corporation, 2019).

OriginPro 9.1 is an appropriate statistical software that allows users to monitor, evaluate, and generate charts and figures. Perhaps OriginPro 9.1's most advanced features are the graphing capabilities. OriginPro 9.1 is highly adaptable, allowing users to set the image appropriately. The user can choose from several 2-D and 3-D graphs, including histograms, line graphs, scatter plots, 3-D colored surface graphs, and 3-D

scatter plots. The interface for creating such graphs is straightforward, enabling even novice users to generate complicated graphs effortlessly. Almost every component of the plot is incredibly flexible, ensuring that the program produces graphics of extremely high quality that are suitable for publication or presentation. OriginPro enables users to save produced graphs in a variety of file formats. This program includes robust analysis techniques, curve-fitting algorithms, and graphical depiction. Various nonlinear data fitting functions are available, including exponential and logarithmic, polynomial, and waveform functions. If research methodology necessitates fitting to customized functions, OriginPro enables users to develop their data fitting algorithms, allowing them to adapt the software to their requirements. Additionally, the application allows the user to examine enormous data sets fast and effectively by continuously evaluating many groups of similar data.

Furthermore, while determining any fitting, OriginPro 9.1 automates various helpful statistical tests, including ANOVA tests, correlation coefficients, and residual plots, allowing users to verify the fit's accuracy easily. OriginPro features code-building software that enables users to customize the program for various uses. It complies with the C programming language and includes tools for writing, compiling, and executing such applications. OriginPro is, in general, among the most powerful data analysis applications available to academics nowadays. OriginPro 9.1 is a leading competitor among available data due to its sophisticated data analysis methodologies and varied, convenient data presentation capabilities (Seifert, 2014).

4 METHODOLOGY

This chapter describes the methodologies followed in this research to evaluate and justify modifying the failure functions suggested by the Austroads mechanistic pavement design guideline. This research only focused on modifying failure function for asphalt fatigue.

Initially, a separate study was conducted to compare the design thicknesses given by the default performance relationships suggested by the Austroads guideline. Section 2 of the Central Expressway from Meerigama to Kurunegala (39.9 km) was selected for the analysis. Different design methods, such as Road Note 31, AASHTO, and Austroads, were incorporated into the design procedure. Traffic distributions for A1 – (Colombo - Kandy Road) and A6 (Ambepussa – Trincomalee Road) were assumed for the thickness design. The distribution at the A6 road was observed to have the highest ESA (Equivalent Standard Axles) in both 10 years and 15 years.

Consequently, pavement thickness design by the AASHTO design was done only for A6 distribution. Mechanistic design software – CIRCLY, based on Austroads- was used to verify. The outcomes of this analysis are presented in the chapter 5.

Fatigue damage in asphalt layers is usually exhibited as asphalt fatigue cracking/alligator cracking. Alligator cracks are formed due to the horizontal tensile strains present at the bottom of the asphalt layer. Thus, it is considered the critical strain responsible for fatigue cracking. An asphalt layer's cumulative damage factor (CDF) indicates the accumulated fatigue damage over the lifetime. There are other methods to quantify the fatigue damage in an asphalt layer, such as visual surveys. Visual surveys allow the observer to identify alligator cracks related to fatigue damage in asphalt layers and rate them according to their quantity and severity. Using visual surveys to rate and quantify the distresses present in the pavements is an effective way of assessing pavement conditions. The alligator cracking index (ACI) effectively determines alligator cracks in the pavement, quantifying the accumulated fatigue damage in the asphalt layers over time. CDF and ACI, representing the accumulated fatigue damage in the asphalt layer, were incorporated to derive the modified damage models, which involved an extensive analysis. The analysis also included several other

parameters and the CDF and ACI. Derivation of the modified damage model for asphalt fatigue is presented in the following sections accordingly.

4.1 Data collection for the model development and model validation

In this research, the most time-consuming part was the data collection. Due to the unavailability of necessary data, a considerable amount of time was spent collecting the data. However, considering the availability and accessibility of data, two A- class trunk roads were selected for model development and verification, respectively. The two chosen roads are as follows.

i. A11 - Maradankadawala-Habarana-Thirukkondaiadimadu
   It connects the Maradankadawala with Tirikkondiadimadu. The A-11 passes through Ganewalpola, Habarana, Moragaswewa, Minneriya, Polonnaruwa, Kaduruwela, Manampitiya, Welikanda, Punani and Vakaneri to reach Tirikkondiadimadu and

ii. A10 - Katugasthota – Kurunegala – Puttalam
   It connects Katugastota with Puttalam. The A10 passes through Galagedara, Mawathagama, Kurunegala, Wariyapola, Padeniya, Nikavaratiya, Anamaduwa, and Kalladi to reach Puttalam.

The summary of the data obtained for the analysis is mentioned below.

4.1.1 Calculation of traffic parameters

The calculation of traffic parameters involved several data types. Data obtained for traffic calculations are summarized below.

i. Axle load survey data
ii. Average annual daily traffic (AADT) data
iii. Manual classified count (MCC) data

Data required for the traffic analysis, such as Axle load survey data, Average annual daily traffic (AADT) data and Manual classified count (MCC) data, were obtained from the Planning Division of the Road Development Authority (RDA), Sri Lanka.

4.1.2 Estimation of layer moduli

Estimating layer moduli using the KUAB PVD back-calculation software involved several data types. Data obtained for the analysis of layer moduli is summarized below.

i. Falling weight deflectometer (FWD) data
ii. Temperature data to estimate the Weighted mean annual pavement temperature (WMAPT) required for the FWD analysis.
iii. Test pit data to obtain layer thicknesses.

Data required to estimate layer moduli, such as Falling weight deflectometer (FWD) data and Test pit data to obtain layer thicknesses, were obtained from the RDA, Research and Development division. RDA is the only government body conducting FWD testing procedures in Sri Lanka. RDA also follows a dynamic testing method for FWD data collection so that the reliability of the collected data is satisfactory. Referring to recommendations by previous research in literature and available resources now, this research used FWD data provided by RDA.

4.1.3 Calculation of Alligator Cracking Index (ACI)

Calculating the alligator cracking index (ACI) involved visual images of the road sections and the crack areas. Data obtained for the estimation of the Alligator cracking index are summarized below.

i. Alligator cracking data – Severity and crack areas

Data required to calculate the ACI were also obtained from the Planning Division, RDA. Digital images and surface areas of the distress were collected to detect and classify alligator cracking data. The same road sections selected for calculating the Cumulative Damage Factor (CDF) following the Austroads guideline were considered to estimate the Alligator Cracking Index (ACI). Considering the availability of the data, only the first 6km (0+000- 6+250) of the A11 (Maradankadawala-Habarana-Thirukkondaiadimadu) road was selected for the model development purpose.

4.1.4 Software packages used for CDF calculation.

The following software packages were required for the CDF calculation.

i. Mechanistic design software – CIRCLY

ii. Back-calculation software – KUAB PVD

4.2 Model Development

4.2.1 Cumulative Damage Factor (CDF) analysis using mechanistic design software- CIRCLY for A11 road.

Estimating the Cumulative damage factor (CDF) by the mechanistic design software – CIRCLY had several steps, including.

i. Estimation of material properties such as layer moduli of pavement layers.
ii. Estimation of the cumulative heavy vehicle axle groups in the design lane over the design period (N_{DT})

4.2.2 Phase 1: Estimation of Layer moduli of pavement layers of A11 road

Layer moduli were input to the mechanistic design software – CIRCLY, representing one of two significant material properties of pavement layers to be input. Stage 1 of the research consisted of back-calculating layer moduli of the A11 (Maradankadawala-Habarana-Thirukkondaiadimadu) road. The FWD deflection data for the A11 road obtained from the Research and Development Division, RDA, was utilized in the back-calculation procedure. An extensive analysis was conducted using the back-calculation software KUAB-PVD available at the Research and Development Division, RDA, to obtain the moduli values of pavement layers. Layer moduli values were estimated at the in-service pavement temperature or the Weighted mean annual pavement temperature (WMAPT), as recommended in the Austroads guide. The back-calculation software – KUAB PVD has a separate option to include the WMAPT value to output the temperature-corrected layer moduli values at the WMAPT.

4.2.3 Estimation of Weighted Mean Annual Pavement Temperature (WMAPT)

Weighted Mean Annual Pavement Temperature (WMAPT) (°C) is used in estimating asphalt moduli at in-service temperatures. Calculation of the WMAPT was done as recommended in the Austroads guideline. A summary of the WMAPT calculation is mentioned below.

The following method was used to calculate the WMAPT.

i. Obtain the monthly average daily maximum air temperature and the annual, monthly daily minimum air temperature (Obtained the direct values from the Department of Meteorology – Sri Lanka).
ii. Calculate the monthly average air temperatures by averaging the maximum and minimum air temperatures.
iii. Using Equation 11 in the Austroads guide and the monthly average air temperature, calculate each month's temperature weighting factors (WF).
iv. For each site, average the 12 WFs obtained in Step iii.
v. Using average WF from Step iv and Equation 12 in the Austroads guide, estimate each site's weighted mean annual air temperature (WMAAT).
vi. Using the WMAAT and Equation 13 in the Austroads guide, estimate the WMAPT for each site (Austroads, 2010).

For the estimation of the WMAPT, the following data were obtained from the Department of Meteorology, Sri Lanka.

i. The monthly average daily maximum air temperature
ii. The monthly average daily minimum air temperature
iii. The monthly average air temperature

Since the FWD data were obtained in 2012, the temperature data collected was also for 2012. Temperature data for 2012 is presented in Table 4.1.

Table 4.1: Temperature data for the year 2012

Month	The monthly average daily maximum air temperature (°C)	The monthly average daily minimum air temperature (°C)	The monthly average air temperature (°C)
January	30	19	26
February	31	20	27
March	34	20	29
April	34	23	30
May	35	24	31
June	34	24	30
July	34	24	30
August	34	24	31
September	35	24	31
October	33	23	29
November	31	22	27
December	29	21	26

Once the temperature data was collected, the next step was calculating the weighting factors (WF). The following equation recommended in the Austroads guide was accommodated to calculate the weighting factors for each month of 2012.

Shell Weighting Factors (Chart W of Shell International Petroleum Company (1978)) (Equation 4.1).

$$\boldsymbol{WF = 10^{(-1.224+0.0650T_{air}-0.000145T_{air}^{2})}} \quad \text{----------}\textit{Equation 4.1}$$

A summary of the calculated weighing factors is given in the results chapter.

WF values for the 2012 year were calculated as presented in Table 4.2.

Table 4.2: WF Values for the months of 2012

Month	The monthly average daily maximum air temperature (°C)	The monthly average daily minimum air temperature (°C)	The monthly average air temperature (°C)	Weighting Factors (WF)
January	30	19	26	2.345
February	31	20	27	2.676
March	34	20	29	3.478
April	34	23	30	3.962
May	35	24	31	4.510
June	34	24	30	3.962
July	34	24	30	3.962
August	34	24	31	4.510
September	35	24	31	4.510
October	33	23	29	3.478
November	31	22	27	2.676
December	29	21	26	2.345

The average value of WF= 3.534313

The weighted mean annual air temperature (WMAAT) values were calculated using the following equation by accommodating the WF values.

WMAAT from average WF (Chart W of Shell International Petroleum Company (1978)) (Equation 4.2).

$$\boldsymbol{WMAAT = 19.66 + 16.91\, logWF + 0.3117 \times (logWF)^2}$$ *-----Equation 4.2*

WMAAT = 29.0255

The Weighted mean annual pavement temperature (WMAPT) was calculated using the following equation.

Estimating WMAPT from WMAAT (Chart RT Shell International Petroleum Company (1978), 100 mm asphalt) (Equation 4.3).

$$\boldsymbol{WMAPT = -12.4 + \frac{6.32(WMAAT)}{ln(WMAAT)}}$$ *----------Equation 4.3*

WMAPT for A11 road = 42°C

Calculated in-service pavement temperature - WMAPT was then input to the back-calculation software to obtain the layer moduli at the in-service pavement temperature.

4.2.4 Back-calculation of Layer moduli using Falling weight deflectometer (FWD) data for A11 road.

A11 road consisted of asphalt, macadam base, subbase, and subgrade layers. Pavement layer thicknesses obtained from the A11 road were used to input the FWD back-calculation procedure. The layer thicknesses of the road were not uniform throughout the length of the selected section for the analysis. A cross-section of the A11 road is illustrated in Figure 4.1.

Figure 4.1: Typical cross-section of the A11 road

Since the road had varying thicknesses of pavement layers, an average value of pavement thickness was used for the back-calculation procedure. The average values of the pavement layer thicknesses used for the FWD back-calculation procedure are mentioned in Table 4.3. Average values of the thicknesses were obtained by averaging the layer thicknesses given in the test pit report for the A11 road section.

*Table 4.3:*Average values of the pavement layer thicknesses used for the FWD back-calculation procedure.

Pavement layer	Layer thickness
Asphalt	150mm
Macadam base	120mm
Subbase	250mm
Subgrade	N/A

Falling weight deflectometer (FWD) data for the A11 road was then analysed using the back-calculation software- KUAB PVD.

4.2.5 Obtaining modulus values of pavement layers from Falling Weight Deflectometer (FWD) back-calculation for the A11 road

Data obtained for the estimation of layer moduli:

i. Falling weight deflectometer (FWD) data
ii. Temperature data to estimate the Weighted mean annual pavement temperature (WMAPT) required for the FWD analysis.
iii. Test pit data to obtain layer thicknesses.

Secondly, Falling Weight Deflectometer (FWD) data obtained from the Road Development Authority (RDA) was required to obtain the moduli of pavement layers. A separate analysis was conducted using the back-calculation software KUAB-PVD available at the RDA Research and Development Division, to get the moduli values of pavement layers. The moduli values were corrected at the Weighted Mean Annual Pavement Temperature (WMAPT) before inputting the mechanistic design software. The back-calculation software – KUAB PVD, has a separate option to include the WMAPT value to output the corrected Moduli values at the WMAPT. WMAPT was calculated for the A11 road as mentioned in the Austroads guideline, and WMAPT for the A11 road was found to be 42°C. This calculated WMAPT value was the value input to the KUAB PVD back-calculation software for the temperature correction of layer moduli.

4.3 Phase 2 - Analysis by Mechanistic Design Software – CIRCLY to obtain cumulative damage factor (CDF)

4.3.1 Material properties for the Mechanistic Design Software – CIRCLY

The mechanistic Design procedure in the Austroads pavement design guide uses two significant material properties. Mechanistic design software-CIRCLY, based on the Austroads pavement design guide, facilitates the input of the following material properties manually to the software, reducing the complexity of the analysis.

1. Resilient Modulus (Obtained from FWD analysis)
2. Poisson’s Ratio (Typical values were used)

Table 4.4: Typical Poisson's ratio values for pavement layers

Pavement Layer	Poisson's Ratio
Asphalt	0.40
Aggregate Base Course (ABC)	0.35
Subbase	0.45

Mechanistic design software-CIRCLY also allows inputting values for each material type's 'K' and 'b' parameters. In addition to default values for 'K' and 'b,' different values were also assumed during the analysis for 'K' and 'b' parameters to obtain the most suitable modified failure function. Consequently, Different Cumulative Damage Factor (CDF) values were calculated at changing 'K; and 'b' parameters. The CDF for Asphalt represents the fatigue damage in the asphalt layer. In contrast, CDF for Subgrade represents the rutting damage present in the subgrade layer.

4.3.2 Traffic Estimation for Mechanistic Design Software- CIRCLY

The mechanistic design software-CIRCLY requires the cumulative heavy vehicle axle groups (in the design lane) over the design period (N_{DT}) on the pavement during the lifetime for estimating the applied strain repetitions. Applied strain repetitions during the pavement's consumed life are significant in the Austroads pavement design guide. This is a crucial parameter required to determine the damage caused to the pavement structure during the pavement's lifetime. Austroads has assigned specified empirical formulae to estimate the strain repetitions for failure under the following failure criteria.

i. Fatigue Cracking of Asphalt
ii. Permanent Deformation of Subgrade

Austroads also has an additional criterion for fatigue cracking in cement-treated materials. Fatigue cracking in asphalt layers was only considered in this research.

4.5.3 Estimation of Cumulative Heavy Vehicle Axle Groups (in the Design Lane) over the Design Period (N_{DT}) for mechanistic software - CIRCLY

Traffic parameters are to be input into the mechanistic design software CIRCLY.

i. Cumulative number of Heavy Vehicle Axle Groups over the design period (N_{DT})
ii. Traffic load distribution (TLD)

As the first step of the CDF calculation, traffic data were analyzed to obtain the traffic load distribution file of the A11 road and the N_{DT} (cumulative number of heavy vehicle axle groups). The traffic load distribution file and the N_{DT} values were derived following the Austroads guidelines.

4.5.4 Estimation of N_{DT} for A11 Road

The following data were required to estimate N_{DT} for the A11 road. Data were obtained from the Planning Division, Road Development Authority (RDA), Sri Lanka.

i. Axle load survey data
ii. Average Annual Daily Traffic Data (AADT) and Manual Classified Count Data (MCC)

The following procedure was conducted to estimate the N_{DT} for the A11 road.

i. Use of Axle load survey data

a) The axles were separated into axle groups. The axle load unit was kept in Kilo Newtons (kN).

When calculating the axle loads for TADT and TRDT axle groups (which were mentioned as -22- and -222- respectively in Austroads notations), the loads were combined accordingly to obtain the total axle load of the axle groups.

b) All the axles were categorized into desired load groups.
c) The number of axles and their percentages in each load group were calculated.
d) The total axles in each axle group, the total number of all the axles, the percentage of axles in each group, and the Heavy Vehicle Axle Groups (HVAG) were calculated.

The total axel percentage can be calculated using Equation 4.4.

$$\textbf{\textit{Total SAST axle}}\ \% = \frac{\textbf{\textit{Total SAST Axle}}}{\textbf{\textit{Total All Axle}}} \times \mathbf{100}\% \text{ -------- } \textit{Equation 4.4}$$

All axle group types (i.e., SAST, SADT, TAST) were considered HVAG in this calculation. Thus, HVAG is always equal to 1.

e) The ESA value for each axle group and each axle type were estimated separately and combined with the total ESA value. The Equation 4.5 using the Equation 4.5.

$$\boldsymbol{ESA\ from\ SAST} = \frac{\boldsymbol{Axle}\ \%}{\mathbf{100}} \times \boldsymbol{SAST\ Axle\ Proportion} \times \left(\frac{\boldsymbol{Axle\ Group\ Load}}{\boldsymbol{Standard\ Axle\ Load}}\right)^{\mathbf{4}} \text{-----}$$

- Equation 4.5

Calculation of Total ESA values can be done by following the Austroads guideline (Austroads, 2017). The first step of calculating total ESA is to add the ESA values for each axle type that were calculated in the previous step.

Then the Pavement Damage in Terms of Equivalent Standard Axle Repetitions were calculated referring to the methodology given in the chapter 7.6.2 of the Austroads guideline (Austroads, 2017).

The Standard Axle is defined as a single axle with dual tires (SADT) applying a load of 80 kN to the pavement. To determine Design Traffic in terms of ESAs the loads on axle configurations that are considered to cause the same damage (i.e., overall pavement damage when using the empirical procedure, and rutting and loss of surface shape in the mechanistic-empirical design procedure) are given in Table 7.7 and Table 7.8. Denoting this axle group load (which causes the same damage as a Standard Axle) as the axle group's Standard Load ($UULL\ ii$), ESAs of damage is evaluated as follows.

f) Standard Axle Repetitions for asphalt - (SAR5 - Asphalt), Standard Axle Repetitions for subgrade (SAR7 - Subgrade), and Standard Axle Repetitions for Cement Treated Materials (SAR12 - Cement Treated Materials) were calculated by changing the exponent value to 5, 7, and 12, respectively.

g) Then, the total ESA values were calculated by adding them.

The general equation to calculate the traffic multiplier value is given by Equation 4.6.

$$\boldsymbol{Traffic\ Multiplier} = \frac{\boldsymbol{SAR_x}}{\boldsymbol{ESA}} \text{-------} \textit{Equation 4.6}$$

Equation to calculate the traffic multiplier values for Asphalt, Subgrade and Cement Treated Materials are given by Equation 4.7, Equation 4.8, and Equation 4.9 respectively.

$$\boldsymbol{Traffic\ Multiplier\ (Asphalt)} = \frac{\boldsymbol{SAR_5}}{\boldsymbol{ESA}} \text{ ----------Equation 4.7}$$

$$\boldsymbol{Traffic\ Multiplier\ (Subgrade)} = \frac{\boldsymbol{SAR_7}}{\boldsymbol{ESA}} \text{ ----------Equation 4.8}$$

$$\boldsymbol{Traffic\ Multiplier\ (Cement\ Treated\ Materials)} = \frac{\boldsymbol{SAR_{12}}}{\boldsymbol{ESA}}. \text{ ---- Equation 4.9}$$

ii. Use of AADT and MCC data

a) The number of years that the pavement was operated was found by the historical data obtained from RDA (Years)
b) The most heavily trafficked lane in the carriageway was identified.
c) The percentage of heavy vehicles (%HV) in the traffic stream was estimated using MCC data.

The percentage of heavy vehicles is given by Equation 4.10.

$$\boldsymbol{Percentage\ Heavy\ Vehicles} = \frac{\boldsymbol{Total\ Heavy\ Vehicles}}{\boldsymbol{Total\ Vehicles}} \times \mathbf{100}\% \text{ -------- Equation 4.10}$$

d) The Lane Distribution Factor (LDF) was determined.
e) Heavy vehicle growth throughout the consumed period was estimated using the equation for Cumulative Growth Factor (CDF)

Cumulative Growth Factor (CGF) is given by Equation 4.11.

$$\boldsymbol{Cumulative\ Growth\ Factor(CGF)} = \frac{(\mathbf{1+0.01}\boldsymbol{R})^{\boldsymbol{P}}\mathbf{-1}}{\mathbf{0.01}\boldsymbol{R}}, \boldsymbol{for\ R > 0} \text{ ----- Equation 4.11}$$

R= Annual heavy vehicle growth rate (%)

P = Consumed period (years)

f) The average number of axle groups per heavy vehicle (N_{HVAGs}) was estimated using Equation 4.12.

$$N_{HVAGs} = \frac{Total\ Number\ of\ Heavy\ Vehicle\ Axles}{total\ Number\ of\ Heavy\ Vehicles}$$ ----------*Equation 4.12*

g) The cumulative number of heavy vehicle axle groups over the consumed period (N_{DT}) was calculated using Equation 4.13.

$$N_{DT} = 365 \times AADT \times DF \times \%HV \times N_{HVAGs} \times LDF \times CGF$$ -------*Equation 4.13*

N_{DT} = Cumulative number of heavy vehicle axle groups (When axles are less than 2.1 m apart, they are considered as axle group)

AADT = Average Annual Daily Traffic

DF = Direction Factor

%HV = Percentage of Traffic That Are Heavy Vehicles

N_{HVAGs} = Average Number of Axle Groups Per Heavy Vehicle

LDF = Lane Distribution Factor

CGF = Cumulative Growth Factor

Calculations of the values for lane distribution factor (LDF) and direction factor (DF) were conducted as recommended in the Austroads guideline. Average annual daily traffic (AADT) values for the A11 road could be obtained from the Planning Division, Road Development Authority. The %HV was calculated using the vehicle composition in the Manual Classified Count (MCC) data obtained from the Planning Division, Road Development Authority, Sri Lanka, for the A11 road.

h) Calculation of Design number of Equivalent Standard Axles (DESA) of traffic loading is done by employing Equation 4.14.

$$DESA = \frac{ESA}{HVAG} \times N_{DT}$$ ----------*Equation 4.14*

ESA/HVAG = Average number of Equivalent Standard Axles per Heavy Vehicle Axle Group

N_{DT} = cumulative number of Heavy Vehicle Axle Groups over the design period

4.5.5 Traffic Load Distribution for A11 road

It was required to obtain the Traffic Load Distribution (TLD) file as an input to the mechanistic design software-CIRCLY. Axle distribution (%) obtained from the axle load survey data was used to derive the TLD file. Guidelines given by the Mechanistic design software-CIRCLY manual were followed to get the TLD file. Once the traffic load distribution file is imported to CIRCLY, it automatically calculates the Average number of Equivalent Standard Axles per Heavy Vehicle Axle Group (ESA/HVAG) value. Consequently, manually calculating the NDT value was only necessary to get the Design number of Equivalent Standard Axles (DESA) traffic loading.

4.5.6 Obtaining Cumulative Damage Factor (CDF) Values for A11 Road using mechanistic design software-CIRCLY.

Once the layer moduli were found, the next step was to estimate the CDF values according to the Austroads guidelines. Since the mechanistic design software-CIRCLY was available, it was easy to calculate the CDF values time efficiently.

Material properties to be input to the mechanistic design software-CIRCLY are summarized below.

i. Modulus (MPa)
ii. Poisson's ratio
iii. Bitumen content (VB%)
iv. Performance exponent (b in the performance relationship)
v. Shift factor (presumptive value = 6)

Consequently, these material properties, such as the resilient modulus (obtained from FWD back-calculation), Poisson's ratio, Bitumen content (VB%), Performance exponent (b), and Shift factor of the pavement layers, were input to the mechanistic design software-CIRCLY manually. It was only required to input the resilient modulus (MR) and Poisson's ratio for the macadam base course, subbase, and subgrade layers. The performance exponent (b) range was set from b=4.5 to b=5.5 for the analysis. The default performance exponent (b) is b=5, given in the Austroads mechanistic pavement guideline. The shift factor (SF) value was kept at the default SF=6, as shown in the Austroads pavement design guideline. When the VB (%) is input manually, the

mechanistic design software automatically calculates the performance constant (k). The VB value is non-zero; therefore, the modulus and VB calculate the performance constant (k).

Once the material properties of the pavement layers were input, the pavement systems were introduced to the software for each selected location of the A11 road. The pavement systems for the A11 road consisted of layers, Asphalt, macadam base course, subbase, and subgrade layers. Material properties of the pavement layers differed from location to location, so it was required to introduce them individually for each selected location of the A11 road. Consequently, a separate pavement system was introduced to the software for each chosen location on the road. Pavement layer thicknesses of the pavement system were obtained from the test pit data of the A11 road. Then, each pavement system was detailed with the layer thicknesses as given in the test pit data obtained from the RDA. Since some of the locations in the test pit data varied significantly, an average thickness values for each layer were used as input for the CDF calculations. Pavement layer thicknesses used for CDF calculations are given in Table 4.5. The basis for using the average values is that during the FWD analysis, it only allowed inputting one pavement layer system. CDF calculation also accommodated the same layer thicknesses, averaged from test pit data for the A11 road.

Table 4.5: Pavement layer thicknesses for CDF calculations

Pavement Layer	Thickness
Asphalt layer	150mm
Macadam base layer	120mm
Subbase Layer	250mm

4.5.7 Calculation of Cumulative Damage Factor (CDF) for the A11 road

Calculating cumulative damage factor (CDF) was done for the selected locations of the A11 road. The methodology mentioned in the previous chapter to calculate the CDF values was followed during the CDF analysis.

The Total Damage Factor is defined by the Equation 4.15:

$$\boldsymbol{CDF_{Total}} = \sum_{\boldsymbol{i=1}}^{\boldsymbol{LoadCases}} \boldsymbol{CDF_i} \quad \text{----------}\textit{Equation 4.15}$$

i is summed over the mix of loads, for example, different container vehicles.

The calculation of the CDF incorporates several design parameters in materials, traffic, and environment.

Cumulative damage factor (CDF) values, representing the damage present in the pavement layers, were calculated for each selected location of the A11 road at each project reliability level given in the mechanistic design software-CIRCLY at varying performance exponents and shift factors. The project reliability levels in the Austroads guide were 50%, 80%,85%,90%, 95% and 97.5%. Austroads (2017) was chosen as the design method from the drop-down menu in the software.

4.6 Calculation of Alligator Cracking Index (ACI)

The Alligator Cracking Index (ACI) is a numerical indicator that rates the surface condition of an asphalt pavement. ACI is calculated by quantifying alligator cracking areas and their severities. It is also a good measure of the present condition of the pavement. ACI can show the pavement's structural integrity and surface operational condition (localized roughness and safety). It cannot measure structural capacity nor directly measure skid resistance or roughness.

Consequently, ACI can determine maintenance and repair needs and priorities. Continuous monitoring of the ACI is essential to establishing pavement deterioration rate, which allows the early identification of significant rehabilitation needs. The ACI provides feedback on pavement performance to validate or improve current pavement design and maintenance procedures. Usually, A new pavement section is considered theoretically distress-free and has an ACI value of 100.

A field survey was conducted to identify the alligator cracks and their severity in the A11 road. Only the left-hand side (LHS) of the A11 road was selected for the data collection. Digital images and surface areas of the distress were collected from the Planning Division, Road Development Authority (RDA), Sri Lanka, to detect and classify alligator cracking data. The exact locations selected for calculating the Cumulative Damage Factor (CDF) were considered to estimate the Alligator Cracking

Index (ACI). Only the first 6km (0+000- 6+250) of the A11 road was selected for the model development purpose considering the availability of the required data.

The pavement consisted of varying thicknesses throughout the selected section. Alligator cracks were rated according to the severity of the cracks, and the areas of the alligator cracks and their severities were incorporated in calculating the alligator cracking index (ACI). The methodology mentioned in the previous chapter to calculate the ACI was followed during the calculation process. The Equation 4.16 was used for the estimation of ACI.

$$\boldsymbol{AC\ Index = 100 - 40 \times \left[\left(\frac{\%LOW}{70}\right) + \left(\frac{\%MED}{30}\right) + \left(\frac{\%HI}{10}\right)\right]} \text{-------} \textit{Equation 4.16}$$

The values %LOW, %MED and %HI report the percentage of the observed pavement (32m, primary lane) that contains alligator cracking within the respective severities.

These values range from ≥ 0 to ≤ 100.

%LOW = Percent of total area (primary lane, 32m in length), low severity

%MED = Percent of total area (primary lane, 32m in length), medium severity

%HI = Percent of total area (primary lane, 32m in length), high severity

Percent of the total area is given in Equation 4.17.

$$\boldsymbol{Percent\ of\ total\ area = \frac{square\ meter\ area\ of\ alligator\ crack\ severity\ (m^2)}{32\ m \times lane\ width\ (m)}} \text{----}$$

Equation 4.17

Once the ACI values were calculated from the Alligator cracking data collected from the A11 road, cumulative damage factor (CDF) values were calculated for the exact locations using the mechanistic design software-CIRCLY.

4.7 Regression Model Development

Since the objective of this research was to find the most suitable modified performance relationship that gives the best fatigue prediction, the researchers focused on checking the CDF values for different damage exponent values (b) and for various shift factors (SF) to find the best combination of the damage exponent and the shift factor. OriginPro statistical analysis software was used for the data analysis. The damage exponent (b) was varied from 4.5 to 5.5 in 0.1 steps starting from 4.5 (the default damage exponent recommended in the Austroads guide is 5 for asphalt fatigue). This analysis was done at six reliabilities beginning from 50% to 97.5%, as given in the mechanistic design software-CIRCLY, to check the variation of the CDF.

Previously calculated Alligator cracking index (ACI) values for each location of the A11 road were incorporated to check the relationship between the Alligator Cracking Index (ACI) and the Cumulative Damage Factor (CDF) obtained at varying damage exponents and shift factors. Regression models were derived at each reliability available in the mechanistic analysis tools design software -CIRCLY and the Austroads mechanistic pavement design guideline at each damage exponent value (b) ranging from b=4.5 to b=5.5. The best-fit regression model between the Alligator cracking index (ACI) and Cumulative damage factor (CDF) was chosen based on the least mean squared error (MSE) value.

4.8 Model Validation

Once the regression model between the ACI and CDF was derived, the following requirement was to validate the derived regression model. Validation of the derived regression model representing the relationship between the ACI and CDF incorporated data obtained from the A10 road (Katugasthota – Kurunegala – Puttalam). A section of the A10 road (Katugasthota – Kurunegala – Puttalam) was selected for the data analysis. The selected road section is from 63+000 to 83+500. The following data were obtained from the Road Development Authority (RDA), Sri Lanka, for the validation procedure.

4.8.1 Estimation of Cumulative Damage Factor (CDF) for A-10 road using the mechanistic-design software – CIRCLY

The model validation procedure consisted of two main phases. The first phase calculated the Estimation of Cumulative Heavy Vehicle Axle Groups (in the Design Lane) over the Design Period (N_{DT}). The second phase was estimating the layer moduli values of the pavement layers of the A10 road. The mechanistic design software CIRCLY required these calculated NDT and layer moduli values to estimate the cumulative damage factor (CDF). A summary of the data obtained is mentioned below.

Data obtained for traffic calculations:

i. Axle load survey data
ii. Average annual daily traffic (AADT) data
iii. Manual classified count (MCC) data

Data obtained for the estimation of layer moduli:

i. Falling weight deflectometer (FWD) data
ii. Temperature data to estimate the Weighted mean annual pavement temperature (WMAPT) required for the FWD analysis.
iii. Test pit data to obtain layer thicknesses.

4.8.2 Phase 1: Estimation of Cumulative Heavy Vehicle Axle Groups (in the Design Lane) over the Design Period (N_{DT}) for A10 road

Axle load survey data, Manually classified count data, and average annual daily traffic data obtained from the Planning Division, Road Development Authority (RDA), Sri Lanka, were incorporated to estimate N_{DT} for the A10 road. Traffic parameters such as the N_{DT} and the traffic load distribution (TLD) were assessed according to the steps mentioned in the Austroads design guideline. A similar methodology, as mentioned in the Austroads guideline followed for the A11 road, was incorporated to obtain the N_{DT} and the traffic load distribution of the A10 road. The calculated N_{DT} was manually input, and the TLD was manually imported to the mechanistic design software – CIRCLY.

4.8.3 Phase 2: Estimation of layer moduli of A10 road

i. Calculation of Weighted Mean Annual Pavement Temperature (WMAPT) for A-10 Road

Weighted mean annual pavement temperature (WMAPT) for the selected section of the A10 road, i.e., 63+000 to 83+500 of the A10 road, was calculated following the steps given in the Austroads guideline to estimate the WMAPT. Similar steps for calculating the WMAPT for the A11 road were followed during this procedure. The following data were obtained from the A10 for WMAPT calculation.

i. The monthly average daily maximum air temperature
ii. The monthly average daily minimum air temperature
iii. The monthly average air temperature

Since the FWD data for A10 were obtained in 2014, the temperature data collected was also for 2014. Temperature data for 2014 is presented in Table 4.6.

Table 4.6: Temperature data for the year 2014

Month	The monthly average daily maximum air temperature (°C)	The monthly average daily minimum air temperature (°C)	The monthly average air temperature (°C)
January	32	20	27
February	35	18	29
March	38	22	30
April	35	19	29
May	33	24	29
June	32	24	29
July	32	25	28
August	32	23	28
September	33	23	28
October	33	23	27
November	32	22	26
December	32	22	26

Once the temperature data was collected, the next step was calculating the weighting factors (WF). The Equation 4.18 recommended in the Austroads guide was accommodated to calculate the weighting factors for each month of 2014.

Shell Weighting Factors (Chart W of Shell International Petroleum Company (1978)).

$$\boldsymbol{WF = 10^{(-1.224+0.0650T_{air}-0.000145T_{air}^{2})}} \quad \textit{----Equation 4.18}$$

WF values for the months of the 2014 year were calculated as presented in Table 4.7

Table 4.7: WF values for the months of 2014

Month	**The monthly average daily maximum air temperature (°C)**	**The monthly average daily minimum air temperature (°C)**	**The monthly average air temperature (°C)**	**Weighting Factors (WF)**
January	32	20	27	2.676
February	35	18	29	3.478
March	38	22	30	3.962
April	35	19	29	3.478
May	33	24	29	3.478
June	32	24	29	3.478
July	32	25	28	3.052
August	32	23	28	3.052
September	33	23	28	3.052
October	33	23	27	2.676
November	32	22	26	2.345
December	32	22	26	2.345

The average value of WF = 3.089294

The weighted mean annual air temperature (WMAAT) values were calculated using the following equation by accommodating the WF values.

WMAAT from average WF (Chart W of Shell International Petroleum Company (1978)). WMAAT was calculated using Equation 4.19.

$$\boldsymbol{WMAAT = 19.66 + 16.91\, logWF + 0.3117 \times (logWF)^2} \quad \textit{-----Equation 4.19}$$

WMAAT = 28.0183

The Weighted mean annual pavement temperature (WMAPT) was calculated using the Equation 4.20.

Estimating WMAPT from WMAAT (Chart RT Shell International Petroleum Company (1978), 100 mm asphalt).

$$\boldsymbol{WMAPT = -12.4 + \frac{6.32(WMAAT)}{ln(WMAAT)}}$$ -------*Equation 4.20*

WMAPT for A10 road = 41°C

Calculated in-service pavement temperature - WMAPT of the A10 road was then input to the back-calculation software- KUAB PVD to obtain the layer moduli at the in-service pavement temperature.

4.8.4 Back-calculation of Layer moduli using Falling weight deflectometer (FWD) data.

Falling weight deflectometer (FWD) data for the A10 road was then analysed using the back-calculation software- KUAB PVD.

A10 road consisted of asphalt, aggregate base course, subbase, and subgrade layers. Pavement layer thicknesses obtained from the A10 road were used to input the FWD back-calculation procedure. The layer thicknesses of the road were not uniform throughout the length of the selected section for the analysis. A typical cross-section of the A10 road is illustrated in Figure 4.2.

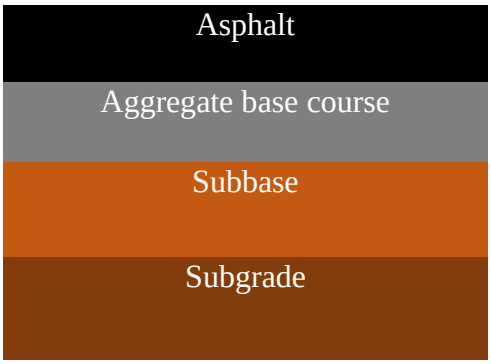

Figure 4.2: Typical cross-section of the A10 road

Since the road had varying thicknesses of pavement layers, an average value of pavement thickness was used for the back-calculation procedure. The average values of the pavement layer thicknesses used for the FWD back-calculation procedure are mentioned in Table 4.8.

Table 4.8: Thickness used for the FWD back-calculation procedure.

Pavement layer	Layer thickness
Asphalt	110mm
Macadam base	150mm
Subbase	250mm
Subgrade	N/A

Then, the calculated WMAPT value for the A10 road was input to the KUAB PVD back-calculation software to back-calculate the layer moduli at the in-service pavement temperature - WMAPT. Once the FWD data were back-calculated to get the moduli of the pavement layers, back-calculated and temperature-corrected moduli were introduced to the mechanistic design software –CIRCLY. A separate pavement system was introduced for each selected location of the A10 road.

Consequently, the pavement layers' back-calculated layer moduli values from the FWD analysis and the typical Poisson's ratio values (Table 4.3) were input as the material properties to the mechanistic design software-CIRCLY. Then, the CDF values for each selected location of the A10 road were calculated.

4.9 Calculation of Alligator cracking index (ACI) for A10 road

Alligator cracking index (ACI) values of the selected locations of the A10 road were estimated by incorporating the derived regression model by substituting the previously calculated CDF values for the A10 road. In the meantime, the actual ACI values from the in-service pavement were also estimated following the steps mentioned before. Consequently, the variation of observed ACI with the predicted ACI from the derived regression model was checked to assess the accuracy of the derived regression model. When the observed ACI values were plotted against the predicted ACI values, it could be identified that the data lies around the 1:1 line, emphasizing the accuracy of the derived regression model.

5 RESULTS

5.1 Understanding the importance of adapting the Austroads mechanistic guideline for tropical climates

Initially, a separate analysis was conducted to understand the requirement of adapting the Austroads mechanistic pavement design methodology for tropical climatic conditions—the analysis involved three pavement design guidelines. Two were conventional empirical pavement design methods; Transport Research Laboratory (TRL) Overseas Road note 31 and American Association of State Highway and Transportation Officials (AASHTO) pavement design guides. However, it was found by a previous research by Jayarathna and Mampearachchi (2017) that the mechanistic design software CIRCLY which is based on Austroads pavement design guideline could be introduced as a good analytical tool for designing road pavements in tropical climatic conditions. The researcher also used the mechanistic design software CIRCLY to investigate pavement failure and to propose suitable reclamation methods successfully in her research. Consequently, considering the justification and the validation of using mechanistic design software - CIRCLY for the design and analysis of pavements in tropical climates, the pavement designs obtained from TRL Road Note 31 and AASHTO design guidelines were then verified by Austroads mechanistic pavement design guide by accommodating the mechanistic design software CIRCLY to check for any possible discrepancies or improvements to be made. The mechanistic design software – CIRLCY accompanied default failure functions suggested by the Austroads guide.

A summary of design thicknesses given by TRL Road Note 31, AASHTO, and Austroads is presented in Table 5.1.

Table 5.1: Summary of design thicknesses given by TRL Road Note 31, AASHTO, and Austroads - CIRCLY

Design life (Years)	Layers	Thickness assuming A1 distribution		Thickness assuming A6 distribution			
		Road Note 31	Verification by Austroads	Road Note 31	Verification by Austroads	AASHTO	Verification by Austroads
10	Asphalt	100mm	130mm	100mm	160mm	178 mm	178 mm
	Base	200mm	200mm	200mm	200mm	153 mm	153 mm
	Subbase	250mm	250mm	250mm	250mm	178 mm	178 mm
15	Asphalt	125mm	140mm	125mm	170mm	178 mm	178 mm
	Base	225mm	225mm	225mm	225mm	153 mm	153 mm
	Subbase	250mm	250mm	250mm	250mm	153 mm	153 mm

It was observed that the Austroads mechanistic procedure outputs different layer thicknesses than the thickness designs given by the other two conventional empirical pavement design methods, i.e., TRL Road Note 31 and AASHTO. This observation was prominent, especially for the asphalt layer thicknesses. When default failure functions suggested by Austroads were accompanied, it was observed that the output layer thicknesses were improved compared to that of the empirical pavement design methods. Consequently, calibrating the performance models to suit the local conditions will enable the effective use of available and novel materials, thereby reducing the constraints in the design and construction of flexible pavements in tropical climates. Calibrating the default performance models will also result in improved layer thicknesses compared to the pavement systems given by traditional pavement design methods such as TRL Road Note 31 and AASHTO. The designs will be more reliable as every pavement system is mechanistically analysed for each pavement material and their strength parameters and environmental conditions and traffic conditions. Additionally, it will reduce the hauling cost of materials from far sites, leading to more user-friendly, cost-effective, and time-efficient pavement design procedures by utilizing an integrated mechanistic design software – CIRCLY. This will help nations to save a lot of time and money wasted due to design and construction

constraints we face due to the conventional pavement design guidelines such as TRL Road Note 31 and AASHTO.

5.2 Calculation of Cumulative damage factor (CDF)

5.2.1 Estimation of Weighted Mean Annual Pavement Temperature (WMAPT)

It was necessary to assess the material properties, such as the resilient moduli of the pavement layers, to estimate the Cumulative damage factor (CDF) using the mechanistic design software-CIRCLY. Consequently, the Weighted Mean Annual Pavement Temperature (WMAPT) for the A11 road (for model development) and A10 road (for model validation) were estimated to back-calculate the Falling weight deflectometer (FWD) data at the in-service pavement temperature (WMAPT), thereby obtaining the temperature corrected resilient moduli values of pavement layers. WMAPT value for the A11 road was incorporated during the model development stage to estimate the layer moduli of the A11 road. Consequently, WMAPT values for the A10 road were used during the model validation stage to estimate the layer moduli values of the A10 road. The calculation of WMAPT incorporated various temperature data and steps as given in the Austroads mechanistic pavement design guideline. Steps mentioned in chapter 4 to calculate the WMAPT were followed during the WMAPT analysis.

Results of the WMAPT calculation of the A11 road for 2012 are illustrated in Table 5.2.

Table 5.2: WMAPT for A-11 road for the year 2012

Month	Max	Min	Avg	WF
Jan	30	19	26	2.345
Feb	31	20	27	2.676
Mar	34	20	29	3.478
Apr	34	23	30	3.962
May	35	24	31	4.510
Jun	34	24	30	3.962
Jul	34	24	30	3.962
Aug	34	24	31	4.510
Sep	35	24	31	4.510
Oct	33	23	29	3.478
Nov	31	22	27	2.676
Dec	29	21	26	2.345
Average WF				3.534
WMAAT				29.026
WMAPT				42.063

5.2.2 Back-Calculation of layer moduli

Deflection data obtained from the non-destructive testing (NDT) of the Falling weight deflectometer (FWD) were utilized to estimate the back-calculated layer moduli of the two selected roads for model development and model verification. KUAB PVD software is available at the Research and Development Division at RDA and was used for the moduli back-calculation procedure. These back-calculated moduli were corrected at the Weighted Mean Annual Pavement Temperature (WMAPT) as recommended in the Austroads mechanistic pavement guideline. WMAPT for the A11 road was 42°C, and the WMAPT for the A10 road was found to be 41°C. The model development stage used the back-calculated layer moduli for the A11 road (Maradankadawala-Habarana-Thirukkondaiadimadu). In contrast, the model verification stage used layer moduli values for the A10 (Katugasthota – Kurunegala – Puttalam). These back-calculated layer moduli of the A11 road and A10 roads

estimated at the in-service pavement temperature (WMAPT) were input to the mechanistic pavement design software-CIRCLY as material parameters to obtain Cumulative damage factor (CDF) values for the model development and the model validation respectively.

A summary of the back-calculated layer moduli values at the in-service pavement temperature (WMAPT) for the A11 road obtained from Non-destructive testing is summarized in Table 5.3.

Table 5.3: Moduli of pavement layers – A11 road

Position	**Asphalt**	**Base**	**Subbase**	**Subgrade**
m	**MPa**	**MPa**	**MPa**	**MPa**
0	1022.61	511.31	187.17	79.56
260	1103.79	543.27	160.64	123.46
501	1184.96	575.22	134.11	167.36
742	2077.13	537.64	200.25	181.63
1000	2969.30	500.05	266.38	195.90
1255	2162.22	500.03	370.01	342.01
1500	1355.14	500.00	473.64	488.11
1820	1489.03	516.44	262.86	352.98
2000	1622.92	532.87	52.07	217.84
2280	1332.61	516.44	156.32	181.58
2505	1042.29	500.00	260.57	145.32
2763	1482.97	508.47	181.81	116.89
3003	1923.65	516.93	103.05	88.46
3256	1471.89	513.50	158.92	84.56
3502	1020.12	510.06	214.78	80.66
3759	1020.35	510.17	211.52	78.49
4001	1020.57	510.28	208.25	76.32
4302	1020.71	510.35	206.57	78.04
4500	1020.85	510.42	204.88	79.76
4771	1454.94	506.86	138.25	95.25

Table 5.3: Moduli of pavement layers – A11 road

5003	1889.02	503.30	71.62	110.74
5272	1889.70	501.67	97.85	114.93
5500	1890.37	500.04	124.08	119.12
5808	1459.10	506.98	134.97	108.88
6004	1027.83	513.91	145.86	98.64
6250	1083.11	533.01	111.64	94.60
6500	1138.38	552.11	77.42	90.56

5.3 Cumulative Damage Factor (CDF) analysis for Model Development

Back-calculated layer moduli values obtained at the in-service pavement temperature (WMAPT) for the A11 road were used to obtain the Cumulative damage factor (CDF) values for model development. CDF values were estimated for each selected location of the A11 road, and the mechanistic design software- CIRCLY, based on the Austroads mechanistic pavement design guideline, was utilized for CDF analysis. Material properties such as resilient modulus, Poisson's ratio, and traffic parameters such as N_{DT} (cumulative number of heavy vehicle axle groups) and the traffic load distribution were manually input into the software before the analysis. N_{DT} for A11 road (10 years) was N_{DT} =1.546E+7.

Since the objective of this research was to find the most suitable modified performance relationship that gives the best fatigue prediction, the researchers focused on checking the CDF values for different damage exponent values (b) and for various shift factors (SF) to find the best combination of the damage exponent and the shift factor. The damage exponent (b) was varied from 4.5 to 5.5 in 0.1 steps starting from 4.5 (the default damage exponent recommended in the Austroads guide is 5 for asphalt fatigue). This was done at six reliabilities beginning from 50% to 97.5% to check the variation of the CDF.

5.4 Alligator Cracking Index (ACI) Analysis for Model Development

A summary of the alligator cracking index (ACI) for the first 6km of the A11 road is presented in Table 5.4.

Table 5.4: Alligator cracking index (ACI) for A11 road

Location	Alligator Cracking Index (ACI)
0+006	78
0+260	80
0+500	83
0+742	69
01+001	88
01+255	90
01+503	91
1+820	84
02+000	42
2+280	66
02+500	71
02+763	66
03+003	47
03+256	63
03+503	44
03+759	87
04+002	84
04+302	81
04+501	85
04+771	56
05+001	41
05+272	46
05+501	55
05+808	60
06+002	67
06+250	65

5.5 Regression Model Development

In parallel with the CDF calculation, the alligator cracking index was also calculated for each location of the A11 road to check the relationship between the Alligator Cracking Index (ACI) and the Cumulative Damage Factor (CDF) obtained for varying damage exponents (b). Regression models were derived for each damage exponent value ranging from b=4.5 to b=5.5 at each reliability. The best-fit regression model between the Alligator cracking index (ACI) and Cumulative damage factor (CDF) was chosen based on the least mean squared error (MSE) value.

The regression model having the least MSE was observed to be at the reliability = 80% with a damage exponent = 5.1. It should be noted that at the reliability = 80%, the reliability factor (RF) = 2.4. Since the reliability factor (RF) at reliability = 50% is one, the researchers' checked the requirement of changing the shift factor to get the same CDF values at reliability=80% and b=5.1. At Reliability=50% and b=5.1, the same results could be obtained when the SF is reduced to 2.5.

Table 5.5 shows the parameters of the statistical analysis.

Table 5.5: Parameters of the statistical analysis

		Value	**Standard Error**	**t-Value**	**Prob>|t|**
Alligator Cracking Index	Intercept	100	--	--	--
	B1	-7.45546	3.09739	-2.40701	0.02451
	B2	-11.56903	2.91818	-3.96447	6.14406E-4
	B3	2.56778	0.62297	4.12185	4.15514E-4

5.6 Regression model

The derived regression model is presented in Equation 5.1

$$\boldsymbol{ACI = -7.455\,CDF^3 - 11.569\,CDF^2 + 2.568\,CDF + 100} \quad \text{---}\textit{Equation 5.1}$$

Table 5.6, Table 5.7, and Table 5.8 are the statistics, summary, and ANOVA results of the statistical analysis.

Table 5.6: Statistics

	Alligator Cracking Index
Number of Points	26
Degrees of Freedom	23
Residual Sum of Squares	289.836
R-Square (COD)	0.998
Adj. R-Square	0.997

Table 5.7: Summary

	Intercept		**B1**		**B2**		**B3**		**Statistics**
Alligator Cracking Index	Value	Standard Error	Value	Standard Error	Value	Standard Error	Value	Standard Error	Adj. R-Square
	100	--	-7.45546	3.09739	-11.56903	2.91818	2.56778	0.62297	0.99747

Table 5.8: ANOVA

		DF	**Sum of Squares**	**Mean Square**	**F Value**	**Prob>F**
Alligator Cracking Index	Model	3	129418.41131	43139.47044	3423.34278	0
	Error	23	289.83595	12.60156		
	Total	26	129708.24727			

Variation of the Alligator cracking index (ACI) with Cumulative damage factor (CDF) is presented in Figure 5.1.

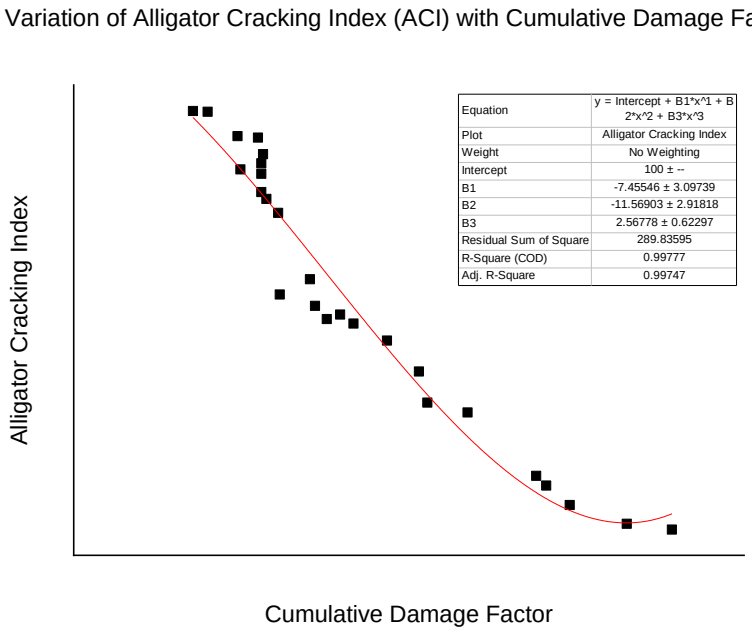

Figure 5.1: Variation of Alligator cracking index (ACI) with Cumulative damage factor (CDF)

Residual plots of the statistical analysis are presented in Figure 5.2

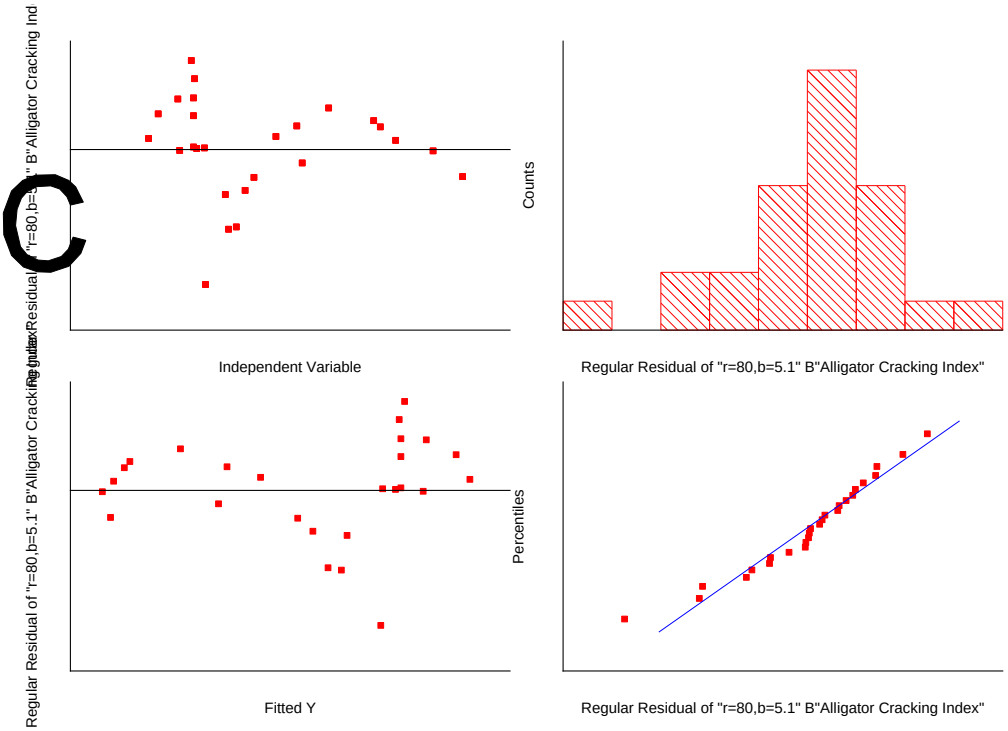

Figure 5.2: Residual plots

The 3rd order regression model fitted to the variation of the ACI with the CDF has an adjusted R-square = 0.997 and a mean squared error (MSE) = 12.602 at the Reliability = 50% (where RF=1), damage exponent for asphalt fatigue (b) = 5.1 and shift factor (SF) = 2.5.

5.7 Regression Model Validation

A separate analysis was conducted using the OriginPro statistical analysis software to validate the derived regression model. Considering the data available, a section of the A10 road (Katugasthota – Kurunegala – Puttalam) was selected for the model validation procedure. The selected road section is from 63+000 to 83+500 of the A10 road.

The weighted mean annual pavement temperature (WMAPT) for the selected road section was initially calculated following the Austroads guideline. WMAPT for A10 road = 41°C.

Results of the WMAPT calculation of the A10 road for 2014 are illustrated in Table 5.9.

Table 5.9: WMAPT for A10 road for the year 2014

Month	Max	Min	Avg	WF
Jan	32	20	27	2.676
Feb	35	18	29	3.478
Mar	38	22	30	3.962
Apr	35	19	29	3.478
May	33	24	29	3.478
Jun	32	24	29	3.478
Jul	32	25	28	3.052
Aug	32	23	28	3.052
Sep	33	23	28	3.052
Oct	33	23	27	2.676
Nov	32	22	26	2.345
Dec	32	22	26	2.345
Average WF				3.089
WMAAT				28.018
WMAPT				41

It was observed that the WMAPT for the A11 road (42°C) is higher than WMAPT for the A10 road (41°C), indicating that the A11 road experiences higher pavement temperatures during the year. This observation is justifiable since the A11 experience warmer temperatures leading to higher in-service pavement temperatures during the year.

Then, the calculated WMAPT value was input to the KUAB PVD back-calculation software to correct the moduli values at the in-service pavement temperature (WMAPT). A summary of the back-calculated layer moduli values at the in-service pavement temperature (WMAPT) for the A10 road obtained from Non-destructive testing is summarized in Table 5.10.

Table 5.10: Moduli of pavement layers – A10 road

Position	**Asphalt**	**Base**	**Subbase**	**Subgrade**
m	**MPa**	**MPa**	**MPa**	**MPa**
63003	2565.42	605.51	654.25	87.44
63500	3079.2	507.22	291.69	108.47
64004	2406.94	519.9	378.74	93.62
64501	3098.07	799.04	915.93	86.55
65007	3148.29	583.69	412.83	81.26
65500	2272.12	421.25	863.72	83.32
66001	2779.74	600.42	611.51	110.11
66504	2334.32	351.89	550.24	58.78
67001	1559.46	509.51	654.09	98.95
67503	3331.36	499.7	343.13	42.27
68001	1640.23	510.18	748.22	141.05
68503	1643.12	425.9	408.86	156.62
69000	1527.22	419.96	940.93	104.08
69503	2601.23	413.95	310.6	162.44
69999	3017.94	543.23	174.65	398.1
70502	3019.67	527.71	244.31	110.98
71006	2122.21	481.5	385.2	227.64
71505	2437.58	413.58	662.79	141.21
72004	2852.99	498.58	478.64	190.46
72501	2284.82	523.58	639.89	200.48
73007	3021.57	560.2	684.65	222
73505	2026.13	734.22	664.39	160.9
74001	3030.92	315.72	647.35	122.13
74506	2631.91	431.39	287.6	59.46
75005	2303.75	497.61	276.45	63.23
75501	2540.18	502.12	326.61	89.77
76000	2975.13	642.63	380.64	82.35

Table 5.10: Moduli of pavement layers – A10 road

76500	2774.33	617.23	411.49	52.91
77003	2721.85	554.17	484.45	57.56
77500	2670.12	559.95	362.43	73.24
78000	2716.55	518.76	356.21	81.43
78500	2379.68	441.19	365.35	75.69
79002	2216.79	423.32	319.22	86
79501	2660.53	423.38	274.03	144.48
80002	2628.78	502	401.6	148.51
80500	2935.18	453.48	303.83	75.94
81003	2702.48	550.23	335.69	79.88
81502	2514.13	543.05	362.04	135.92
82000	2578.38	556.93	534.65	263.22
82500	2963.39	659.3	200.79	88.04
83002	2776.92	416.54	424.23	151
83501	3088.35	707.71	515.55	243.77

Once the FWD data were back-calculated to get the moduli of the pavement layers, back-calculated and temperature-corrected moduli were introduced to the mechanistic design software –CIRCLY by introducing a pavement system for each selected location of the A10 road. The software also imported traffic parameters such as the NDT and the traffic load distribution. The CDF values for each location of the A10 road were estimated afterwards. Consequently, ACI values for the selected locations of the A10 road were predicted by substituting the calculated CDF values for the derived regression model. The actual ACI values from the in-service pavement were also noted. The variation of observed ACI with the predicted ACI is presented in Figure 5.3.

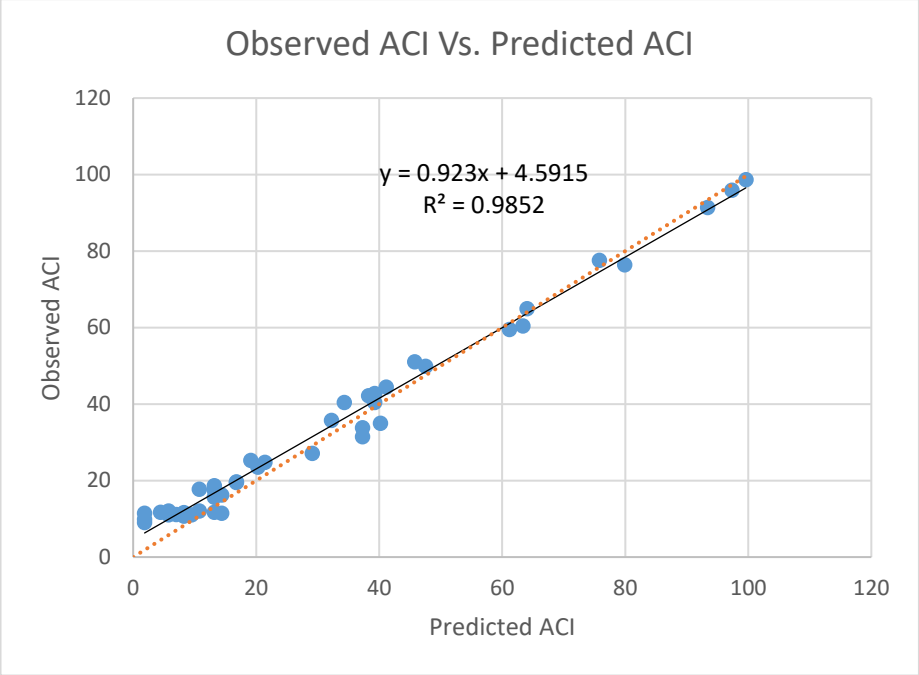

Figure 5.3: The variation of observed ACI with the predicted ACI

A vital stage in research is testing model predictions. One of the most popular methods for assessing the accuracy of model predictions is the scatter plot of predicted vs observed (or vice versa) data. Regressing predicted versus observed values (or vice versa) and comparing slope and intercept parameters to the 1:1 line is a widespread and straightforward model evaluation method (Piñeiro et al., 2008). Piñeiro et al. (2008) strongly recommend that scientists evaluate their models by regressing OP (observed and predicted) values and testing the significance of slope = 1 and intercept = 0.

The black line represents the best fit for the plotted points, whereas the red line represents where the points would fall if all predicted values perfectly matched the observed ones. The closer the two lines are, the better the model's performance is (Martini et al., 2021). In this study, when the observed ACI values were plotted against the predicted ACI values, it can be noticed that the slope of the observed ACI and predicted ACI is slope = 0.923, and the intercept value of the observed ACI and predicted ACI is intercepted = 4.592. This observation emphasizes the accuracy of the derived model, thereby justifying its use for the design and analysis of flexible pavements for tropical climatic conditions.

5.8 Application of the modified fatigue model for the design and analysis of flexible pavements

The data used to understand the requirement of adapting the Austroads mechanistic pavement design methodology for tropical climatic conditions was again used to identify the design and analysis improvements with the newly modified fatigue cracking model obtained from this research. The design thicknesses given by Transport Research Laboratory (TRL) Overseas Road note 31, American Association of State Highway and Transportation Officials (AASHTO), Austroads mechanistic pavement design guideline before adaptation was verified by accommodating the modified fatigue model for Austroads mechanistic pavement design guides. Mechanistic design software-CIRCLY based on the Austroads mechanistic pavement design guide, was accommodated for the new analysis by inputting the modified parameters such as damage exponent (b) and the shift factor (SF).

It was observed that when the modified fatigue failure function for Austroads mechanistic pavement design method was accommodated for designing and analysing flexible pavements, it improved the asphalt layer thicknesses given by conventional flexible pavement design guidelines such as TRL Road Note 31 and AASHTO. It was especially significant that the asphalt layer thicknesses given by default Austroads failure functions were also optimized and improved when the modified fatigue failure function for Austroads was accommodated. This observation was prominent, especially for the asphalt layer thicknesses. This output emphasizes the success of adapting the Austroads mechanistic pavement design method for tropical climates by accommodating the modified fatigue damage model derived in this study.

A summary of design thicknesses given by TRL Road Note 31, AASHTO, and Austroads before and after adaptation for tropical climates is presented in Table 5.11.

Table 5.11: A summary of design thicknesses given by TRL Road Note 31, AASHTO, and Austroads before and after adaptation to tropical climates.

Design life (Years)	Layers	Thickness for A1 distribution			Thickness for A6 distribution					
		(1) Road Note 31	(2) Austroads – Road Note 31	(3) Modified Austroads – Road Note 31	(4) Road Note 31	(5) Austroads – Road Note 31	(6) Modified Austroads – Road Note 31	(7) AASHTO	(8) Austroads – AASHTO	(9) Modified Austroads – AASHTO
		Thickness (mm)								
10	Asphalt	100	130	105	100	160	140	178	178	140
	Base	200	200	200	200	200	200	153	153	153
	Subbase	250	250	250	250	250	250	178	178	178
15	Asphalt	125	140	120	125	170	150	178	178	147
	Base	225	225	225	225	225	225	153	153	153
	Subbase	250	250	250	250	250	250	153	153	153

6 CONCLUSION

This research was focused on adapting the Austroads Mechanistic-Empirical (M-E) pavement design guidelines for tropical climatic conditions. Since the performance models suggested by the Austroads M-E guideline were laboratory-derived under controlled conditions, validating and modifying before adapting to local tropical climates was imperative. Austroads M-E guideline is mainly based on asphalt fatigue cracking and subgrade rutting performance models.

An extensive analytical procedure was initially conducted to identify the requirement of calibrating the default performance models suggested by the Austroads mechanistic pavement design guideline. Two major conventional pavement design guidelines (TRL Road Note 31 and AASHTO) were used to derive pavement systems. Then, these derived pavement systems were validated by the Austroads mechanistic pavement design guideline to identify any requirement for calibration of default failure functions. Mechanistic design software – CIRCLY, based on the default performance models of the Austroads mechanistic pavement design guide, was incorporated for the verification process. Subsequently, it was observed that the Austroads mechanistic pavement design guideline computes different layer thicknesses compared to other conventional empirical pavement design guidelines such as Transport Research Laboratory (TRL) Overseas Road note 31 (Transport Research Laboratory, 1993) and American Association of State Highway and Transportation Officials (AASHTO) (AASHTO, 1993)guidelines.

Furthermore, a recent study by Jayarathna (2017) validated that the Austroads mechanistic design method can be used to design and analyze flexible pavements in local tropical climatic conditions. Even though it was validated that the Austroads mechanistic pavement design method can be accommodated for local tropical climatic conditions, the differences among the pavement thicknesses provided by conventional pavement design methods and Austroads raised the requirement of adapting the Austroads mechanistic pavement design guideline for local tropical climatic conditions. The Austroads mechanistic pavement design guideline is mainly based on two performance models, i.e., asphalt fatigue cracking and subgrade rutting. These

damage models recommended in the Austroads pavement design guide could not directly apply to local tropical conditions due to the differences in the thickness designs provided by the analysis.

Consequently, this finding raised the requirement of adapting the Austroads mechanistic pavement design methods to suit tropical climatic conditions before applying them to designing and analyzing pavements in tropical climates directly. Therefore, these models required specific modifications to suit local tropical climatic conditions. It was identified that the Austroads mechanistic pavement design and analysis procedures could be adapted by modifying/calibrating the default failure functions as suggested in the Austroads mechanistic pavement design guideline. Since there is less effect from the subgrade rutting, only the performance model for asphalt fatigue cracking was selected for the calibration procedure. Adaptation of the fatigue model suggested by the Austroads accompanied by calibration of the damage exponent (b) and the shift factor (SF) as given in the default fatigue relationship.

This study incorporated all the necessary aspects, such as materials, traffic, and the environment, as recommended by the Austroads guide during the analysis process. Data from two A-class roads were obtained for model development and validation. The traffic data, visual survey data, and the falling weight deflectometer (FWD) deflection data required for the research analysis were collected from the Road Development Authority (RDA), Sri Lanka. Temperature data required to estimate the Weighted mean annual pavement temperature (WMAPT) were obtained from the Meteorological Department of Sri Lanka.

Using the mechanistic pavement design software-CIRCLY has made the research analysis time-efficient and user-friendly, making the analysis procedure successful and reliable. Mechanistic design software-CIRCLY incorporated all the recommended elements, such as material properties and traffic conditions, in the Austroads. The use of mechanistic design software-CIRCLY to analyse pavements according to the Austroads mechanistic pavement design guide emphasized the utility of mechanistic tools to design and analyse pavements, ensuring the reliability of such tools in pavement design and analysis procedures in tropical climates. Using the mechanistic

design software-CIRCLY made the research analysis procedure time-efficient in adapting Austroads mechanistic pavement design procedures for tropical climates.

Calculation of the Cumulative damage factor (CDF) included many steps. It was necessary to assess the material properties, such as the resilient moduli of the pavement layers, to estimate the Cumulative damage factor (CDF) using the mechanistic design software CIRCLY. Consequently, the Weighted Mean Annual Pavement Temperature (WMAPT) for the A11 road (for model development) and A10 road (for model validation) were estimated to back-calculate the Falling weight deflectometer (FWD) data at the in-service pavement temperature (WMAPT), thereby obtaining the temperature corrected resilient moduli values of pavement layers. WMAPT values were calculated following the Austroads mechanistic pavement design guide steps. WMAPT for the A11 road was 42°C, and the WMAPT for the A10 road was found to be 41°C. It was observed that the WMAPT for the A11 road (42°C) is higher than WMAPT for the A10 road (41°C), indicating that the A11 road experiences higher pavement temperatures during the year. This observation is justifiable since the A11 experience warmer temperatures leading to higher in-service pavement temperatures during the year. Consequently, with the WMAPT values, back-calculated layer moduli values at the in-service pavement temperature (WMAPT) for both A11 road and A10 were obtained from Non-destructive testing. KUAB PVD back-calculation software was used for the back-calculation of layer moduli.

Back-calculated layer moduli values obtained at the in-service pavement temperature (WMAPT) for the A11 road were used to obtain the Cumulative damage factor (CDF) values for model development. Material properties such as resilient modulus, Poisson's ratio, and traffic parameters such as NDT (cumulative number of heavy vehicle axle groups) and the traffic load distribution were manually input into the software before the analysis. NDT for A11 road (10 years) was N_{DT} =1.546E+7. Mechanistic design software – CIRCLY, based on Austroads mechanistic pavement design guide, was utilized to calculate $N_{DT.}$ Then the CDF values were calculated for different damage exponent values (b) and various shift factors (SF) to find the best combination of the damage exponent and the shift factor. The damage exponent (b) was varied from 4.5 to 5.5 in 0.1 steps starting from 4.5 (the default damage exponent

recommended in the Austroads guide is 5 for asphalt fatigue). This was done at six reliabilities beginning from 50% to 97.5% to check the variation of the CDF. Only the calibration of the fatigue damage model, as suggested in Austroads, was focused on the analysis.

For the model development stage, the alligator cracking index (ACI), a numerical indicator that rates the surface condition of asphalt pavement, was calculated for the first 6km of A11 road using the visual survey data (visual images and surface areas) obtained. The exact locations selected for calculating the Cumulative Damage Factor (CDF) were considered to estimate the ACI. "Distress Identification Manual for the National Park Service Road Inventory Program" was followed for crack detection and classification to determine the severity and extent of distress and calculate distress index values for the FHWA RIP Cycle 4. ACI, suggested by the Federal Highway Administration (FHWA), was successfully applied to quantify fatigue damage in flexible pavements (Federal Highway Administration, 2006).

Then, ppreviously calculated Alligator cracking index (ACI) values for each location of the A11 road were incorporated to check the relationship between the Alligator Cracking Index (ACI) and the Cumulative Damage Factor (CDF) obtained at varying damage exponents and shift factors. The best-fit regression model between the Alligator cracking index (ACI) and Cumulative damage factor (CDF) was chosen based on the least mean squared error (MSE) value. The regression model having the least MSE was observed to be at the reliability = 80% with a damage exponent (b) = 5.1. It should also be noted that at the reliability = 80%, the reliability factor (RF) = 2.4. Since the reliability factor (RF) at reliability = 50% is one, the researchers checked the requirement of changing the shift factor to get the same CDF values at reliability=80% and b=5.1. It was observed that the same results could be obtained at Reliability=50% and b=5.1 when the SF is reduced to SF=2.5. The 3rd order regression model fitted to the variation of the ACI with the CDF has an adjusted R-square = 0.997 and a mean squared error (MSE) = 12.602 at the Reliability = 50% (where RF=1), damage exponent for asphalt fatigue (b) = 5.1 and shift factor (SF) = 2.5.

The regression model is presented by Equation 5.2.

$$ACI = -7.455\,CDF^3 - 11.569\,CDF^2 + 2.568\,CDF + 100$$ ------ *Equation 5.2*

Figure 5.1 shows the variation of the alligator cracking index (ACI) with cumulative damage factor (CDF).

Subsequently, this derived model was validated using the data obtained from the A10 road. A separate analysis was conducted using the OriginPro statistical analysis software to validate the derived regression model. Previously calculated WMAPT value (WMAPT A10 = 41°C) for the A10 road was used to back-calculate layer moduli values at the in-service pavement temperature (WMAPT) for the A10 road obtained from Non-destructive testing. Once the FWD data were back-calculated to get the moduli of the pavement layers, back-calculated and temperature-corrected moduli were introduced to the mechanistic design software –CIRCLY by introducing a pavement system for each selected location of the A10 road. The software also imported traffic parameters such as the NDT and the traffic load distribution. The CDF values for each location of the A10 road were estimated afterwards. Consequently, ACI values for the selected locations of the A10 road were predicted by substituting the calculated CDF values for the derived regression model. The actual ACI values from the in-service pavement were also noted. The variation of observed ACI with the predicted ACI is presented in Figure 5.3.

The black line represents the best fit for the plotted points, whereas the red line represents where the points would fall if all predicted values perfectly matched the observed ones. The closer the two lines are, the better the model's performance is (Martini et al., 2021). In this study, when the observed ACI values were plotted against the predicted ACI values, it can be noticed that the best-fit curve for the observed ACI and predicted ACI has $R^2 = 0.99$ and slope = 1.007. This observation emphasizes the accuracy of the derived model, thereby justifying its use for the design and analysis of flexible pavements for tropical climatic conditions.

The modified performance function for asphalt fatigue damage is presented in Equation 5.3.

6.1 Modified Austroads fatigue criteria for tropical climates.

$$N = \frac{SF}{RF}\left[\frac{6918(0.856V_b + 1.08)}{E^{0.36}\mu\varepsilon}\right]^{5.1} \quad \text{-----}\textit{Equation 5.3}$$

N = allowable number of repetitions of the load-induced tensile strain

με = load-induced tensile strain at the base of the asphalt (micro-strain)

V_b = percentage by volume of bitumen in the asphalt (%)

E = asphalt modulus (MPa)

SF = shift factor between laboratory and in-service fatigue lives (For tropical climates, SF = 2.5)

RF = reliability factor for asphalt fatigue

The data used to understand the requirement of adapting the Austroads mechanistic pavement design methodology for tropical climatic conditions was again used to identify the design and analysis improvements with the newly modified fatigue cracking model obtained from this research. The design thicknesses given by Transport Research Laboratory (TRL) Overseas Road note 31, American Association of State Highway and Transportation Officials (AASHTO), Austroads mechanistic pavement design guideline before adaptation was verified by accommodating the modified fatigue model for Austroads mechanistic pavement design guides. Mechanistic design software-CIRCLY based on the Austroads mechanistic pavement design guide, was accommodated for the new analysis by inputting the modified parameters such as damage exponent (b) and the shift factor (SF).

It was observed that when the modified fatigue failure function for Austroads mechanistic pavement design method was accommodated for designing and analysing flexible pavements, it improved the layer thicknesses given by conventional flexible pavement design guidelines such as TRL Road Note 31 and AASHTO. It was especially significant that the pavement thicknesses given by default Austroads failure functions were also optimized and improved when the modified fatigue failure function for Austroads was accommodated. This observation was prominent,

especially for the asphalt layer thicknesses. This output emphasizes the success of adapting the Austroads mechanistic pavement design method for tropical climates by accommodating the modified fatigue damage model derived in this study.

It can be concluded that adapting the Austroads mechanistic pavement design guideline for tropical climatic conditions is highly favourable by modifying/calibrating the default performance functions by calibrating the damage exponent (b) and the shift factor (SF) to suit the local tropical climatic conditions. The use of mechanistic design software – CIRCLY, which is an integral tool of the Austroads mechanistic pavement design guide, allows the designers and engineers to accommodate the Austroads mechanistic pavement design effectively and time-efficiently given that the damage models based in the software suit the conditions of the road construction project. It was observed that the mechanistic design software – CIRCLY is a user-friendly mechanistic tool for tropical climates as the designer can directly input this damage exponent (b=5.1) and shift factor (SF=2.5) values to the software and proceed with the pavement design and analysis procedure according to the Austroads mechanistic pavement design guideline, effectively and reliably. These modified parameters can be used directly for tropical conditions, which will help the designer use the mechanistic design procedure accurately and efficiently. Adapting the Austroads mechanistic design procedure will address the significant constraints in road construction projects, such as material constraints, time constraints and cost constraints, and it will be highly beneficial to deliver more cost-effective, long-lasting pavement designs promptly. These research findings will finally help reduce any possible overestimation or underestimation of pavement systems, thereby reducing undesirable expenditure and improving the economic aspect of road construction projects.

REFERENCES

AASHTO, A. A. o. S. H. a. T. O. (1993). *AASHTO Guide for Design of Pavement Structures* (Vol. 1). AASHTO.

Aguib, A. A. (2021). Flexible pavement design AASHTO 1993 versus mechanistic-empirical pavement design.

Aher, N. S., & Loya, A. (2019). Structural Evaluation of Flexible Pavement and Rehabilitation using Falling Weight Deflectometer (FWD). *International Journal for Research in Engineering Application & Management (IJREAM), 05*(03).

Ahmed, A. W., & Erlingsson, S. (2015). Evaluation of a permanent deformation model for asphalt concrete mixtures using extra-large wheel-tracking and heavy vehicle simulator tests. *Road Materials and Pavement Design, 16*(1), 154-171.

Al-Suleiman, T. I., Hamici, Z. M., Bazlamit, S. M., & Ahmad, H. S. (2017). Assessment of the effect of alligator cracking on pavement condition using WSN-image processing. International Conference on Engineering, Project, and Product Management,

Austroads. (2010). Guide to pavement technology—Part 2: Pavement structural design. In: Austroads Sydney, Australia.

Austroads. (2012). *Guide to pavement technology: Part 2: Pavement structural design*. Austroads.

Austroads. (2017). Guide to pavement technology-Part 2: Pavement structural design. In. Sydney, Australia: Austroads

Baburamani, P. (1999). *Asphalt fatigue life prediction models: a literature review*.

Bentsen, R. A., Bush III, A. J., & Harrison, J. A. (1989). *Evaluation of Nondestructive Test Equipment for Airfield Pavements. Phase 1. Calibration Test Results and Field Data Collection*.

Brown, S. (1996). Soil mechanics in pavement engineering. *Géotechnique, 46*(3), 383-426.

Ceylan, H., Guclu, A., Tutumluer, E., & Thompson, M. R. (2005). Backcalculation of full-depth asphalt pavement layer moduli considering nonlinear stress-

dependent subgrade behavior. *International Journal of Pavement Engineering*, *6*(3), 171-182.

Chou, Y., & Lytton, R. L. (1991). Accuracy and consistency of backcalculated pavement layer moduli. *Transportation research record*, *1293*, 72-85.

Claessen, A., Edwards, J., Sommer, P., & Uge, P. (1977). Asphalt pavement design--the shell method. Volume I of proceedings of 4th International Conference on Structural Design of Asphalt Pavements, Ann Arbor, Michigan, August 22-26, 1977,

Cook, M. C., Seeds, S. B., Zhou, H., & Hicks, R. G. (2004). Guide for investigating and remediating distress in flexible pavements: california department of transportation's New procedure. *Transportation research record*, *1896*(1), 147-161.

Das, A. (2010). Interpretation of Falling Weight Deflectometer data. Seloflex World Conference,

Dorman, E., & Metcalf, C. (1965). Design Guide. *Austroads Sidney. Sidney, Austrália*.

Elnashar, G., Bhat, R. B., & Sedaghati, R. (2019). Modeling pavement damage and predicting fatigue cracking of flexible pavements based on a combination of deterministic method with stochastic approach using Miner's hypothesis. *SN Applied Sciences*, *1*(3), 1-9.

Erlingsson, S. (2013). Failure modes in pavements. *KTH AF2903 Road Construction and MaintenanceAF2903 Road Construction and Maintenance*.

Federal Highway Administration. (2006). *Pavement Distress Identification Manual for The NPS Road Inventory Program*.

Ferreira, A., Picado-Santos, L. d., Wu, Z., & Flintsch, G. (2011). Selection of pavement performance models for use in the Portuguese PMS. *International Journal of Pavement Engineering*, *12*(1), 87-97.

Finn, F., Saraf, C., Kulkarni, R., Nair, K., Smith, W., & Abdullah, A. (1977). The use of distress prediction subsystems for the design of pavement structures. Volume I of proceedings of 4th International Conference on Structural Design of Asphalt Pavements, Ann Arbor, Michigan, August 22-26, 1977.,

Gillett, S. D. (2001). *Accuracy in mechanistic pavement design consequent upon unbound material testing* University of Nottingham].

Goktepe, A. B., Agar, E., & Lav, A. H. (2006). Advances in backcalculating the mechanical properties of flexible pavements. *Advances in engineering software*, *37*(7), 421-431.

Gribble, M., & Patrick, J. (2008). *Adaptation of the AUSTROADS pavement design guide for New Zealand conditions*. Land Transport New Zealand.

Guide, M.-E. P. D. (2004). Guide for mechanistic empirical design of new and rehabilitated pavement structures. *NCHRP Rep*.

Haas, R., Tighe, S., Dore, G., & Hein, D. (2007a). Mechanistic-empirical pavement design: Evolution and future challenges. Proceedings, Transportation Association of Canada Annual Conference, Saskatoon,

Haas, R., Tighe, S., Dore, G., & Hein, D. (2007b). Mechanistic-empirical pavement design: Evolution and future challenges. Annual Conference and Exhibition of the Transportation Association of Canada, Saskatoon, SK,

Hall, K. D., Xiao, D. X., & Wang, K. C. (2011). Calibration of the mechanistic–empirical pavement design guidefor flexible pavement design in Arkansas. *Transportation Research Record*, *2226*(1), 135-141.

Hall, K. T., & Mohseni, A. (1991). Backcalculation of asphalt concrete-overlaid Portland cement concrete pavement layer moduli. *Transportation research record*(1293).

Hicks, R., Finn, F., Monismith, C., & Leahy, R. (1993). Validation of SHRP binder specification through mix testing (with discussion). *Journal of the Association of Asphalt Paving Technologists*, *62*.

Hoffman, M. S., & Thompson, M. R. (1982). *Backcalculating nonlinear resilient moduli from deflection data*.

Horak, E., & Emery, S. (2006). Falling weight deflectometer bowl parameters as analysis tool for pavement structural evaluations. Research into Practice: 22nd ARRB ConferenceARRB Group Limited,

Huang, Y. H. (1993). *Pavement analysis and design*.

Husain, S., & George, K. (1982). In Situ Pavement Moduli from Dynaflect Deflection. *Transportation research record*, *1043*.

Islam, M. R., & Tarefder, R. A. (2016). Developing temperature-induced fatigue model of asphalt concrete for better prediction of alligator cracking. *Journal of Materials in Civil Engineering*, *28*(5), 04015193.

Jayarathna, K. A. R. N. (2017). *Validation of mechanistic empirical design approach for pavement design – Case study for Sri Lanka* University of Moratuwa].

Jayarathna, K. A. R. N., & Mampearachchi, W. K. (2017). *Validation of mechanistic empirical design approach for pavement design-case study for Sri Lanka*

Khattak, M. J., & Baladi, G. Y. (2013). Analysis of fatigue and fracture of hot mix asphalt mixtures. *International Scholarly Research Notices*, *2013*.

Kim, Y.-R., Little, D., & Lytton, R. (2003). Fatigue and healing characterization of asphalt mixtures. *Journal of Materials in Civil Engineering*, *15*(1), 75-83.

Lee, H., & Kim, J. (2005). Development of a crack type index. *Transportation research record*, *1940*(1), 99-109.

Leonards, G. A. (1982). Investigation of failures. *Journal of the Geotechnical Engineering Division*, *108*(2), 187-246.

Li, Z. (2005). *A probabilistic and adaptive approach to modeling performance of pavement infrastructure*. The University of Texas at Austin.

Lytton, R. L. (1987). Concepts of pavement performance prediction and modelling. North American Conference on Managing Pavements, 2nd, 1987, Toronto, Ontario, Canada,

Lytton, R. L. (1989). Backcalculation of pavement layer properties. In *Nondestructive Testing of Pavements and Backcalculation of Moduli*. ASTM International.

Mamlouk, M. S. (1985). Use of Dynamic Analysis 1n Predicting Field Multilayer Pavement Moduli. *Transportation research record*, *1043*, 113.

Martini, G., Bracci, A., Jaiswal, S., Corea, M., Riches, L., Rivers, J., & Omodei, E. (2021). Nowcasting food insecurity on a global scale. *medRxiv*, 2021.2006. 2023.21259419.

May, R. W., & Von Quintus, H. L. (1994). The quest for a standard guide to NDT backcalculation. In *Nondestructive Testing of Pavements and Backcalculation of Moduli: Second Volume*. ASTM International.

McGovern, M. E., Buttlar, W. G., & Reis, H. (2016). Field assessment of oxidative aging in asphalt concrete pavements with unknown acoustic properties. *Construction and Building Materials*, *116*, 159-168.

McQueen, J. M. (2004). *A Study of Manual Vs Automated Pavement Condition Surveys* Auburn University].

Mehta, Y., & Roque, R. (2003). Evaluation of FWD data for determination of layer moduli of pavements. *Journal of Materials in Civil Engineering*, *15*(1), 25-31.

Mehta, Y. A., Sauber, R. W., Owad, J., & Krause, J. (2008). *Lessons learned during implementation of mechanistic-empirical pavement design guide*.

Meier, R. W., & Rix, G. J. (1995). Backcalculation of flexible pavement moduli from dynamic deflection basins using artificial neural networks. *Transportation research record*(1473).

Miller, J. S., & Bellinger, W. Y. (2003). *Distress identification manual for the long-term pavement performance program*.

Minnesota Department of Transportation. (2011). *Mn/DOT Pavement Distress Identification Manual*.

Moghaddam, T. B., Karim, M. R., & Abdelaziz, M. (2011). A review on fatigue and rutting performance of asphalt mixes. *Scientific Research and Essays*, *6*(4), 670-682.

Monismith, C. (2004, June 7-9). Evolution of long-lasting asphalt pavement design methodology: A perspective. International Symposium on Designand Construction of Long Lasting Asphalt Pavements, Auburn University.

Monismith, C., Epps, J., & Finn, F. (1985). Improved asphalt mix design (with discussion). Association of Asphalt Paving Technologists Proc,

Monismith, C., Sousa, J., & Lysmer, J. (1988). Modern pavement design technology including dynamic load conditions. *SAE Transactions*, 747-766.

Newcomb, D. E. (1987). DEVELOPMENT AND EVALUATION OF A REGRESSION METHOD TO INTERPRET DYNAMIC PAVEMENT DEFLECTIONS.

OriginLab Corporation. (2019). *Origin and OriginPro*. Origin and OriginPro. Retrieved 1/21/2022 from https://www.originlab.com/origin#Introduction

Pan, P., Wu, S., Xiao, Y., & Liu, G. (2015). A review on hydronic asphalt pavement for energy harvesting and snow melting. *Renewable and Sustainable Energy Reviews*, *48*, 624-634.

Piñeiro, G., Perelman, S., Guerschman, J. P., & Paruelo, J. M. (2008). How to evaluate models: observed vs. predicted or predicted vs. observed? *Ecological modelling*, *216*(3-4), 316-322.

Powell, W., Potter, J., Mayhew, H., & Nunn, M. (1984). The structural design of bituminous roads, TRRL Laboratory Report 1132. *Transportation and Road Research Laboratory, Crowthorne, Berkshire, UK*, *62*.

Richter, C. A. (2006). *Seasonal variations in the moduli of unbound pavement layers*.

Safaei, F., Castorena, C., & Kim, Y. R. (2016). Linking asphalt binder fatigue to asphalt mixture fatigue performance using viscoelastic continuum damage modeling. *Mechanics of Time-Dependent Materials*, *20*(3), 299-323.

Saudy, M., Breakah, T., Kaloop, M. R., & El-Badawy, S. (2023). Regional Implementation of the Mechanistic Empirical Pavement Design and Analysis Approach: Egyptian Case Study. *Case Studies in Construction Materials*, e01863.

Schwartz, C., & Carvalho, R. (2007). Evaluation of mechanistic-empirical design procedure. *Final Report, MDSHA Project No. SP0077B41, Maryland*.

Sebaaly, B., Davis, T. G., & Mamlouk, M. S. (1985). Dynamics of falling weight deflectometer. *Journal of Transportation Engineering*, *111*(6), 618-632.

Seifert, E. (2014). OriginPro 9.1: scientific data analysis and graphing software-software review. *Journal of chemical information and modeling*, *54*(5), 1552.

Sengoz, B., & Topal, A. (2005). Use of asphalt roofing shingle waste in HMA. *Construction and Building Materials*, *19*(5), 337-346.

Seyhan, U., Tutumluer, E., & Yesilyurt, H. (2005). Anisotropic aggregate base inputs for mechanistic pavement analysis considering effects of moving wheel loads. *Journal of Materials in Civil Engineering*, *17*(5), 505-512.

Shah, Y. U., Jain, S., Tiwari, D., & Jain, M. (2013). Development of overall pavement condition index for urban road network. *Procedia-Social and Behavioral Sciences*, *104*, 332-341.

Sharma, J., & Stubstad, R. (1980). EVALUATION OF PAVEMENT IN FLORIDA BY USING THE FALLING-WEIGHT DEFLECTOMETER. *Transportation research record*(755).

Shell International Petroleum Company, l. (1978). *Shell pavement design manual: Asphalt pavements and overlays for road traffic*. Shell International Petroleum Company.

Shen, X. (1993). *Simulation dual load fwd systems for determination of pavement layer moduli in flexible pavement* University of Florida].

Shook, J. F. (1982). Thickness design of asphalt pavements-the Asphalt Institute method. Proceedings, 5th International Conference on Structural Design of Asphalt Pavements, Delft University of Technology, The Netherlands, 1982,

Singh, A. K., & Sahoo, J. P. (2021). Rutting prediction models for flexible pavement structures: a review of historical and recent developments. *Journal of Traffic and Transportation Engineering (English Edition)*.

Smith, B. J., & Hesp, S. A. (2000). Crack pinning in asphalt mastic and concrete: regular fatigue studies. *Transportation research record*, *1728*(1), 75-81.

Stolle, D. (1991). Modelling of dynamic response of pavements to impact loading. *Computers and Geotechnics*, *11*(1), 83-94.

Stubbs, A. P. (2011). Fatigue Behaviour of Hot Mix Asphalt for New Zealand Pavement Design.

Tawfiq, K., Armaghani, J., & Sobanjo, J. (2000). Seismic pavement analyzer vs. FWD for pavement evaluation: comparative study. *NDT of pavements and backcalculation of moduli*, *3*, 327-345.

Tholen, O., Sharma, J., & Terrel, R. L. (1985). Comparison of falling weight deflectometer with other deflection testing devices. *Transportation research record*, *1007*, 20-26.

Transport Research Laboratory. (1993). Overseas Road Note 31. In *A Guide to The Structural Design of Bitumen-Surfaced Roads in Tropical and Sub-Tropical countries*.

Ullidtz, P. (2000). Will nonlinear backcalculation help? In *Nondestructive Testing of Pavements and Backcalculation of Moduli: Third Volume*. ASTM International.

Ullidtz, P., & Stubstad, R. N. (1985). Analytical-empirical pavement evaluation using the falling weight deflectometer. *Transportation research record*, *1022*, 36-44.

Uzan, J. (1994). Dynamic linear back calculation of pavement material parameters. *Journal of Transportation Engineering*, *120*(1), 109-126.

Uzan, J. (2004). Permanent deformation in flexible pavements. *Journal of Transportation Engineering*, *130*(1), 6-13.

Vallejo, L. E. (2012). Fractal evaluation of the level of alligator cracking in pavements. *Geomechanics & engineering*, *4*(3), 219-227.

Van Cauwelaert, F. J., Alexander, D. R., White, T. D., & Barker, W. R. (1989). Multilayer elastic program for backcalculating layer moduli in pavement evaluation. In *Nondestructive Testing of Pavements and Backcalculation of Moduli*. ASTM International.

Walther, A., & Wistuba, M. (2012). Mechanistic pavement design considering bottom-up and top-down-cracking. 7th RILEM International Conference on Cracking in Pavements,

Wardle, L. (2010). CIRCLY and mechanistic pavement design: the past, present and towards the future. *Minicad Systems, Australia*.

Williams, D. A. (1998). *Microdamage healing in asphalt concretes: relating binder composition and surface energy to healing rate*. Texas A&M University.

Xiao, F. (2006). Development of Fatigue Predictive Models of Rubberized Asphalt Concrete (RAC) Containing Reclaimed Asphalt Pavement (RAP) Mixtures.

Yoder, E. J., & Witczak, M. W. (1991). *Principles of pavement design*. John Wiley & Sons.

Yoo, P. J., & Park, H. M. (2018). Developing pavement thickness design incorporating the catalogue and mechanistic approach [Case study]. Retrieved 25/01/2023, from https://development.asia/case-study/developing-pavement-thickness-design-incorporating-catalogue-and-mechanistic-approach

Zhang, W., Huang, X., Yang, J., & Chen, X. (2017). RETRACTED: Effect of segregation on rutting resistance of asphalt pavement. In: Elsevier.

Zhaoyun, S., Chaofan, W., & Aimin, S. (2009). Study of image-based pavement cracking measurement techniques. 2009 9th International Conference on Electronic Measurement & Instruments,

Zhou, H. (2000). Comparison of backcalculated and laboratory measured moduli on AC and granular base layer materials. In *Nondestructive Testing of Pavements and Backcalculation of Moduli: Third Volume*. ASTM International.

APPENDICES

Appendix A - Traffic Load distribution (TLD) file for A11 road

Load	SAST	SADT	TAST	TADT	TRDT	QADT
2.5	0.00597	0	0	0	0	0
7.5	0.044776	0.002985	0	0	0	0
12.5	0.029851	0.035821	0	0	0	0
17.5	0.050746	0.032836	0.002985	0	0	0
22.5	0.038806	0.041791	0.00597	0	0	0
27.5	0.032836	0.056716	0	0.002985	0	0
32.5	0.116418	0.053731	0	0	0	0
37.5	0.089552	0.026866	0.002985	0	0	0
42.5	0.026866	0.026866	0	0	0	0
47.5	0.01194	0.023881	0	0	0	0
52.5	0.01194	0.00597	0	0.00597	0	0
57.5	0.014925	0.01194	0	0.008955	0	0
62.5	0.008955	0.00597	0	0.01194	0	0
67.5	0.01791	0.008955	0	0	0	0
72.5	0.01194	0	0	0.002985	0.002985	0
77.5	0.002985	0.008955	0	0	0	0
82.5	0.002985	0.00597	0	0	0	0
87.5	0	0	0	0.00597	0	0
92.5	0	0	0	0	0	0
97.5	0	0	0	0	0	0
102.5	0	0.00597	0	0	0	0
107.5	0	0.008955	0	0	0	0
112.5	0	0	0	0	0	0
117.5	0	0	0	0	0	0
122.5	0	0.002985	0	0	0	0
127.5	0	0.002985	0	0	0	0
132.5	0	0	0	0	0	0
137.5	0	0.002985	0	0	0	0
142.5	0	0	0	0	0	0
147.5	0	0.002985	0	0	0	0
152.5	0	0.002985	0	0	0	0
157.5	0	0.01194	0	0	0	0
162.5	0	0.002985	0	0	0	0
167.5	0	0.002985	0	0	0	0
172.5	0	0.008955	0	0	0	0
177.5	0	0.002985	0	0	0	0
182.5	0	0.002985	0	0	0	0
187.5	0	0	0	0.002985	0	0
192.5	0	0.002985	0	0	0	0
197.5	0	0	0	0	0	0
202.5	0	0	0	0	0	0

207.5	0	0	0	0.002985	0	0
212.5	0	0	0	0	0	0
217.5	0	0	0	0	0	0
222.5	0	0	0	0	0	0
227.5	0	0	0	0	0	0
232.5	0	0	0	0	0	0
237.5	0	0	0	0	0	0
242.5	0	0	0	0.002985	0	0
247.5	0	0	0	0	0	0
252.5	0	0	0	0.002985	0	0
257.5	0	0	0	0	0	0
262.5	0	0	0	0	0	0
267.5	0	0	0	0	0	0
272.5	0	0	0	0	0	0
277.5	0	0	0	0	0	0
282.5	0	0	0	0	0	0
287.5	0	0	0	0	0	0
292.5	0	0	0	0	0	0
297.5	0	0	0	0	0	0
302.5	0	0	0	0	0	0
307.5	0	0	0	0	0	0
312.5	0	0	0	0	0	0
317.5	0	0	0	0	0	0
322.5	0	0	0	0	0	0
327.5	0	0	0	0	0	0
332.5	0	0	0	0	0	0
337.5	0	0	0	0	0	0
342.5	0	0	0	0	0	0
347.5	0	0	0	0	0	0
352.5	0	0	0	0	0	0
357.5	0	0	0	0	0	0
362.5	0	0	0	0	0	0
367.5	0	0	0	0	0	0
372.5	0	0	0	0	0	0
377.5	0	0	0	0	0	0
382.5	0	0	0	0	0	0
387.5	0	0	0	0	0	0
392.5	0	0	0	0	0	0
397.5	0	0	0	0	0	0

Appendix B – CDF calculation for model development

Table 1: CDF variation at Reliability = 50%

Location	ACI	b=5	b=5.1	b=5.2	b=5.3	b=5.4	b=5.5	b=4.9	b=4.8	b=4.7	b=4.6	b=4.5
		CDF										
0+006	78	0.907	0.507	0.391	0.302	0.234	0.181	0.851	1.1	1.43	1.86	2.42
0+260	80	0.619	0.477	0.368	0.284	0.22	0.17	0.803	1.04	1.36	1.76	2.29
0+500	83	0.442	0.468	0.361	0.279	0.215	0.166	0.787	1.02	1.33	1.73	2.25
0+742	69	0.662	0.511	0.395	0.306	0.237	0.183	0.857	1.11	1.44	1.87	2.43
01+001	88	0.243	0.408	0.314	0.242	0.187	0.144	0.689	0.896	1.17	1.52	1.98
01+255	90	0.435	0.333	0.255	0.196	0.15	0.115	0.569	0.744	0.973	1.27	1.67
01+503	91	0.196	0.297	0.227	0.173	0.132	0.101	0.51	0.669	0.878	1.15	1.52
1+820	84	0.539	0.415	0.319	0.246	0.189	0.146	0.702	0.914	1.19	1.55	2.03
02+000	42	1.75	1.38	1.09	0.858	0.678	0.536	2.22	2.81	3.57	4.54	5.78
2+280	66	0.813	0.63	0.489	0.38	0.295	0.23	1.05	1.35	1.75	2.26	2.93
02+500	71	0.757	0.586	0.454	0.352	0.273	0.211	0.979	1.27	1.64	2.13	2.76
02+763	66	0.854	0.663	0.515	0.401	0.312	0.243	1.1	1.42	1.83	2.37	3.06
03+003	47	1.46	1.15	0.903	0.711	0.56	0.441	1.86	2.37	3.02	3.86	4.93
03+256	63	1	0.78	0.608	0.475	0.37	0.289	1.29	1.65	2.12	2.73	3.52
03+503	44	1.57	1.23	0.971	0.763	0.601	0.473	2	2.55	3.26	4.16	5.31
03+759	87	0.593	0.456	0.352	0.271	0.209	0.162	0.77	1	1.3	1.7	2.21
04+002	84	0.605	0.466	0.359	0.277	0.214	0.165	0.786	1.02	1.33	1.73	2.25
04+302	81	0.606	0.467	0.36	0.278	0.214	0.165	0.786	1.02	1.33	1.73	2.25
04+501	85	0.609	0.469	0.362	0.279	0.216	0.166	0.791	1.03	1.34	1.74	2.27
04+771	56	1.12	0.878	0.686	0.537	0.42	0.329	1.44	1.85	2.37	3.04	3.91
05+001	41	1.88	1.49	1.18	0.929	0.736	0.583	2.38	3.02	3.83	4.86	6.18
05+272	46	1.5	1.18	0.926	0.729	0.574	0.452	1.91	2.43	3.09	3.95	5.04
05+501	55	1.25	0.981	0.769	0.603	0.473	0.371	1.6	2.05	2.62	3.35	4.3
05+808	60	1.1	0.86	0.672	0.526	0.411	0.322	1.41	1.81	2.32	2.99	3.84
06+002	67	0.772	0.598	0.464	0.36	0.279	0.217	0.997	1.29	1.67	2.16	2.8
06+250	65	0.896	0.697	0.542	0.422	0.328	0.256	1.15	1.49	1.92	2.47	3.19

Table 2: CDF variation at Reliability = 80%

Location	ACI	b=5	b=5.1	b=5.2	b=5.3	b=5.4	b=5.5	b=4.9	b=4.8	b=4.7	b=4.6	b=4.5
		CDF										
0+006	78	1.58	1.22	0.939	0.726	0.561	0.434	2.04	2.65	3.44	4.47	5.81
0+260	80	1.49	1.15	0.884	0.683	0.527	0.408	1.93	2.5	3.25	4.23	5.51
0+500	83	1.46	1.12	0.866	0.669	0.517	0.399	1.89	2.45	3.19	4.15	5.4
0+742	69	1.59	1.23	0.949	0.734	0.568	0.44	2.06	2.66	3.45	4.48	5.82
01+001	88	1.27	0.978	0.754	0.581	0.448	0.345	1.65	2.15	2.8	3.65	4.76

01+255	90	1.04	0.799	0.613	0.47	0.36	0.277	1.36	1.78	2.34	3.06	4.01
01+503	91	0.933	0.712	0.544	0.416	0.318	0.243	1.22	1.6	2.11	2.77	3.64
1+820	84	1.29	0.995	0.765	0.589	0.454	0.35	1.68	2.19	2.86	3.73	4.87
02+000	42	4.19	3.3	2.61	2.06	1.63	1.29	5.32	6.75	8.58	10.9	13.9
2+280	66	1.95	1.51	1.17	0.912	0.708	0.551	2.52	3.25	4.2	5.43	7.02
02+500	71	1.82	1.41	1.09	0.844	0.654	0.507	2.35	3.04	3.94	5.11	6.62
02+763	66	2.05	1.59	1.24	0.962	0.748	0.582	2.64	3.41	4.4	5.68	7.34
03+003	47	3.51	2.76	2.17	1.71	1.34	1.06	4.47	5.69	7.26	9.26	11.8
03+256	63	2.4	1.87	1.46	1.14	0.889	0.694	3.09	3.96	5.1	6.56	8.45
03+503	44	3.77	2.96	2.33	1.83	1.44	1.14	4.8	6.12	7.81	9.97	8.45
03+759	87	1.42	1.1	0.844	0.651	0.502	0.388	1.85	2.4	3.13	4.07	5.31
04+002	84	1.45	1.12	0.862	0.665	0.513	0.397	1.89	2.45	3.19	4.15	5.4
04+302	81	1.45	1.12	0.863	0.666	0.514	0.397	1.89	2.45	3.19	4.15	5.41
04+501	85	1.46	1.13	0.868	0.67	0.517	0.4	1.9	2.47	3.21	4.17	5.44
04+771	56	2.7	2.11	1.65	1.29	1.01	0.789	3.46	4.43	5.68	7.3	9.38
05+001	41	4.52	3.57	2.82	2.23	1.77	1.4	5.72	7.25	9.2	11.7	14.8
05+272	46	3.59	2.82	2.22	1.75	1.38	1.09	4.57	5.82	7.42	9.47	12.1
05+501	55	3.01	2.35	1.84	1.45	1.13	0.891	3.84	4.91	6.28	8.05	10.3
05+808	60	2.64	2.06	1.61	1.26	0.987	0.772	3.39	4.35	5.58	7.17	9.21
06+002	67	1.85	1.44	1.11	0.863	0.67	0.52	2.39	3.09	4	5.18	6.72
06+250	65	2.15	1.67	1.3	1.01	0.788	0.614	2.77	3.57	4.6	5.93	7.66

Table 3: CDF variation at Reliability = 85%

Location	ACI	b=5	b=5.1	b=5.2	b=5.3	b=5.4	b=5.5	b=4.9	b=4.8	b=4.7	b=4.6	b=4.5
		CDF										
0+006	78	1.97	1.52	1.17	0.907	0.702	0.543	2.55	3.31	4.3	5.59	7.27
0+260	80	1.86	1.43	1.11	0.853	0.659	0.51	2.41	3.13	4.07	5.29	6.88
0+500	83	1.82	1.4	1.08	0.836	0.646	0.499	2.36	3.07	3.99	5.19	6.75
0+742	69	1.98	1.53	1.19	0.918	0.711	0.55	2.57	3.33	4.32	5.6	7.28
01+001	88	1.59	1.22	0.942	0.726	0.56	0.432	2.07	2.69	3.5	4.56	5.95
01+255	90	1.31	0.999	0.766	0.587	0.45	0.346	1.71	2.23	2.92	3.82	5.01
01+503	91	1.17	0.89	0.68	0.519	0.397	0.304	1.53	2.01	2.63	3.46	4.55
1+820	84	1.62	1.24	0.957	0.737	0.567	0.437	2.11	2.74	3.57	4.66	6.09
02+000	42	5.24	4.13	3.26	2.57	2.03	1.61	6.65	8.44	10.7	13.6	17.3

2+280	66	2.44	1.89	1.47	1.14	0.886	0.689	3.15	4.06	5.25	6.78	8.78
02+500	71	2.27	1.76	1.36	1.05	0.818	0.634	2.94	3.8	4.92	6.38	8.28
02+763	66	2.56	1.99	1.55	1.2	0.935	0.728	3.3	4.26	5.49	7.1	9.17
03+003	47	4.38	3.45	2.71	2.13	1.68	1.32	5.58	7.11	9.07	11.6	14.8
03+256	63	3	2.34	1.82	1.42	1.11	0.868	3.86	4.96	6.37	8.2	10.6
03+503	44	4.72	3.7	2.91	2.29	1.8	1.42	6.01	7.66	9.77	12.5	15.9
03+759	87	1.78	1.37	1.05	0.813	0.628	0.485	2.31	3	3.91	5.09	6.63
04+002	84	1.81	1.4	1.08	0.832	0.642	0.496	2.36	3.06	3.98	5.19	6.75
04+302	81	1.82	1.4	1.08	0.833	0.643	0.496	2.36	3.07	3.99	5.19	6.76
04+501	85	1.83	1.41	1.09	0.837	0.647	0.499	2.37	3.08	4.01	5.22	6.8
04+771	56	3.37	2.63	2.06	1.61	1.26	0.987	4.32	5.54	7.11	9.12	11.7
05+001	41	5.64	4.46	3.53	2.79	2.21	1.75	7.15	9.06	11.5	14.6	18.5
05+272	46	4.49	3.53	2.78	2.19	1.72	1.36	5.72	7.28	9.28	11.8	15.1
05+501	55	3.76	2.94	2.31	1.81	1.42	1.11	4.8	6.14	7.85	10.1	12.9
05+808	60	3.31	2.58	2.02	1.58	1.23	0.965	4.24	5.43	6.97	8.96	11.5
06+002	67	2.32	1.79	1.39	1.08	0.837	0.65	2.99	3.87	5	6.48	8.4
06+250	65	2.69	2.09	1.63	1.27	0.985	0.768	3.46	4.46	5.75	7.42	9.58

Table 4: CDF variation at Reliability = 90%

Location	ACI	b=5	b=5.1	b=5.2	b=5.3	b=5.4	b=5.5	b=4.9	b=4.8	b=4.7	b=4.6	b=4.5
		CDF										
0+006	78	2.56	1.98	1.53	1.18	0.912	0.706	3.32	4.31	5.59	7.26	9.45
0+260	80	2.41	1.86	1.44	1.11	0.857	0.662	3.13	4.07	5.29	6.88	8.95
0+500	83	2.37	1.82	1.41	1.09	0.839	0.649	3.07	3.99	5.18	6.74	8.78
0+742	69	2.58	1.99	1.54	1.19	0.924	0.716	3.34	4.33	5.61	7.28	9.46
01+001	88	2.07	1.59	1.22	0.944	0.728	0.561	2.69	3.5	4.55	5.93	7.73
01+255	90	1.7	1.3	0.995	0.763	0.585	0.449	2.22	2.9	3.79	4.97	6.52
01+503	91	1.52	1.16	0.884	0.675	0.516	0.395	1.99	2.61	3.42	4.5	5.92
1+820	84	2.1	1.62	1.24	0.958	0.738	0.568	2.74	3.57	4.65	6.06	7.91
02+000	42	6.81	5.37	4.24	3.35	2.64	2.09	8.64	11	13.9	17.7	22.6
2+280	66	3.17	2.46	1.91	1.48	1.15	0.895	4.09	5.28	6.82	8.82	11.4
02+500	71	2.95	2.29	1.77	1.37	1.06	0.825	3.82	4.94	6.4	8.3	10.8
02+763	66	3.33	2.59	2.01	1.56	1.22	0.946	4.29	5.54	7.14	9.23	11.9

03+003	47	5.7	4.48	3.52	2.77	2.18	1.72	7.26	9.25	11.8	15	19.2
03+256	63	3.9	3.04	2.37	1.85	1.44	1.13	5.01	6.44	8.28	10.7	13.7
03+503	44	6.13	4.82	3.79	2.98	2.34	1.85	7.81	9.95	12.7	16.2	20.7
03+759	87	2.31	1.78	1.37	1.06	0.816	0.63	3	3.9	5.08	6.62	8.62
04+002	84	2.36	1.82	1.4	1.08	0.834	0.644	3.06	3.98	5.18	6.74	8.78
04+302	81	2.36	1.82	1.4	1.08	0.835	0.645	3.07	3.99	5.18	6.75	8.79
04+501	85	2.37	1.83	1.41	1.09	0.84	0.649	3.08	4.01	5.21	6.78	8.83
04+771	56	4.38	3.42	2.68	2.09	1.64	1.28	5.62	7.2	9.24	11.9	15.2
05+001	41	7.34	5.8	4.58	3.62	2.87	2.27	9.29	11.8	14.9	19	24.1
05+272	46	5.84	4.59	3.61	2.84	2.24	1.76	7.43	9.46	12.1	15.4	19.6
05+501	55	4.88	3.83	3	2.35	1.84	1.45	6.24	7.98	10.2	13.1	16.8
05+808	60	4.3	3.36	2.62	2.05	1.6	1.25	5.51	7.06	9.07	11.6	15
06+002	67	3.01	2.33	1.81	1.4	1.09	0.845	3.89	5.03	6.51	8.42	10.9
06+250	65	3.5	2.72	2.11	1.65	1.28	0.998	4.5	5.8	7.47	9.64	12.5

Table 5: CDF variation at Reliability = 95%

Location	ACI	b=5	b=5.1	b=5.2	b=5.3	b=5.4	b=5.5	b=4.9	b=4.8	b=4.7	b=4.6	b=4.5
		CDF										
0+006	78	3.94	3.04	2.35	1.81	1.4	1.09	5.11	6.63	8.6	11.2	14.5
0+260	80	3.71	2.86	2.21	1.71	1.32	1.02	4.82	6.26	8.13	10.6	13.8
0+500	83	3.64	2.81	2.17	1.67	1.29	0.998	4.72	6.14	7.98	10.4	13.5
0+742	69	3.97	3.07	2.37	1.84	1.42	1.1	5.14	6.66	8.64	11.2	14.6
01+001	88	3.18	2.45	1.88	1.45	1.12	0.863	4.13	5.38	7	9.12	11.9
01+255	90	2.61	2	1.53	1.17	0.901	0.691	3.41	4.46	5.84	7.65	10
01+503	91	2.33	1.78	1.36	1.04	0.794	0.608	3.06	4.01	5.27	6.92	9.1
1+820	84	3.24	2.49	1.91	1.47	1.13	0.874	4.21	5.48	7.15	9.33	12.2
02+000	42	10.5	8.26	6.52	5.15	4.07	3.22	13.3	16.9	21.4	27.3	34.7
2+280	66	4.88	3.78	2.94	2.28	1.77	1.38	6.29	8.12	10.5	13.6	17.6
02+500	71	4.54	3.52	2.72	2.11	1.64	1.27	5.88	7.6	9.85	12.8	16.6
02+763	66	5.12	3.98	3.09	2.4	1.87	1.46	6.6	8.52	11	14.2	18.3
03+003	47	8.77	6.89	5.42	4.26	3.36	2.65	11.2	14.2	18.1	23.1	29.6
03+256	63	6.01	4.68	3.65	2.85	2.22	1.74	7.71	9.91	12.7	16.4	21.1
03+503	44	9.43	7.41	5.82	4.58	3.61	2.84	12	15.3	19.5	24.9	31.9
03+759	87	3.56	2.74	2.11	1.63	1.26	0.969	4.62	6.01	7.82	10.2	13.3
04+002	84	3.63	2.8	2.16	1.66	1.28	0.991	4.71	6.13	7.97	10.4	13.5
04+302	81	3.63	2.8	2.16	1.67	1.29	0.993	4.72	6.13	7.98	10.4	13.5
04+501	85	3.65	2.82	2.17	1.67	1.29	0.999	4.74	6.16	8.02	10.4	13.6
04+771	56	6.75	5.27	4.12	3.22	2.52	1.97	8.64	11.1	14.2	18.2	23.4

05+001	41	11.3	8.92	7.05	5.58	4.41	3.5	14.3	18.1	23	29.2	37.1
05+272	46	8.98	7.06	5.55	4.37	3.44	2.71	11.4	14.6	18.6	23.7	30.2
05+501	55	7.51	5.88	4.61	3.62	2.84	2.23	9.6	12.3	15.7	20.1	25.8
05+808	60	6.61	5.16	4.03	3.15	2.47	1.93	8.47	10.9	13.9	17.9	23
06+002	67	4.63	3.59	2.78	2.16	1.67	1.3	5.98	7.74	10	13	16.8
06+250	65	5.38	4.18	3.25	2.53	1.97	1.54	6.92	8.92	11.5	14.8	19.2

Table 6: CDF variation at Reliability = 97.5%

Location	ACI	b=5	b=5.1	b=5.2	b=5.3	b=5.4	b=5.5	b=4.9	b=4.8	b=4.7	b=4.6	b=4.5
		CDF										
0+006	78	5.91	4.56	3.52	2.72	2.11	1.63	7.66	9.94	12.9	16.8	21.8
0+260	80	5.57	4.3	3.32	2.56	1.98	1.53	7.23	9.39	12.2	15.9	20.7
0+500	83	5.46	4.21	3.25	2.51	1.94	1.5	7.09	9.2	12	15.6	20.3
0+742	69	5.95	4.6	3.56	2.75	2.13	1.65	7.71	9.99	13	16.8	21.8
01+001	88	4.77	3.67	2.83	2.18	1.68	1.3	6.2	8.07	10.5	13.7	17.8
01+255	90	3.92	3	2.3	1.76	1.35	1.04	5.12	6.69	8.76	11.5	15
01+503	91	3.5	2.67	2.04	1.56	1.19	0.911	4.59	6.02	7.9	10.4	13.7
1+820	84	4.85	3.73	2.87	2.21	1.7	1.31	6.32	8.23	10.7	14	18.3
02+000	42	15.7	12.4	9.78	7.72	6.1	4.82	19.9	25.3	32.2	40.9	52
2+280	66	7.31	5.67	4.4	3.42	2.66	2.07	9.44	12.2	15.7	20.4	26.3
02+500	71	6.82	5.27	4.08	3.16	2.45	1.9	8.81	11.4	14.8	19.1	24.8
02+763	66	7.69	5.97	4.64	3.61	2.81	2.18	9.91	12.8	16.5	21.3	27.5
03+003	47	13.2	10.3	8.13	6.4	5.04	3.97	16.7	21.3	27.2	34.7	44.3
03+256	63	9.01	7.02	5.47	4.27	3.33	2.6	11.6	14.9	19.1	24.6	31.7
03+503	44	14.1	11.1	8.74	6.87	5.41	4.26	18	23	29.3	37.4	47.8
03+759	87	5.33	4.11	3.16	2.44	1.88	1.45	6.93	9.01	11.7	15.3	19.9
04+002	84	5.44	4.19	3.23	2.49	1.93	1.49	7.07	9.19	12	15.6	20.3
04+302	81	5.45	4.2	3.24	2.5	1.93	1.49	7.08	9.2	12	15.6	20.3
04+501	85	5.48	4.22	3.26	2.51	1.94	1.5	7.12	9.25	12	15.7	20.4
04+771	56	10.1	7.9	6.18	4.83	3.78	2.96	13	16.6	21.3	27.4	35.2
05+001	41	16.9	13.4	10.6	8.37	6.62	5.24	21.4	27.2	34.5	43.8	55.6
05+272	46	13.5	10.6	8.33	6.56	5.17	4.07	17.1	21.8	27.8	35.5	45.3
05+501	55	11.3	8.83	6.92	5.42	11.3	3.34	14.4	18.4	23.6	30.2	38.7
05+808	60	9.92	7.74	6.05	4.73	3.7	2.9	12.7	16.3	20.9	26.9	34.6
06+002	67	6.95	5.38	4.17	3.24	2.51	1.95	8.98	11.6	15	19.4	25.2
06+250	65	8.07	6.27	4.88	3.8	2.96	2.3	10.4	13.4	17.2	22.3	28.7

Appendix C - Traffic load distribution (TLD) file for A10 road

Load	SAST	SADT	TAST	TADT	TRDT	QADT
2.5	0.008451	0	0	0	0	0
7.5	0.087324	0.016901	0	0	0	0
12.5	0.08169	0.064789	0	0	0	0
17.5	0.11831	0.056338	0	0	0	0
22.5	0.070423	0.059155	0	0	0	0
27.5	0.03662	0.014085	0	0	0	0
32.5	0.042254	0.039437	0	0	0	0
37.5	0.042254	0.025352	0	0	0	0
42.5	0.022535	0.025352	0	0.002817	0	0
47.5	0.011268	0.008451	0	0.005634	0	0
52.5	0.019718	0.011268	0	0.016901	0	0
57.5	0.019718	0.014085	0	0.008451	0	0
62.5	0.002817	0.008451	0	0.005634	0	0
67.5	0	0.002817	0	0.002817	0	0
72.5	0.002817	0.014085	0	0.005634	0	0
77.5	0	0.002817	0	0.002817	0	0
82.5	0	0.002817	0	0.002817	0	0
87.5	0	0	0	0	0	0
92.5	0	0	0	0	0	0
97.5	0	0.002817	0	0	0	0
102.5	0	0	0	0	0	0
107.5	0	0	0	0	0	0
112.5	0	0	0	0	0	0
117.5	0	0	0	0	0	0
122.5	0	0	0	0	0	0
127.5	0	0.002817	0	0	0	0
132.5	0	0	0	0	0	0
137.5	0	0.002817	0	0	0	0
142.5	0	0	0	0	0	0
147.5	0	0	0	0	0	0
152.5	0	0	0	0	0	0
157.5	0	0	0	0	0	0
162.5	0	0	0	0	0	0
167.5	0	0	0	0	0	0
172.5	0	0	0	0	0	0
177.5	0	0	0	0	0	0
182.5	0	0.002817	0	0	0	0
187.5	0	0	0	0	0	0
192.5	0	0	0	0	0	0
197.5	0	0	0	0	0	0
202.5	0	0	0	0	0	0
207.5	0	0.002817	0	0	0	0
212.5	0	0	0	0	0	0

217.5	0	0	0	0	0	0
222.5	0	0	0	0	0	0
227.5	0	0	0	0	0	0
232.5	0	0	0	0	0	0
237.5	0	0	0	0	0	0
242.5	0	0	0	0	0	0
247.5	0	0	0	0	0	0
252.5	0	0	0	0	0	0
257.5	0	0	0	0	0	0
262.5	0	0	0	0	0	0
267.5	0	0	0	0	0	0
272.5	0	0	0	0	0	0
277.5	0	0	0	0	0	0
282.5	0	0	0	0	0	0
287.5	0	0	0	0	0	0
292.5	0	0	0	0	0	0
297.5	0	0	0	0	0	0
302.5	0	0	0	0	0	0
307.5	0	0	0	0	0	0
312.5	0	0	0	0	0	0
317.5	0	0	0	0	0	0
322.5	0	0	0	0	0	0
327.5	0	0	0	0	0	0
332.5	0	0	0	0	0	0
337.5	0	0	0	0	0	0
342.5	0	0	0	0	0	0
347.5	0	0	0	0	0	0
352.5	0	0	0	0	0	0
357.5	0	0	0	0	0	0
362.5	0	0	0	0	0	0
367.5	0	0	0	0	0	0
372.5	0	0	0	0	0	0
377.5	0	0	0	0	0	0
382.5	0	0	0	0	0	0
387.5	0	0	0	0	0	0
392.5	0	0	0	0	0	0
397.5	0	0	0	0	0	0

Appendix D - Model validation calculations

Table 7: Observed ACI Vs. Observed ACI calculations.

Location	CDF	ACI	
		Model Prediction	Observed
63003	1.58E+00	45.770	51.038
63500	1.91E+00	10.751	17.725
64004	1.75E+00	29.107	27.088
64501	1.08E+00	79.887	76.395
65007	1.84E+00	19.113	25.227
65500	1.67E+00	37.300	31.456
66001	1.70E+00	34.302	40.431
66504	1.94E+00	7.005	11.136
67001	1.67E+00	37.300	33.817
67503	1.83E+00	20.265	23.470
68001	1.65E+00	39.249	40.431
68503	1.64E+00	40.209	34.999
69000	1.72E+00	32.254	35.736
69503	1.93E+00	8.265	11.602
69999	1.66E+00	38.279	42.200
70502	1.89E+00	13.194	17.480
71006	1.96E+00	4.453	11.732
71505	1.89E+00	13.194	18.637
72004	1.98E+00	1.857	11.466
72501	1.65E+00	39.249	42.767
73007	1.88E+00	14.399	11.464
73505	1.35E+00	64.039	64.932
74001	1.89E+00	13.194	15.624
74506	1.98E+00	1.857	8.974
75005	1.92E+00	9.513	11.026
75501	1.63E+00	41.160	44.394
76005	1.88E+00	14.399	16.255
76500	1.95E+00	5.735	11.009
77003	1.91E+00	10.751	12.039
77500	1.82E+00	21.406	24.775
78000	1.86E+00	16.777	19.495
78500	1.86E+00	16.777	19.646
79002	1.95E+00	5.735	11.994
79501	1.98E+00	1.857	9.876
80002	1.36E+00	63.340	60.379
80500	1.89E+00	13.194	11.682
81003	1.39E+00	61.194	59.525

81502	1.16E+00	75.774	77.546
82000	7.08E-01	93.373	91.361
82500	1.93E+00	8.265	10.650
83002	1.56E+00	47.547	49.826
83500	5.09E-01	97.327	95.885
84000	2.88E-01	99.602	98.617

Appendix E – Axle distribution of A1 Road

Table 8: Axle distribution of A1 Road.

Axle Load	Axle distribution					
	SAST	**SADT**	**TAST**	**TADT**	**TRDT**	**QADT**
5	10	0	0	0	0	0
10	121	30	0	0	0	0
15	510	121	0	0	0	0
20	466	281	0	0	0	0
25	372	181	0	1	0	0
30	324	243	0	3	0	0
35	383	143	0	1	0	0
40	235	202	0	2	0	0
45	267	94	0	3	0	0
50	120	112	0	2	0	0
55	107	75	0	3	0	0
60	224	52	0	4	0	0
65	98	63	0	4	0	0
70	95	92	0	4	0	0
75	13	40	0	7	0	0
80	40	92	0	1	0	0
85	12	30	0	4	0	0
90	51	41	0	4	0	0
95	0	30	0	5	0	0
100	0	40	0	2	0	0
105	0	0	0	5	0	0
110	0	23	0	2	0	0
115	0	0	0	1	0	0
120	0	40	0	0	0	0
125	0	50	0	5	0	0
130	0	101	0	1	0	0
135	0	20	0	3	0	0
140	0	70	0	2	0	0
145	0	40	0	2	0	0
150	0	91	0	2	0	0
155	0	40	0	0	0	0
160	0	10	0	1	0	0
165	0	31	0	1	0	0
170	0	20	0	1	0	0
175	0	0	0	1	0	0
180	0	20	0	1	0	0
185	0	10	0	3	0	0
190	0	10	0	2	0	0

195	0	0	0	3	0	0
200	0	0	0	0	0	0
205	0	0	0	0	0	0
210	0	30	0	1	1	0
215	0	0	0	1	0	0
220	0	0	0	4	0	0
225	0	0	0	3	0	0
230	0	0	0	2	0	0
235	0	0	0	2	0	0
240	0	0	0	1	0	0
245	0		0	0	0	0
250	0		0	1	0	0
255	0		0	0	0	0
260	0		0	0	0	0
265	0		0	2	0	0
270	0		0	1	0	0
275	0		0	3	0	0
280	0		0	0	0	0
285	0		0	1	0	0
290	0		0	3	0	0
295	0		0	1	0	0
300	0		0	1	0	0
305	0		0	0	0	0
310	0		0	1	0	0
315	0		0	1	0	0
320	0		0	0	0	0
325	0		0	2	0	0
330	0		0	1	0	0
335	0		0	1	0	0
340	0		0	0	0	0
345	0		0	0	0	0
350	0		0	0	0	0
355	0		0	0	0	0
360	0		0	0	0	0
365	0		0	0	0	0
370	0		0	0	1	0
375	0		0	1		0
380	0		0	0		0
385	0		0	0		0
390	0		0			0
395	0		0			0
400	0		0			0
Total:	3448	2568	0	120	2	0

Total (all axles):	6138					
Total axle %:	0.561746	0.418377	0	0.0195503	0.000326	0
Total	1					
HVAG	1					

Appendix F – Axle distribution of A6 Road

Table 9: Axle distribution of A6 Road.

Axle Load	Axle distribution					
	SAST	**SADT**	**TAST**	**TADT**	**TRDT**	**QADT**
5	117	0	0	0	0	0
10	854	21	0	0	0	0
15	201	126	0	0	0	0
20	514	214	0	0	0	0
25	410	192	0	0	0	0
30	414	107	0	0	0	0
35	408	303	0	0	0	0
40	390	217	0	0	0	0
45	416	197	0	2	0	0
50	211	97	0	0	0	0
55	389	117	0	0	0	0
60	176	43	0	0	0	0
65	109	151	0	0	0	0
70	170	174	0	0	0	0
75	65	260	0	0	1	0
80	22	64	0	0	1	0
85	45	21	0	57	0	0
90	17	0	0	0	0	0
95	0	0	0	0	0	0
100		44	0	0	0	0
105		0	0	0	0	0
110		22	0	0	0	0
115		65	0	0	0	0
120		44	0	0	0	0
125		44	0	0	0	0
130		151	0	0	0	0
135		163	0	0	0	0
140		88	0	1	0	0
145		22	0	0	0	0
150		21	0	0	0	0
155		0	0	0	0	0
160		10	0	0	0	0
165		21	0	0	0	0
170		0	0	0	0	0
175		22	0	0	0	0
180		22	0	0	0	0
185		44	0	0	0	0
190		22	0	0	0	0

195		65	0	0	0	0
200		22	0	0	0	0
205		0	0	0	0	0
210		0	0	0	0	0
215		0	0	0	0	0
220		21	0	0	0	0
225		22	0	0	0	0
230		0	0	0	0	0
235		0	0	0	0	0
240		0	0	0	0	0
245			0	0	0	0
250			0	0	0	0
255			0	30	0	0
260			0	44	0	0
265		0	0	0	0	0
270		0	0	0	0	0
275		0	0	0	1	0
280		0	0	0	0	0
285		0	0	0	0	0
290		0	0	0	0	0
295		0	0	0	0	0
300		0	0	0	0	0
305		0	0	30	0	0
310		0	0	0	0	0
315		0	0	45	0	0
320		0	0	0	0	0
325		0	0	0	0	0
330		0	0	0	0	0
335		0	0	0	0	0
340		0	0	0	0	0
345		0	0	0	0	0
350		0	0	0	0	0
355		0	0	0	0	0
360		0	0	0	0	0
365		0	0	0	0	0
370		0	0	0	0	0
375		0	0	0	0	0
380		0	0	0	0	0
385		0	0	0	0	0
390		0	0	0	0	0
395		0	0	0	0	0
400		0	0	0	0	0
425				45		
Total:	4928	3239	0	254	3	0

Total (all axles):	8424					
Total axle %:	0.584995	0.384497	0	0.0301519	0.000356	0
Total	1					
HVAG	1					